IGNITION AND FLAMEHOLDING IN SUPERSONIC FLOW BY INJECTION OF DISSOCIATED HYDROGEN

by

Timothy Charles Wagner

Dissertation submitted to the Faculty of the
Virginia Polytechnic Institute and State University in
Partial Fulfillment of the Requirements for the Degree of

DOCTOR OF PHILOSOPHY

in

Mechanical Engineering

APPROVED:

W. F. O'Brien, Chairman

H. L. Moses

D. R. Jaasma

A. K. Jakubowski

J. A. Schetz

G. B. Northam

May 1987

Blacksburg, Virginia

IGNITION AND FLAMEHOLDING IN SUPERSONIC FLOW BY INJECTION OF DISSOCIATED HYDROGEN

by

Timothy Charles Wagner

Committee Chairman: Walter F. O'Brien

Mechanical Engineering

(ABSTRACT)

The objective of this research was to investigate analytically and experimentally the use of free radicals for ignition and flameholding in supersonic flows. An analytical investigation of the effects of adding small quantities of radicals to a stoichiometric mixture of hydrogen and air was performed using a finite-rate chemical kinetics code. The results of these calculations indicate that small additions of hydrogen atoms, oxygen atoms, nitrogen atoms, or hydroxyl radicals are effective in promoting ignition. These analytical results were qualitatively verified in a Mach 2 flow experiment using hydrogen atoms generated by a plasma torch. The supersonic combustion tests were conducted in a direct-connect mode at atmospheric pressure with either ambient temperature air or burner-heated vitiated air with total temperatures from 1200 to 4000 R. Both semi-freejet and ducted configurations were used. The experimental results indicate that

hydrogen atoms from a low-power plasma torch provide an effective ignition and flameholding source for hydrogen-fueled Mach 2 flows at total temperatures as low as 1065 R, the lowest temperature tested. A reduction in the minimum total temperature required for ignition of several hydrocarbon fuels was also demonstrated.

A piloted fuel injector configuration designed to take maximum advantage of the hydrogen atoms from the plasma torch was conceived and fabricated. The injector design consisted of five small upstream pilot fuel injectors, a rearward-facing step and three primary fuel injectors downstream of the step. The hydrogen atoms from the plasma torch were injected in the recirculation region downstream of the step. Three other ignition sources were also tested as comparisons: an argon plasma, a pyrophoric mixture of silane and hydrogen, and a surface discharge device. Hydrogen-fueled supersonic combustion tests were conducted at conditions similar to those described earlier. Hydrogen atoms generated by the plasma torch proved to be the most effective ignition source, causing ignition for a torch input power of 780 W, the lowest power tested. The combination of the hydrogen atoms and the piloted fuel injector was shown to be a very effective igniter and flameholder for scramjet operation over a simulated flight envelope (Mach 3 to Mach 6, low to moderate altitudes).

ACKNOWLEDGEMENTS

I owe my deepest thanks to Dr. W. F. O'Brien, my advisor, and Dr. G. B. Northam, technical monitor of this project. Their guidance and encouragement have made working on this research both educational and enjoyable. I also want to thank the remaining members of my committee: Professors D. R. Jaasma, A. K. Jakubowski, H. L. Moses, and J. A. Schetz.

I am grateful for the technical support provided by and his staff of technicians. I especially want to thank without whose help the experiments reported herein would not have been possible.

and are to be thanked for their assistance as test engineers during the supersonic combustion tests.

and are also thanked for their assistance in this project.

I also want to thank the National Aeronautics and Space Administration for their support of this project.

Finally, I would like to express a special thanks to my mother, and my brother, for their love and support throughout this endeavor.

TABLE OF CONTENTS

Page

Page

Page

LIST OF FIGURES

Figure Page

Figure Page

LIST OF TABLES

NOMENCLATURE

a,b,c,C	constants
$\overline{C}_p$	mean constant pressure specific heat
d	orifice diameter
$E_{a,r+1}$	ionization energy for the levels r to r+1 in species a
$\Delta E_{a,r+1}$	lowering of the ionization energy due to Coulomb interaction of charged species
h	Planck's constant
H	step height
I	current
k	Boltzmann's constant
$\overline{k}$	mean thermal conductivity
K	Karlovitz number
L	characteristic dimension
m_a	mass of species a
m_{aa}	mass of diatomic species aa
m_e	mass of electron
M_∞	free stream Mach number
n_a	total number density of particles of species a
n_{aa}	number density of diatomic species aa
$n_{a,r}$	number density of atoms or ions of species a in ionization level r
n_e	electron density
p	static pressure
p_t	total pressure
P	power
q_r	dynamic pressure ratio

Q, Q_{TOT}	volumetric flowrate
r	ionization level
$\hat{S}_T$	turbulent flame speed at anchor point
$\bar{S}_T$	mean turbulent flame speed
T	static temperature
T_t	total temperature
v	velocity
v^*	velocity along dividing streamline between recirculation zone and shear layer
V	voltage
x	distance along flow direction
x_ℓ	length for complete mixing
x_ϕ	parameter in mixing efficiency equation (see eqn. 7)
z	distance perpendicular to flow direction
Z_{aa}	partition function of diatomic species
$Z_{a,r}$	partition function of species a in ionization level r
α	argon-hydrogen volumetric flow ratio
γ	ratio of specific heats
η_c	combustion efficiency
η_m	mixing efficiency
μ_{aa}	dissociation energy of diatomic species aa
ρ	density
$\bar{\rho}$	mean density
ϕ	fuel-air equivalence ratio
ϕ_1	bulk equivalence ratio of fuel from upstream injector
ϕ_2	bulk equivalence ratio of fuel from downstream injector

1. INTRODUCTION

The desire to fly higher and faster has captured the imagination of man since the Wright brothers' first successful powered flight. Although rockets may be used to achieve high-speed flight, air-breathing propulsion is much more efficient for flight within the atmosphere. The turbojet is the most efficient device for supersonic flight up to speeds of approximately Mach 3.5. The upper bound of the operating range of the turbojet is limited by the availability of materials for the rotating machinery. However, at these speeds the air may be compressed by utilizing the forward motion of the vehicle to force air through a varying-area inlet. Therefore, the compressor and hence the turbine may be eliminated. This concept is utilized in the conventional subsonic combustion ramjet. The maximum speed of the ramjet is restricted to about Mach 6 because of materials limitations and losses associated with diffusion and dissociation. These limitations and losses may be circumvented by utilizing supersonic combustion. With the advent of the National Aero-Space Plane (NASP) Program, supersonic combustion ramjets (scramjets) are once again an area of great interest to the aerospace community.

Because of the ignition characteristics and finite flame speeds of fuel-air mixtures and the short residence times characteristic of supersonic combustors, the process of igniting and sustaining combustion in a supersonic flow has been and continues to be a difficult engineering problem. The need for ignition, flameholding and combustion enhancement in supersonic flow has been demonstrated during

subscale supersonic combustion ramjet (scramjet) engine tests conducted by the Hypersonic Propulsion Branch of the NASA Langley Research Center and in other investigations. During these tests two flight regimes were identified where a source of ignition or combustion enhancement is required with hydrogen fuel. At low flight Mach numbers the static temperature is below the autoignition temperature for hydrogen, and an igniter is required.[1-3] Possible igniters include chemical torches, pyrophorics, monopropellants, chemical additives, very reactive oxidizers and vacuum ultraviolet radiation. At Mach 7 simulated flight conditions (T_t = 3900 R, well above the autoignition temperature, combustor pressure = 0.3 atmospheres), flame stabilization and augmentation in subscale systems are required to compensate for the short residence times associated with the higher velocity.[4] Geometric flameholders and continuous ignition sources are among the possible flame stabilization techniques for use in supersonic combustion. For the subscale scramjet engine tests conducted at NASA Langley, pyrophoric silane (SiH_4) was mixed with the hydrogen fuel to provide ignition and flame stabilization when required.[4]

Most ignition sources add energetic free radicals (H, O, OH) to the flow either directly (chemical torches) or indirectly through reaction (pyrophorics, monopropellants, very reactive oxidizers, chemical additives and UV radiation). The formation of radicals plays a key role in the rate-determining steps of combustion processes. By adding radicals to a combustible mixture, the rate controlling reactions may be accelerated, thereby enhancing the ignition and flame-

holding characteristics. The concept of using radicals to enhance combustion has been investigated by Weinberg,[5] Clements,[6] Dabora[7-9] and Kimura.[10-12] In these investigations, radicals generated by small plasma torches or chemical torches were used to extend the flammability limits of fuel-air mixtures in nonflowing systems and to ignite and flamehold in flowing systems. Kimura et al.[10] have used a plasma torch to ignite hydrogen-fueled supersonic flows.

The objective of the current research was to analytically and experimentally investigate the use of free radicals for ignition and flameholding in supersonic flow. A review of previous ignition and flameholding methods in supersonic flow was conducted. An analytical investigation of the effects of adding small quantities of radicals to a combustible mixture was performed using a finite-rate chemical kinetics code. An experimental investigation was conducted in a Mach 2 flow using hydrogen atoms generated by a plasma torch. Initial tests were performed using a commercially-available plasma torch. The goals of the initial tests were to demonstrate the ability of hydrogen atoms from the plasma torch to ignite and flamehold in confined supersonic flow with hydrogen fuel and to investigate the use of hydrogen atoms from the plasma torch as an ignition source for hydrocarbon fuels. The effects of power level and the relative location of torch and fuel injectors were also investigated. Based on the promising performance of the hydrogen atoms generated by the commercial torch and the fact that the plasma torch was an effective igniter and flameholder at its lowest stable power level, a new, low-power plasma torch was designed in conjunction with this investigation. A new injector configuration

was also designed to make optimum utilization of the hydrogen atoms generated by the low-power torch. The combination of the plasma torch and the injector configuration were tested in a hydrogen-fueled Mach 2 flow at conditions simulating Mach 3 through Mach 6 flight at low to moderate altitudes. The test program was divided into two parts. The first part of the test program was designed to explore the effects of torch operating conditions on the ignition and flameholding characteristics of the new injector design as a function of total temperature. The second part of the test program was designed to investigate the characteristics of the injector configuration. An argon plasma, a 20/80 volumetric mixture of silane and hydrogen (a pyrophoric), and a surface discharge plug were tested for comparison to the hydrogen atoms from the plasma torch. Diagnostic tests were conducted to verify the presence of hydrogen atoms in the argon-hydrogen plasma generated by the torch.

2. REVIEW OF IGNITION AND FLAMEHOLDING IN HIGH SPEED FLOW

Combustion may occur in any supersonic flow of fuel and oxidizer where the requirements for mixing, ignition and flameholding are satisfied. Many investigations of supersonic combustion have been in support of supersonic combustion ramjet (scramjet) development. (See, for example, Refs. 13-25.) The fuel and oxidizer may be premixed or the fuel may be injected into a supersonic flow. High velocity air provides the oxidizer. For most practical supersonic combustors the fuel and air are not premixed. In these cases the fuel may be injected axially or transversely from the walls or from struts imbedded in the flow. Struts allow for a combination of transverse and axial injection. Transverse injection is typically normal to the flow, although angled injection has also been studied. Fuel, in either liquid or gas phase, may be injected through slots or discrete orifices. The interaction of transverse jets and supersonic crossflows has been extensively studied. (See, for example, Refs. 26-44.)

For short combustors, transverse injection is preferred because it provides greater penetration and faster mixing. A schematic of the flowfield near a sonic, underexpanded wall injector normal to the flow is shown in Fig. 1. A "barrel" shock forms as a result of the underexpansion. The disturbance created by the fuel penetration represents a blockage to the airflow, causing a bow shock to form upstream of the injector. If the blockage is significant, a flow separation occurs upstream of the injector. The penetration of fuel injected transversely into a supersonic crossflow depends primarily on the size of

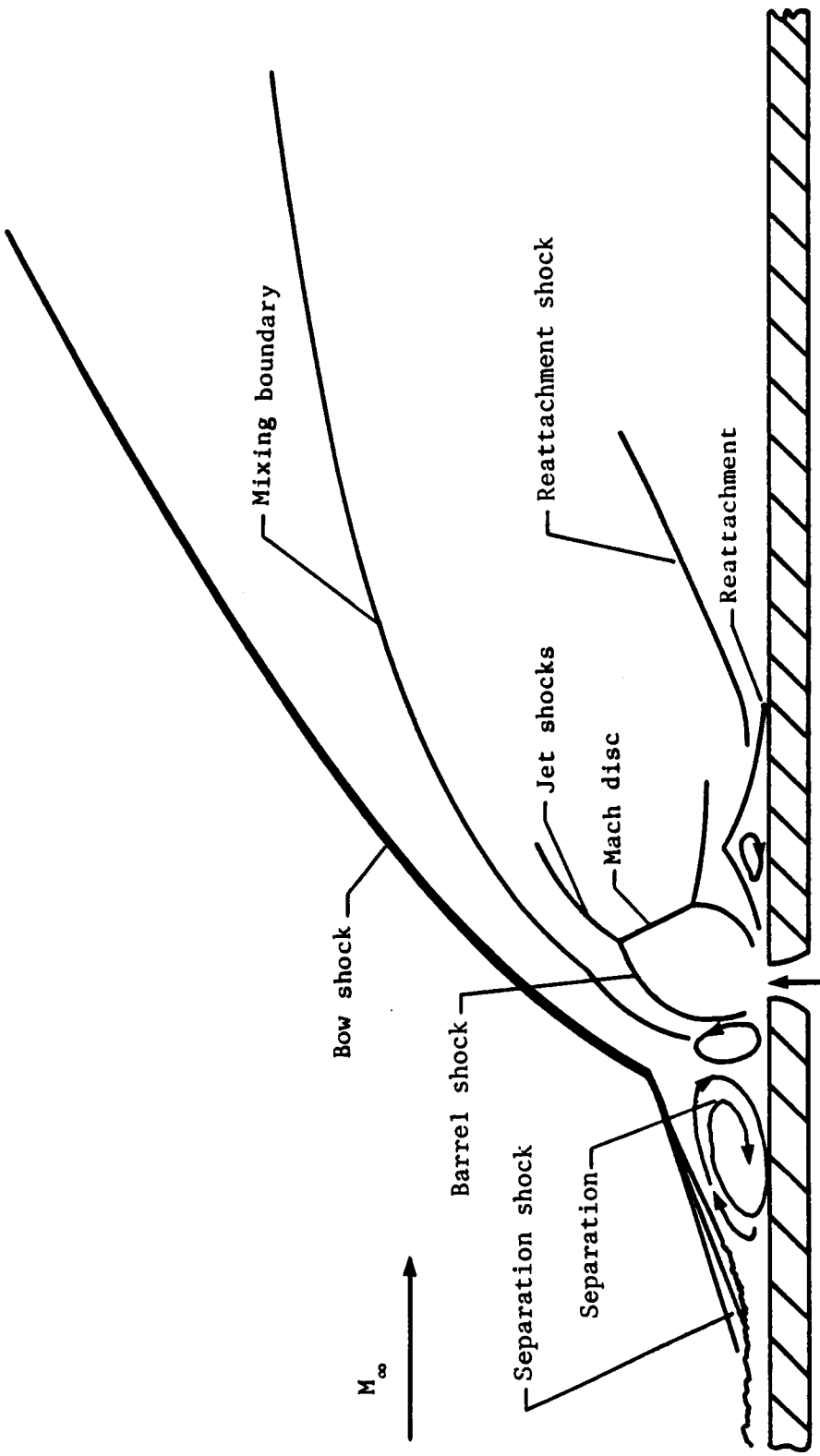

Fig. 1. Schematic of transverse fuel-injection flowfield. (After Refs. 32, 49)

the injector and the ratio of the dynamic pressures of the jet and the freestream, q_r,

$$q_r = \frac{\left(\frac{1}{2} \rho v^2\right)_j}{\left(\frac{1}{2} \rho v^2\right)_\infty} \tag{1}$$

Choked circular sonic orifices are usually employed and are sized and spaced to yield good penetration and mixing at the desired fuel equivalence ratio. The dynamic pressure ratio for a sonic injector with unity discharge coefficient may be expressed as

$$q_r = \left[\frac{\gamma_j}{\gamma_\infty}\right]\left[\frac{p_{t_j}}{p_\infty M_\infty^2}\right]\left[\frac{\gamma_j + 1}{2}\right]^{\left(\frac{\gamma_j}{1 - \gamma_j}\right)} \tag{2}$$

Empirical correlations for the penetration of fuel injected through sonic orifices normal to the airflow have been developed and are of the form[30,37,38]

$$\frac{z}{d} = C \left(q_r\right)^a \left(\frac{x}{d}\right)^b \tag{3}$$

where a and b are both less than one. The variation in the values of the constants has been attributed to differences in the molecular weight of injectants[33] and the ratio of plate boundary-layer thickness to orifice diameter.[40] In general, the penetration increases with increasing orifice diameter and dynamic pressure ratio. Correlations for lateral spreading of transversely injected fuel have also been developed. As a general rule, the lateral spreading is approximately twice the penetration.[39]

Empirical correlations for mixing efficiency for normal injection from multiple injectors, η_m, have also been developed and are of the form[38]

$$\eta_m = c \left(\frac{x}{d} q_r^{-a} \right)^b \tag{4}$$

where the mixing efficiency is defined as the fraction of fuel which would react if complete combustion occurred without further mixing. The injector spacing for optimum mixing was empirically determined to be equal to the gap, which is the distance between opposite walls of the combustor or fuel injection struts.[22] With this configuration the length for complete mixing, x_ℓ, is 60 gaps for an equivalence ratio of 1.0. The mixing efficiency may be estimated from the following relationships:[22]

Perpendicular injection (from 2 opposite walls)

$$\eta_m = 1.01 + 0.176 \ln \left(\frac{x}{x_\phi} \right) \tag{5}$$

Parallel injection

$$\eta_m = \frac{x}{x_\ell} \tag{6}$$

where

$$x_\phi = 0.179\, x_\ell\, e^{1.72\phi} \qquad \phi < 1 \tag{7a}$$

$$x_\phi = 3.33\, x_\ell\, e^{-1.204\phi} \qquad \phi > 1 \tag{7b}$$

2.1 Review of Ignition Schemes

In a flowing combustible mixture, ignition will occur spontaneously if the static temperature, static pressure, residence time and equivalence ratio meet the ignition requirements. These requirements are dependent upon the choice of fuel. The ignition requirements may be minimized by using highly reactive fuels or monopropellants. Aluminum borohydride, a pyrophoric, has been successfully burned in supersonic flows.[45,46] Hydrazine, a monopropellant, has also been used as the primary fuel in supersonic combustion.[47] (The hydrazine was passed through a catalyst prior to injection.) For a discussion of other high energy and reactive fuels for use in supersonic combustion applications, see Ref. 48. The unstable nature of these very reactive fuels renders them undesirable for practical systems. Hydrogen is a fuel of interest for reusable propulsion systems utilizing supersonic combustion because of its high heating value, fast reaction rate and good cooling properties. However, hydrogen requires a higher temperature for ignition than many other fuels. Detailed studies of the autoignition of hydrogen injected transversely into supersonic airstreams are presented in Refs. 49 and 50. When pyrophoric fuels and monopropellants are not used and the requirements for autoignition are not satisfied in the flow, an external ignition source is required.

Several ignition schemes have been tested in supersonic flows. The method which has been most widely used is the pilot flame, which may also be referred to as the chemical torch. A pilot flame provides

a jet of hot, reactive species which is an effective ignition and flameholding source. Coaxial hydrogen-oxygen-air pilot flames have been studied experimentally and analytically as igniters for ambient temperature, premixed, supersonic flows of hydrogen[51,52] or hydrocarbons[53-55] and air. A propane-oxygen pilot flame has been successfully used to ignite premixed supersonic flows of propane, JP-7, TM-MCPD or Shelldyne-H (RP-5) and air.[55] In these tests a two-dimensional combustor was used with the pilot injected parallel to the mainstream. Two of the variables in these tests were the pilot equivalence ratio and the pilot exhaust temperature. The pilot exhaust temperature was varied independent of the pilot equivalence ratio by adding an inert gas to the pilot. An interesting result from this study was that the effectiveness of the torch was independent of the torch equivalence ratio. Combustion was always obtained when the pilot exhaust temperature was greater than 5000 R and was never obtained when the exhaust temperature was below 4000 R. Schmotolocha et al.[4] have also demonstrated piloted supersonic combustion of propane and JP-7. However, during the tests reported on in Ref. 4, the pilot was operated with a mixture of air and a small amount of the primary fuel. The fuel and the exhaust from the pilot were injected almost parallel to the airflow from a "fish-mouth" cowl protruding from the wall. The significant result from this study was the demonstration that the pilot could be operated with a mixture of air and the primary fuel.

An ethylene-oxygen torch has been used to ignite supersonic flows of air with injection of the following fuels: liquid hexane,[56,57]

magnesium slurry[57] and boron slurry.[57] The fuel was injected transversely from the sides of a strut while the torch exhaust was injected axially from the trailing edge of the strut. McFarlin and Kepler[58] found that an oxygen-hydrogen torch located downstream of a step was an effective igniter for hydrogen-fueled supersonic flows. However, neither a spark igniter with 3 sparks per second nor injection of triethylborane were effective for the conditions tested. The spark igniter was not located directly in the combustor but rather in a separate chamber connected to the combustor by a duct.

Very reactive oxidizers have also been used to ignite supersonic flows. During the development of the hydrogen-fueled Dual Mode Scramjet Engine at the Marquardt Corporation, gaseous fluorine was found to be a more effective igniter than pentaborane or a hydrogen-air torch.[59] All injection was normal to the air flow. The fluorine injectors were located between rows of fuel injectors. Chlorine trifluorine (CTF) has also been used effectively.[60]

In an attempt to develop a storable igniter/pilot system, Diskin[61,62] used an ethylene-oxygen preburner to produce fluorine from the dissociation of sulfur hexafluoride (SF_6). This pilot was successfully tested in supersonic flows fueled with ethylene, ethane and methane. However, when the SF_6 was replaced with nitrogen, no decrease in effectiveness was observed. The products of combustion and the large flow disturbance created by the pilot injection were thought to have been responsible for the observed results.

Monopropellant igniters have also been used in supersonic flow. Carlson et al.[63] used OTTO fuel to ignite RJ-5. (OTTO fuel is a

monopropellant used in submarine applications.) The RJ-5 was injected far enough upstream of the igniter to allow for atomization and mixing. The OTTO fuel was injected from the leading edge of a strut. Some of the fuel-air mixture was captured by slots on the side of the strut and directed through a catalyst in the rear of the strut, where ignition occurred.

Chemical additives have been investigated as a means for obtaining supersonic combustion of fuels at flow conditions where the fuel would not otherwise burn. Aluminum borohydride has been added to JP-4 to lower the autoignition temperature, allowing the fuel to be used at lower temperatures without an igniter.[45] Shelldyne-H with additions of 13 percent pentaborane (B_5H_9), 6.7 percent trimethylaluminum (TMA) or 8.9 percent HiCal have been burned successfully in a supersonic flow.[64] The pentaborane additive was the most effective. Siminski and Wright[65] have demonstrated that alkyl nitrates and nitrites are effective in promoting ignition of hydrocarbon fuels in supersonic flows. Additions of NO and NO_2 were nearly as effective as the alkyl nitrates and nitrites.[66]

Silane, SiH_4, has been used as an additive for the supersonic combustion of hydrogen[67] and methane[68,69] fuels. A mixture of 20 percent by volume silane in hydrogen was used to initiate combustion during some scramjet engine tests at the Hypersonic Propulsion Branch of the NASA Langley Research Center.[3,67] The silane was eliminated once combustion was established . The flame was stabilized by an aerodynamic or geometric flameholder. (See Section 2.2.)

Isaac and Cookson[70-73] have demonstrated that combustion of methane injected into a supersonic airstream may be promoted by injecting small amounts of hydrogen into the flow. Injecting the hydrogen upstream of the methane fuel injection was shown to be the optimum configuration. It was also demonstrated that less hydrogen was required to stabilize the flame when the aerodynamic blockage created by transverse injection was present. The ability of transverse injection to aid in autoignition was demonstrated during an investigation of scramjet operation at low Mach numbers at the General Applied Science Laboratories (GASL).[74] In the original design of the GASL scramjet, all of the hydrogen fuel was injected axially. However, the autoignition characteristics were improved by injecting 3 percent of the fuel perpendicular to the airstream.

Flaucher et al.[75] found that methane and octane could be burned in a supersonic flow at temperatures below their autoignition temperature by injecting hydrogen and oxygen separately into a recirculation zone upstream of the primary fuel injection. The recirculation zone was formed by a recessed hole, a recessed step or a projected step. Some methane-fueled configurations required no oxygen injection, similar to the results of Isaac and Cookson.[70-73]

Billig, Waltrup and Stockbridge[76] have proposed a novel variation on the pilot concept: the dual-combustion ramjet. In this design, some of the air is slowed to subsonic speeds, mixed with all of the fuel, and burned in a dump combustor. The fuel-rich exhaust of this pilot is then injected into the remaining supersonic airstream, and the combustion process is completed supersonically. Because of the

high temperatures in the dump combustor, hydrocarbon fuels will burn without additives. However, at some operating conditions, the fuel-rich preburner exhaust contains soot. All of this soot does not burn in the supersonic flow, resulting in reduced efficiency. Brabbs[77,78] has proposed a fuel-rich catalytic preburner which would allow the preburner combustion process to occur without the formation of soot.

The duct hardware may also be modified to promote ignition in supersonic flows. One modification is to tailor the combustor geometry to provide a localized flow of higher static temperature and residence time where ignition is more likely to occur. Catalysts or hot spots created by adiabatic surfaces are other possible modifications. Two researchers have used a platinum catalyst in supersonic combustors.[79,80] The hot spot concept has also been tested by locating a zirconium rod along the combustor wall.[79] The flow obstruction created by this rod produced a recirculating flow of low velocity, which also aided in ignition.

Kimura, Aoki, and Kato[10] have investigated the use of a plasma torch for ignition and piloting of supersonic flows with hydrogen injection. Their investigation will be reviewed in detail because of its relevance to the current investigation. The subsonic exhaust from a plasma torch was injected normal to Mach 2.1 or 2.7 semi-freejet flows. Hydrogen, nitrogen and argon were used as feedstocks for the plasma torch. At the entrance to the test section the static pressure was one atmosphere and the total temperature was 290 K. The hydrogen fuel was injected from a single sonic injector at a pressure of 16 atmospheres. The hydrogen fuel flow rate was 3.68×10^{-3} lb/s. The

fuel injector and the plasma jet were located on the centerline of the bottom wall of the duct. The fuel was injected from either of six locations : 3.0, 2.0, 1.0 or 0.1 inches upstream of the plasma injector, or 1.0 or 0.1 inches downstream of the plasma injector. The net power into the arc was varied between 2 and 4 kW. The flowrates of feedstock to the torch were selected so as to maintain a stable arc. The only torch flowrate reported in the paper was 106 scfh of hydrogen. The results indicated that nitrogen and hydrogen were almost equally effective for enhancing combustion. Argon was ineffective. The maximum combustion efficiency occured with the plasma torch located one inch downstream of the fuel injector. With this configuration, the combustion efficiency at a point four inches downstream of the plasma injector was estimated to be 68 percent, based on thermocouple and pitot probe measurements. The authors attributed the effectiveness of the plasma torch to radicals in the plasma jet. However, they also suggested that the effects of ions and nonequilibrium species such as vibrationally excited molecules might participate in enhancing combustion. The primary result of this investigation was the demonstration of ignition and flameholding in a supersonic flow using a plasma torch.

2.2 Review of Flameholding Studies

Because the velocities in supersonic flow are significantly greater than the flame speed, flame stabilization is usually required. This stabilization may be provided by chemical pilots,

flameholders or a combination of both. Many of the ignition systems discussed in the previous section stabilized a flame by providing a continuous ignition source. A flameholder stabilizes the flame by creating a region of low velocity, recirculating flow. The recirculation zone is in essence a pilot, providing hot gas and radicals to the freestream. The energy and mass transport between the recirculation zone and the freestream are requisite for establishing a propagating flame.

A region of low velocity flow may be created aerodynamically or geometrically. The flow disturbance created by injecting fuel transversely into an airstream is an example of an aerodynamic flameholder. A bluff body protruding into the flow is an example of a geometric flameholder. Although flame stabilization in subsonic premixed flows has been studied extensively (see, for example, Refs. 81-91), no general theory has gained universal acceptance. The models which have been proposed to describe flameholding in premixed subsonic flows may be divided into two categories:

1. Models which assume that blowoff occurs when the rate of energy leaving the recirculation zone just exceeds the rate of energy entering (Refs. 82-85).

2. Models which assume that blowoff occurs when the residence time in the shear layer or in the recirculation zone is equal to the ignition delay time (Refs. 86-88).

Stability limits for premixed subsonic flow have been developed by correlating experimental observations. These correlations are of the form[82]

$$\phi = v\, L^{a} p^{b} T^{c} \qquad (8)$$

where: ϕ = equivalence ratio at blowoff
v = velocity past the flameholder
L = characteristic dimension
p = pressure
T = absolute temperature

The values of the exponents reported in the literature vary over a wide range, depending on the details of the flowfield. A qualitative explanation of the effects of various parameters on flameholding follows.

Velocity - An increase in velocity decreases the residence time in the recirculation zone and increases the influx of cold reactants, thereby destabilizing the flame.

Geometry - The flameholding geometry is typically described by a characteristic dimension. Increasing the size of the flameholder results in a larger recirculation zone and residence time, thereby improving flameholding. The shape of the flameholder may also affect the correlation. Rizk and Lefebvre[91] have incorporated the drag coefficient into their correlation.

Pressure - In general, an increase in pressure reduces the ignition delay time, thereby improving flameholding. However, for hydrogen-air mixtures at temperatures less than 2000 R, the ignition delay time versus pressure curve reaches a minimum and then increases for increasing pressure.[92]

Temperature - An increase in gas temperature reduces the ignition delay time and the reaction time, thereby improving flameholding. The temperature of the flameholder may also be important. A hot flameholder decreases the heat loss from the recirculation zone, resulting in an increased recirculation zone temperature and improved flameholding.

Although the blowoff correlations reported in the literature are for premixed subsonic flows, Winterfeld[93] has demonstrated that the stability limit correlation is a continuous function as the freestream Mach number increases beyond one. However, it is necessary in supersonic flows to specify whether static or total conditions are to be used in the correlation. McClinton and Jakubowski[94,95] have proposed a correlation of the following form for the blowoff limit of supersonic combustion using various configurations with transverse injection of hydrogen.

$$\phi = \frac{M\,T^{0.5}}{L^{a}\,p_t^{\,b}\,T_t^{\,c}} \tag{9}$$

where: M = Mach number of approach flow
T = static temperature of approach flow
p_t = total pressure of approach flow
T_t = total temperature of approach flow
L = characteristic dimension

Large bluff bodies are undesirable for use in hot supersonic flows because they create large total pressure losses and require large amounts of cooling. Therefore, rearward-facing steps, airfoil-shaped struts and the aerodynamic blockage created by fuel injection are typically used for supersonic flame stabilization. Rearward-facing steps may be used for a dual purpose. Besides aiding in flameholding, steps also act to isolate the upstream flow from the pressure rise generated by reaction in the combustor. Since a rearward-facing step was employed in this investigation, a description of the flowfield and a review of the flameholding theories for rearward-facing steps will now be presented.

A schematic of the flowfield past a rearward-facing step is presented in Fig. 2. An expansion fan forms at the top corner of the step as the flow adjusts to the increased flow area. A recirculation zone forms behind the step. The boundary layer of the approach flow becomes a free shear layer between the freestream and the recirculation region. The dividing streamline (DS) marks the boundary between the low velocity gas in the recirculation zone and the high velocity gas of the shear layer. The gas in the high velocity shear layer has sufficient momentum to traverse the pressure rise at the rear attachment point and to continue downstream. A shock forms at the reattachment point as the flow turns to adjust to the constant area.

Huber[96] has proposed a conceptual model for flameholding of premixed supersonic flows stabilized by a rearward-facing step. In this model the flame originates from an anchor point in the recirculation zone where the local flow velocity equals the local turbulent flame velocity and the flame is not stretched too far ($\frac{du}{dy}$ is not too large). (See Fig. 2.) The flame propagates out of the recirculation zone for the case of self-sustaining combustion. As the approach velocity is increased, the anchor point moves toward the center of the recirculation zone in order to maintain a low value of the velocity gradient, $\frac{du}{dy}$, and to maintain equality between the local flow velocity and the local turbulent flame speed. An increase in approach velocity also causes the point at which the flame crosses the dividing streamline to move farther downstream. When the approach velocity is increased to a value just below the blowoff velocity, the flame crossing point moves very near the rear stagnation point (see

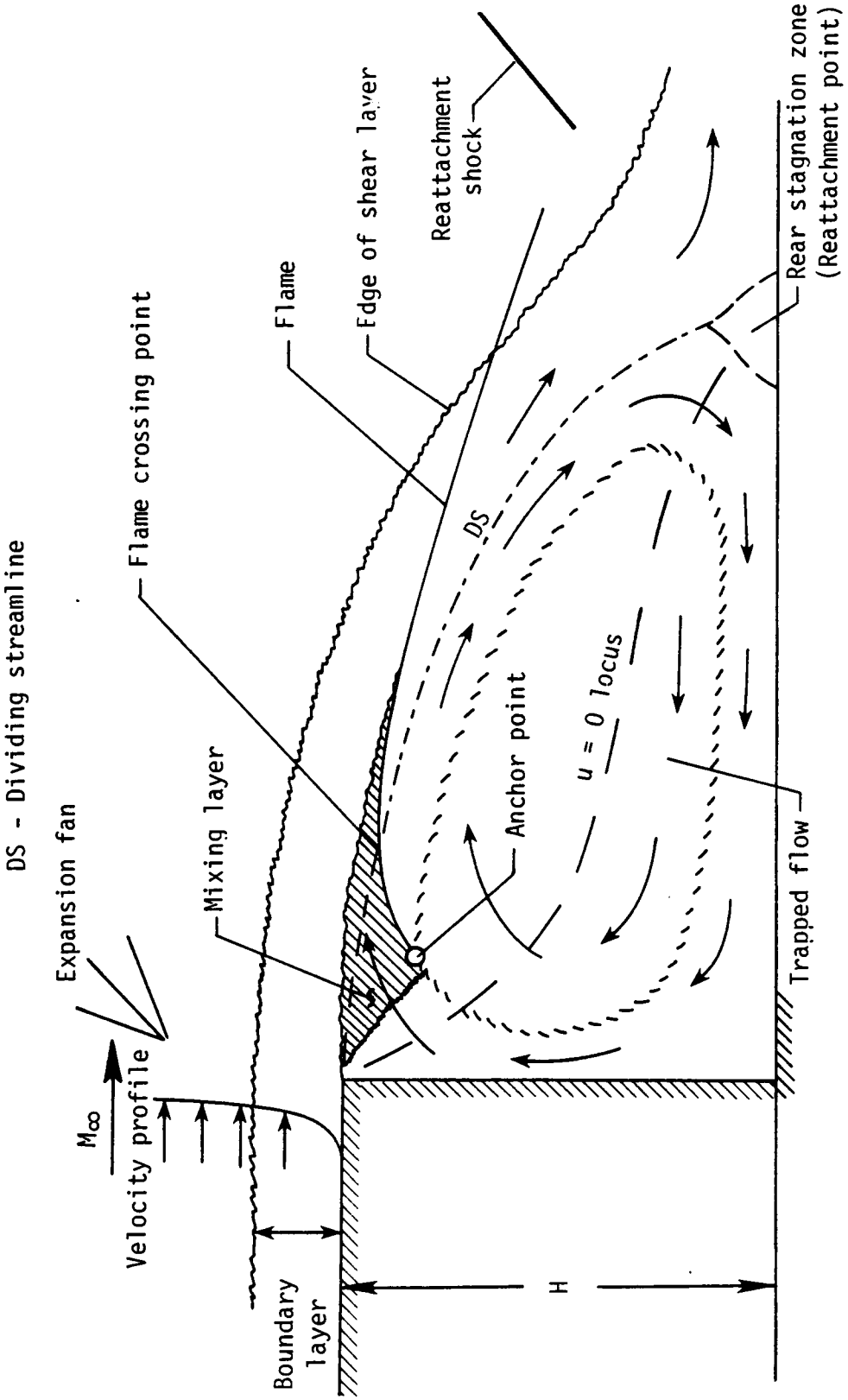

Fig. 2. Schematic of supersonic flow over a rearward-facing step with combustion. (Freestream velocity below blowoff velocity) (From Ref. 96)

Fig. 3). A further increase in approach velocity results in the flame not crossing the dividing streamline. When this occurs, the flame outside the recirculation zone blows off, and unburned mixture is drawn into the recirculation zone. This cooler gas mixes with the hot gas in the recirculation zone, reducing the temperature and the turbulent flame speed. As the flame speed decreases, the flame collapses farther inward, drawing more unburned gas into the recirculation region. This process results in rapid quenching of the flame.

Based on this conceptual model, Huber[96] has proposed an analytical model of flameholding for premixed flow over a step. This model is based on the assumption that the time required for the flame to travel from the anchor point to the dividing streamline must equal the time required for a parcel of gas to pass by the recirculation zone along the dividing streamline. The resulting equation is

$$H = \frac{1}{3K} \frac{1}{\left(S_T \frac{\bar{\rho}\bar{C}_p}{\bar{k}}\right)} \frac{v^*}{\bar{S}_T} \ln\left(\frac{v^*}{\hat{S}_T}\right) \qquad (10)$$

where:

H = step height
$\bar{C}_p$ = mean constant pressure specific heat
K = Karlovitz number
$\bar{k}$ = mean thermal conductivity
v^* = velocity along dividing streamline
$\hat{S}_T$ = turbulent flame speed at anchor point
$\bar{S}_T$ = mean turbulent flame speed
$\bar{\rho}$ = mean density

Huber integrated profiles of properties across the mixing layer to evaluate the average quantities. Several simplifying assumptions were

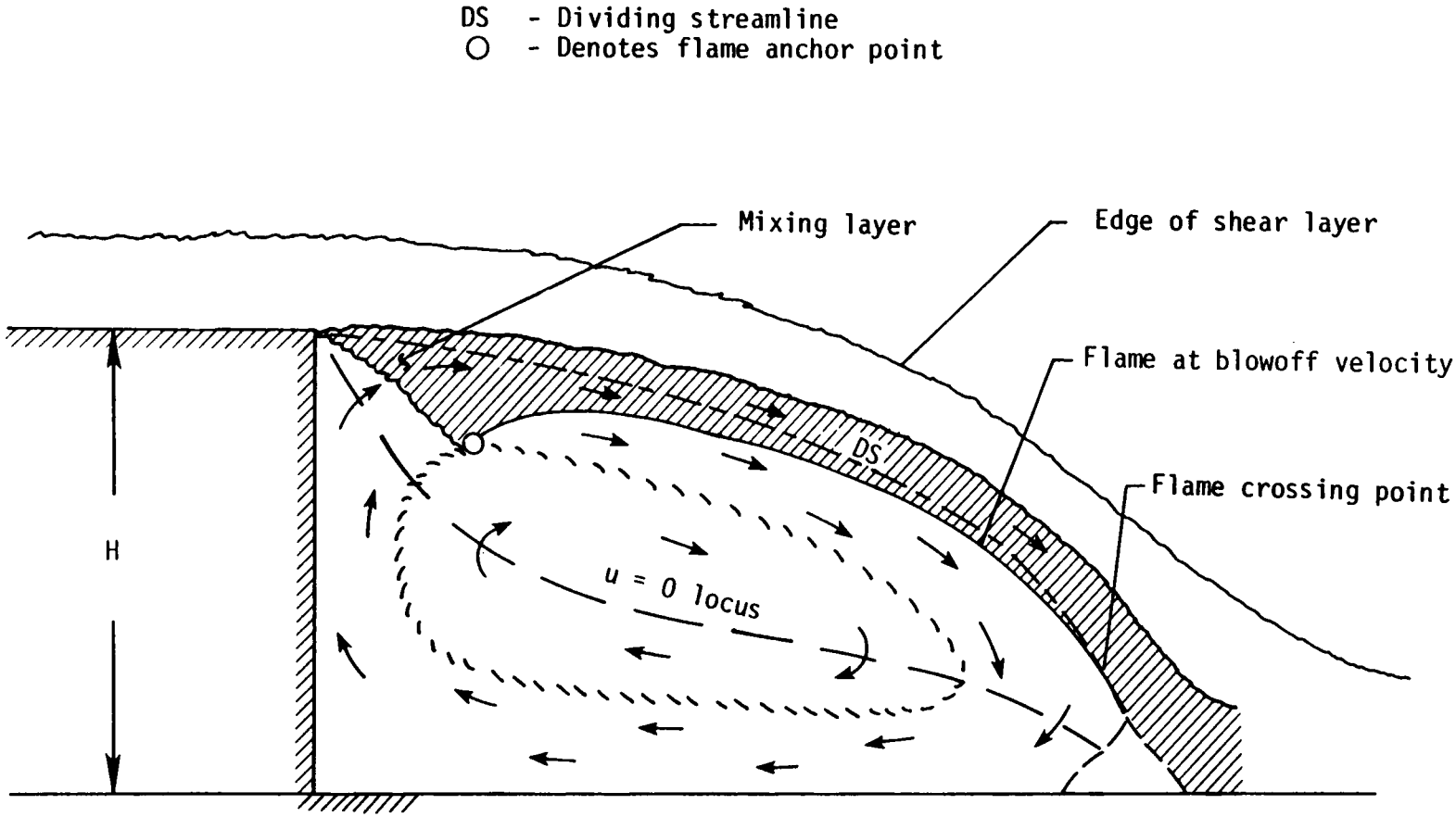

Fig. 3. Schematic of flameholding region behind step at blowoff condition. (From Ref. 96)

made in the development of this model, including assumed constant values of the Karlovitz number and the velocity along the dividing streamline. Even with these assumptions, this model correctly predicts that, for flameholding to occur, the scale of the step must increase as either the pressure or the equivalence ratio decreases.

In practical supersonic combustion systems, where the fuel and air are not premixed, the disturbance created by fuel injection may be sufficient to stabilize the flame. This aerodynamic flameholding was used in the hydrogen-fueled Marquardt Dual Mode Scramjet once ignition was established by the fluorine igniter.[59] The effect of blockage created by injection has been investigated by Isaac and Cookson,[70-73] as was discussed earlier. Depending on the flow conditions, a step or a bluff body may be required to assist the aerodynamic disturbance.

Although the use of bluff bodies for flame stabilization in supersonic flow is rare, Winterfeld[97] has published the results of such an investigation. In this study, hydrogen was injected transversely from a cylinder situated concentrically in a conical Mach 2.1 nozzle. The end of the cylinder formed the bluff body.

Rearward facing steps have been employed in most supersonic combustion applications requiring flame stabilization. Several different injector configurations have been used, including fuel injection upstream[98] or downstream[99-104] of the step. A compilation of injector configurations, including constant area injection as well as injection upstream and downstream of rearward facing steps, has been published in Ref. 49. Several other configurations were tested during the investigations reported in Refs. 50 and 98. From these references

it is clear that almost all tests have been conducted with fuel injection within 6 step heights of the step. As a result of the investigations reported in Refs. 49 and 50, McClinton concluded that the optimum geometry for autoignition was a stepped configuration with fuel injection 3 to 4 step heights downstream of the step.[50] This configuration has become the "standard" for most NASA-Langley combustors. For injection closer to the step or just upstream of the step the recirculation region was too rich and therefore impaired both ignition and flameholding. Anderson and Gooderum[99] found that if the injectors were located too far downstream of the step the recirculation region was not fueled and, therefore, could not assist in autoignition and flameholding. Northam, Trexler and McClinton[105] investigated the effects of step size and injector configuration on flameholding. The best flameholding characteristics were obtained with a deep step and fuel injection through multiple stages downstream of the step.

3. ROLE OF FREE RADICALS IN IGNITION AND FLAMEHOLDING

Radicals such as hydrogen atoms, oxygen atoms and the hydroxyl radical have long been recognized as important species in the combustion process. The role of radicals may be qualitatively demonstrated by considering a simplified eight step kinetic mechanism of the hydrogen-air reaction. (A more comprehensive reaction model is later used for computations.)

$$H + O_2 \rightarrow OH + O \quad (11)$$

$$O + H_2 \rightarrow OH + H \quad (12)$$

$$OH + H_2 \rightarrow H_2O + H \quad (13)$$

$$2OH \rightarrow H_2O + O \quad (14)$$

$$2H + M \rightarrow H_2 + M \quad (15)$$

$$H + OH + M \rightarrow H_2O + M \quad (16)$$

$$H + O + M \rightarrow OH + M \quad (17)$$

$$2O + M \rightarrow O_2 + M \quad (18)$$

The overall reaction may be divided into two periods: the induction period and the recombination period. During the induction period the concentrations of the radicals increase rapidly. The bimolecular reactions (11-14) dominate the induction period. During the recombination period the radicals recombine to produce the equilibrium products and liberate the heat of reaction. The three-body recombination reactions (15-18) dominate the recombination period. The time required for the induction period is referred to as the ignition delay time. There are several definitions of ignition delay time. For the purpose of this study, the ignition delay time was defined as the time

required to achieve the maximum rate of heat release during the combustion process. The time required to complete the reaction after the induction period is referred to as the recombination time. The reaction time is the sum of the ignition delay time and the recombination time.

The formation of radicals is the rate-controlling process for the induction period. If one of the steps in the radical formation process could be identified as rate-limiting, its reaction rate could be accelerated by increasing the concentration of the radical involved in that particular reaction. The necessary radicals could be added from an external source. The reaction which was previously rate-limiting would then proceed at an accelerated rate almost as though the temperature of the mixture had been increased a sufficient amount to create the externally-supplied radicals. This acceleration could be accomplished with only a fraction of the energy required to heat all of the reacting gas to a comparable temperature.

This concept of selectively accelerating the rate-limiting reaction is the basis of the current research. By heating a small quantity of gas and injecting it into a supersonic flow, the global reaction rate could be accelerated. However, the reaction and associated radical which are rate-limiting are not obvious. A discussion of the effects of radicals on combustion and the possible identification of a "key" species will be presented in the following material. A discussion of the possible effects of nitrogen atoms generated by a plasma torch will also be included because of the relevance to the current investigation.

3.1 Oxygen Atoms

Oxygen atoms are important in combustion because they participate in the chain branching reaction

$$O + H_2 \rightarrow OH + H \qquad (12)$$

The effects of oxygen atoms on combustion have been investigated by several researchers.[106-109] In these investigations combustible mixtures were ignited by a vacuum ultraviolet radiation source. The investigators observed that the results were independent of fuel type, indicating that the radiation was absorbed in the photochemical dissociation of molecular oxygen. These experiments demonstrated that the chain branching process could be initiated by increasing the concentration of oxygen atoms.

3.2 Hydrogen Atoms

Hydrogen atoms are important in combustion becau ' they participate in the chain branching reaction

$$H + O_2 \rightarrow OH + O \qquad (11)$$

This reaction is highly endothermic. Therefore, the reaction proceeds slowly at low temperatures and is easily quenched. Three observations indicating the significance of hydrogen atoms in combustion are discussed in the following material.

The importance of hydrogen atoms in combustion was demonstrated by Tanford and Pease,[110-112] who correlated the measured burning

velocity with the equilibrium concentration of hydrogen atoms at the flame temperature. The correlation between hydrogen atom concentration and flame speed for various fuels is illustrated in Fig. 4.

The importance of hydrogen atoms in combustion may also be observed by considering silane-hydrogen-air combustion. As was discussed in Section 2.1, silane is a pyrophoric which may be used to reduce the ignition delay time of a hydrogen-air mixture. Jachimowski and McLain[114] have suggested that the radicals formed during the rapid reaction of the silane are responsible for the reduced ignition delay. More recently, Chinitz[115] has suggested that the reaction

$$SiH_4 + M \rightarrow SiH_3 + H + M \qquad (19)$$

is the principal initiating reaction in the oxidation of silane. If this reaction is the initiating step, then silane is effective in reducing the ignition delay time because it provides hydrogen atoms which participate in the chain branching process.

A third observation indicating the importance of hydrogen atoms in combustion is a result of studies of inhibitors on flames. Biordi et al.[116] have used molecular beam and mass spectrometry to measure the species present in normal methane-air flames and in flames inhibited with CF_3Br. The authors found that the concentrations of CH_3 and hydrogen atoms were reduced when an inhibitor was present. However, the concentrations of atomic oxygen and the hydroxyl radical were unchanged by the presence of an inhibitor. These results indicate that hydrogen atoms may be the significant species in the chain branching process.

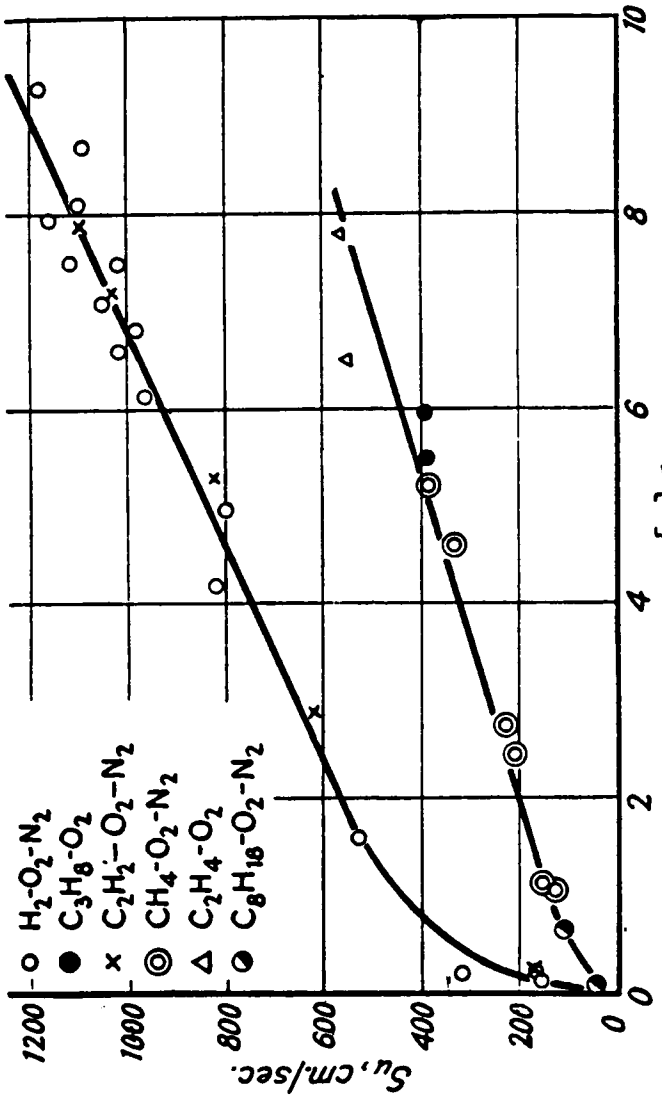

Fig. 4. Burning velocity vs. equilibrium concentration of hydrogen atoms. (From Ref. 113)

3.3 Hydroxyl Radicals

The hydroxyl radical is important in combustion because it participates in the chain propagating reaction

$$OH + H_2 \rightarrow H_2O + H \qquad (13)$$

Therefore, OH is important because it produces hydrogen atoms. However, some investigators have suggested that OH may be more effective in enhancing combustion than hydrogen atoms. Mittinti and Dabora[8] investigated the ignition of lean methane-air mixtures in a bomb. The igniter was a pulsed plasma torch operated with various feedstocks. An index of combustion, representing a normalized average rate of energy release, was used to determine effectiveness. A torch feedstock consisting of a mixture of methane, oxygen and nitrogen dioxide ($CH_4 + 6O_2 + NO_2$) was found to yield a higher index of combustion than a methane-oxygen mixture ($CH_4 + 7O_2$) or pure methane. The authors attributed the increase in effectiveness to the presence of OH radicals in the torch exhaust. However, the NO_2 must have participated, since the index of combustion using $CH_4 + 7O_2$ was only comparable to and in some cases less than that found with pure methane. (NO_2 has been shown to be effective in reducing the ignition delay time of methane-air mixtures.[117-118]) In a later study, Mittinti and Dabora[9] reported results from another ignition study in which a flame jet igniter (chemical torch) was tested. The medium for the igniter was a stoichiometric mixture of hydrogen and oxygen. Again using the index of combustion, they found the flame jet igniter

to be comparable to or slightly better than the plasma torch with $CH_4 + 6O_2 + NO_2$ injection. As in the plasma torch tests, OH was proposed to be responsible for the improved flame propagation, but no further explantation of the kinetic mechanism was given.

3.4 Nitrogen Atoms

Harrison and Weinberg[101] have investigated the use of nitrogen atoms for ignition and stabilization of methane-air flames. The investigators demonstrated that, by adding 10 percent of the total chemical energy by means of electrical input to an argon-nitrogen plasma, it was possible to increase the fuel-air mixture flowrate at blowoff by 700 percent. The combustion enhancement was shown not to be the result of a thermal effect. This investigation will be discussed further in Section 4.2. For hydrocarbons, Hilliard[120] has suggested that nitrogen atoms react with hydrocarbon fragments to produce HCN and hydrogen atoms.

$$CH_n + N \rightarrow HCN + H \qquad (20)$$

The HCN quickly oxidizes to form NO. If this mechanism is correct, nitrogen atoms are effective because they result in the production of hydrogen atoms. Hilliard has presented experimental evidence to support this hypothesis. Furthermore, Hilliard has suggested that nitrogen atoms may be more effective than hydrogen atoms for systems which are mixing controlled because the nitrogen atoms survive longer.

3.5 Analytical Investigation

From the previous discussion it is clear that there is no agreement on which radical species is rate-limiting. All four radicals have been effectively demonstrated as chain initiators. For this reason, an analytical study of the importance of H, O, N and OH on the combustion of hydrogen and air was conducted using a finite-rate chemical kinetics computer code. The hydrogen-air reaction was modeled by 60 equations involving 20 species. The chemical reactions and the associated rate data for this model are presented in Table I. Rogers and Schexnayder[92] have demonstrated excellent agreement between the ignition delay times calculated by this model and experimental data from shock tubes for atmospheric pressure. For the current investigation, the ignition delay time was calculated for a stoichiometric mixture of hydrogen and air at atmospheric pressure. The effect of radicals was investigated by replacing small amounts of the fuel (0.5, 1.0, and 2.0 percent by weight) with radicals. The results of this calculation for hydrogen atom addition are presented in Fig. 5. For temperatures below 2000 R, 0.1 percent hydrogen atoms reduce the calculated ignition delay time by a factor of 2, and the effect becomes more pronounced at lower temperatures. Similar results were obtained for small additions of O, N, and OH. Therefore, from finite-rate chemical kinetics calculations, H, O, N, or OH are all effective in reducing the ignition delay time of hydrogen-air mixtures.

TABLE I.- HYDROGEN-AIR-REACTION MODEL WITH THIRD-BODY EFFICIENCIES*

[Rate constant is given by $k = AT^N \exp(-\text{Activation energy}/1.987T)$]

REACTION NUMBER	REACTION	REACTION RATE VARIABLES A	N	ACTIVATION ENERGY
1	M + 1*O2 = 1*O + 1*O	.72000E+19	-1.0000	117908.00
2	M + 1*H2 = 1*H + 1*H	.55000E+19	-1.0000	103298.00
3	M + 1*H2O = 1*H + 1*OH	.52000E+22	-1.5000	118000.00
4	1*H + 1*O2 = 1*HO2 + M	.23000E+16	0.0000	-800.00
5	M + 1*NO2 = 1*NO + 1*O	.11000E+17	0.0000	64995.00
6	M + 1*NO = 1*N + 1*O	.41000E+19	-1.0000	149680.00
7	1*O + 1*CO = 1*CO2 + M	.30000E+15	0.0000	3000.00
8	1*H + 1*NO = 1*HNO + M	.54000E+16	0.0000	-596.10
9	M + 1*H2O2 = 1*OH + 1*OH	.12000E+18	0.0000	45500.00
10	1*OH + 1*NO = 1*HNO2 + M	.80000E+16	0.0000	-1987.00
11	1*OH + 1*NO2 = 1*HNO3 + M	.13000E+17	0.0000	-2200.00
12	M + 1*O3 = 1*O2 + 1*O	.13000E+22	-2.0000	25433.00
13	M + 1*HCO = 1*CO + 1*H	.20000E+13	.5000	27400.00
14	1*O + 1*H = 1*OH + M	.71000E+19	-1.0000	0.00
15	1*H2O + 1*O = 1*OH + 1*OH	.58000E+14	0.0000	18000.00
16	1*H2 + 1*OH = 1*H2O + 1*H	.20000E+14	0.0000	5166.00
17	1*O2 + 1*H = 1*OH + 1*O	.22000E+15	0.0000	16800.00
18	1*H2 + 1*O = 1*OH + 1*H	.75000E+14	0.0000	11099.00
19	1*H2 + 1*O2 = 1*OH + 1*OH	.10000E+14	0.0000	43000.00
20	1*H + 1*HO2 = 1*H2 + 1*O2	.24000E+14	0.0000	695.00
21	1*H2 + 1*O2 = 1*H2O + 1*O	.41000E+14	0.0000	50470.00
22	1*H + 1*HO2 = 1*OH + 1*OH	.24000E+15	0.0000	1887.00
23	1*H2O + 1*O = 1*H + 1*HO2	.58000E+12	.5000	57000.00
24	1*O + 1*HO2 = 1*OH + 1*O2	.50000E+14	0.0000	1000.00
25	1*OH + 1*HO2 = 1*O2 + 1*H2O	.30000E+14	0.0000	0.00
26	1*H2 + 1*HO2 = 1*H2O + 1*OH	.20000E+14	0.0000	25000.00
27	1*HO2 + 1*H2 = 1*H + 1*H2O2	.73000E+12	0.0000	18677.00
28	1*H2O2 + 1*H = 1*OH + 1*H2O	.32000E+15	0.0000	8950.00
29	1*HO2 + 1*OH = 1*O + 1*H2O2	.52000E+11	.5000	21062.00
30	1*HO2 + 1*H2O = 1*OH + 1*H2O2	.28000E+14	0.0000	32785.00
31	1*HO2 + 1*HO2 = 1*H2O2 + 1*O2	.20000E+13	0.0000	0.00
32	1*O + 1*O3 = 1*O2 + 1*O2	.10000E+14	0.0000	4790.00
33	1*O3 + 1*NO = 1*NO2 + 1*O2	.54000E+12	0.0000	2384.00
34	1*O3 + 1*H = 1*OH + 1*O2	.70000E+14	0.0000	1113.00
35	1*O3 + 1*OH = 1*O2 + 1*HO2	.90000E+12	0.0000	1987.00
36	1*O + 1*N2 = 1*NO + 1*N	.50000E+14	0.0000	75386.00
37	1*H + 1*NO = 1*OH + 1*N	.17000E+15	0.0000	48681.00
38	1*O + 1*NO = 1*O2 + 1*N	.15000E+10	1.0000	38746.00
39	1*NO2 + 1*H = 1*NO + 1*OH	.35000E+15	0.0000	1470.00
40	1*NO2 + 1*O = 1*NO + 1*O2	.10000E+14	0.0000	600.00
41	1*NO2 + 1*H2 = 1*HNO2 + 1*H	.24000E+14	0.0000	29000.00
42	1*NO2 + 1*NO = 1*NO2 + 1*OH	.36000E+13	.5000	2400.00
43	1*NO2 + 1*H2O = 1*HNO2 + 1*OH	.32000E+13	0.0000	43714.00
44	1*NO2 + 1*OH = 1*HNO2 + 1*O	.21000E+13	0.0000	24996.00
45	1*CO + 1*OH = 1*CO2 + 1*H	.70000E+12	0.0000	1987.00
46	1*CO2 + 1*O = 1*O2 + 1*CO	.25000E+12	.5000	55040.00
47	1*H2O + 1*CO = 1*HCO + 1*OH	.65000E+14	.3000	103026.00
48	1*OH + 1*CO = 1*HCO + 1*O	.58000E+13	.3200	86295.00
49	1*H2 + 1*CO = 1*HCO + 1*H	.12000E+14	.2900	85242.00
50	1*HO2 + 1*CO = 1*CO2 + 1*OH	.15000E+15	0.0000	23645.00
51	1*HNO + 1*H = 1*H2 + 1*NO	.48000E+13	0.0000	0.00
52	1*HNO + 1*OH = 1*H2O + 1*NO	.36000E+14	0.0000	0.00
53	1*NO + 1*CO = 1*CO2 + 1*N	.46000E+09	.5000	23983.00
54	1*NO2 + 1*CO = 1*NO + 1*CO2	.10000E+13	0.0000	27600.00
55	1*NO + 1*HO2 = 1*HNO + 1*O2	.72000E+11	.5000	10928.00
56	1*HNO + 1*O = 1*NO + 1*OH	.50000E+12	.5000	0.00
57	1*HNO3 + 1*O = 1*HO2 + 1*NO2	.10000E+12	0.0000	0.00
58	1*HO2 + 1*NO2 = 1*HNO2 + 1*O2	.20000E+12	0.0000	0.00
59	1*HCO + 1*O2 = 1*CO + 1*HO2	.10000E+12	.5000	5400.00
60	1*O3 + 1*HO2 = 2*O2 + 1*OH	.10000E+12	0.0000	2800.00

ALL THIRD BODY RATIOS ARE 1.0 EXCEPT THE FOLLOWING

M(O2	, 1) =	4.00000	M(O2	,12) =	1.50000	M(O	, 1) =	10.00000	M(H2	, 2) =	2.00000
M(H2	, 4) =	2.00000	M(H	, 2) =	5.00000	M(H2O	, 1) =	2.00000	M(H2O	, 2) =	8.00000
M(H2O	, 3) =	6.00000	M(H2O	, 4) =	13.00000	M(H2O	, 8) =	3.00000	M(H2O	, 9) =	6.00000

* From Reference 92

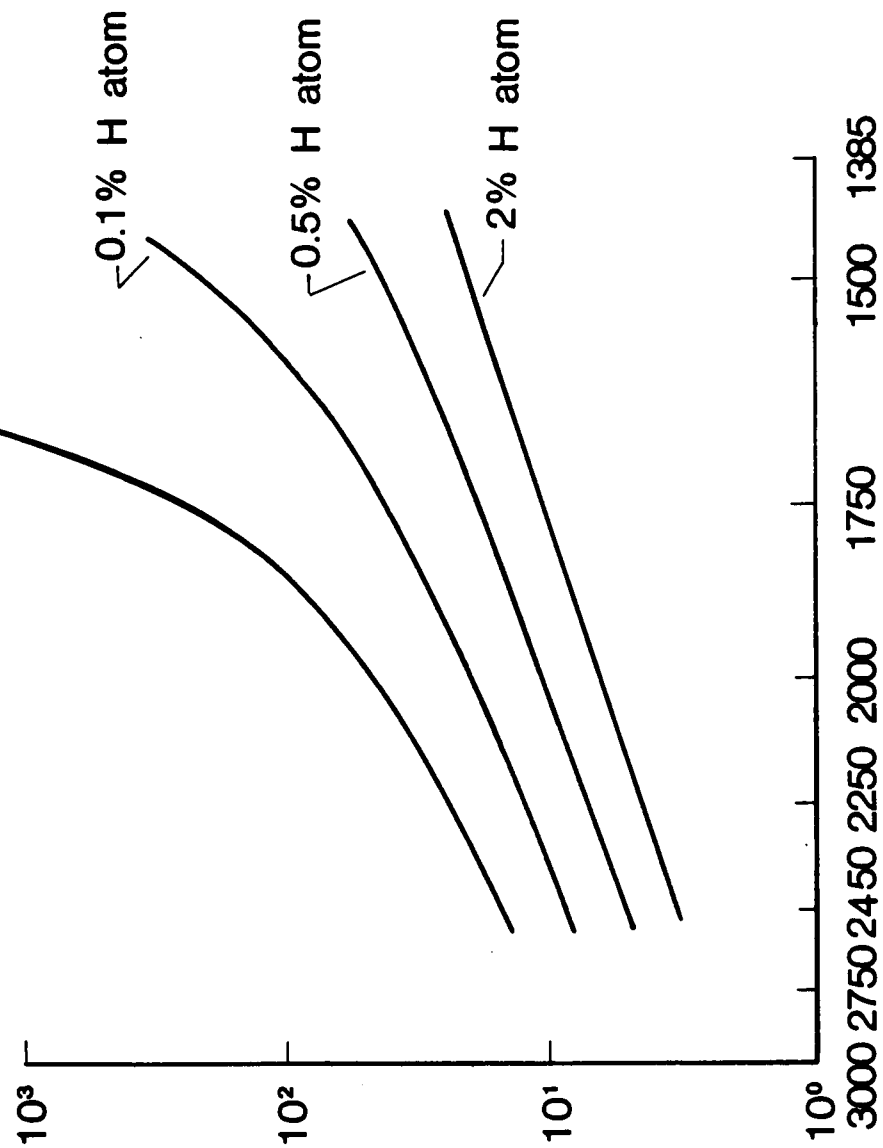

Fig. 5. Calculated ignition delay times. (stoichiometric H_2 - air @ 1 atm.)

Hydrogen atoms were used in the current experimental investigation because they are directly involved in a chain branching reaction and because the results of the investigation on inhibited flames[115] indicated that the hydrogen atom concentration is reduced in inhibited flames while the concentrations of O and OH are unaffected.

The energy to dissociate molecular hydrogen may be introduced by several means, including lasers, microwaves, glow discharges or arc discharges. For the supersonic flows of interest in this study, the hydrogen atom generator was required to operate continuously. This constraint ruled out the use of a laser, since lasers of sufficient power to cause hydrogen dissociation are pulsed devices. A second constraint on the hydrogen atom source was that it be suitable for operation at pressures in excess of atmospheric pressure. This requirement resulted from the need to inject the hydrogen atoms into a supersonic combustor with a static pressure of approximately one atmosphere. Practical application of this technique in scramjet engines may be at different pressures. However, high speed flight at low or medium altitudes will produce combustor pressures on the order of one atmosphere. Although microwave techniques and glow discharges are commonly used to generate plasmas at sub-atmospheric pressures, they are not generally useful at pressures greater than one atmosphere. Ziegler et al.[121] have reported ignition studies of lean quiescent methane-air mixtures at a pressure of approximately 2 atmospheres with a pulsed glow discharge. However, the author is unaware of any devices developed to establish and maintain glow discharges in noncombustible flow at pressures above one atmosphere. For high altitude

flight applications (100,000 feet and above), the glow discharge or the microwave technique may be applicable.

Because of these constraints, an arc discharge was used in the present research as the method to generate atomic hydrogen. A device which uses an arc discharge to dissociate and ionize a gas is referred to as a plasma torch. The next chapter describes the physics of an arc discharge and the use of plasma torches in combustion enhancement.

4. ELECTRIC ARC HIGH PRESSURE TORCHES

4.1 Plasma Physics Review

The mixture of ions, electrons and neutral particles formed as a gas passes through an electric arc is referred to as a plasma. The device which uses an electric arc to generate a plasma is referred to as a plasma torch. A schematic of a commercial plasma torch is shown in Fig. 6. The plasma torch consists of a cathode and an anode. Some plasma torches, such as the one shown in Fig. 6, are water cooled. The gas (feedstock) is introduced through the body of the torch, flows through the arc and exits through the anode. The plasma region may be divided into two parts: the arc region and the recombining region. (See Fig. 6.) In the arc region the gas is ionized and, in the case of diatomic gases, dissociated by Joule heating as a result of the electric current flowing through the gas. In the jet downstream of the anode the plasma recombines. For atmospheric pressure plasmas the arc is a very narrow region of extremely hot gas which forms between two localized spots on the electrodes. Because the arc is narrow, much of the feedstock does not pass through the arc. In most plasma torches the arc is forced to rotate in an attempt to uniformly distribute the energy throughout the gas. The arc may be caused to rotate either by swirling the gas flow as it enters the torch or by applying an external magnetic field.

A brief review of the physics of gaseous electrical discharges will now be presented. For more detailed information, refer to

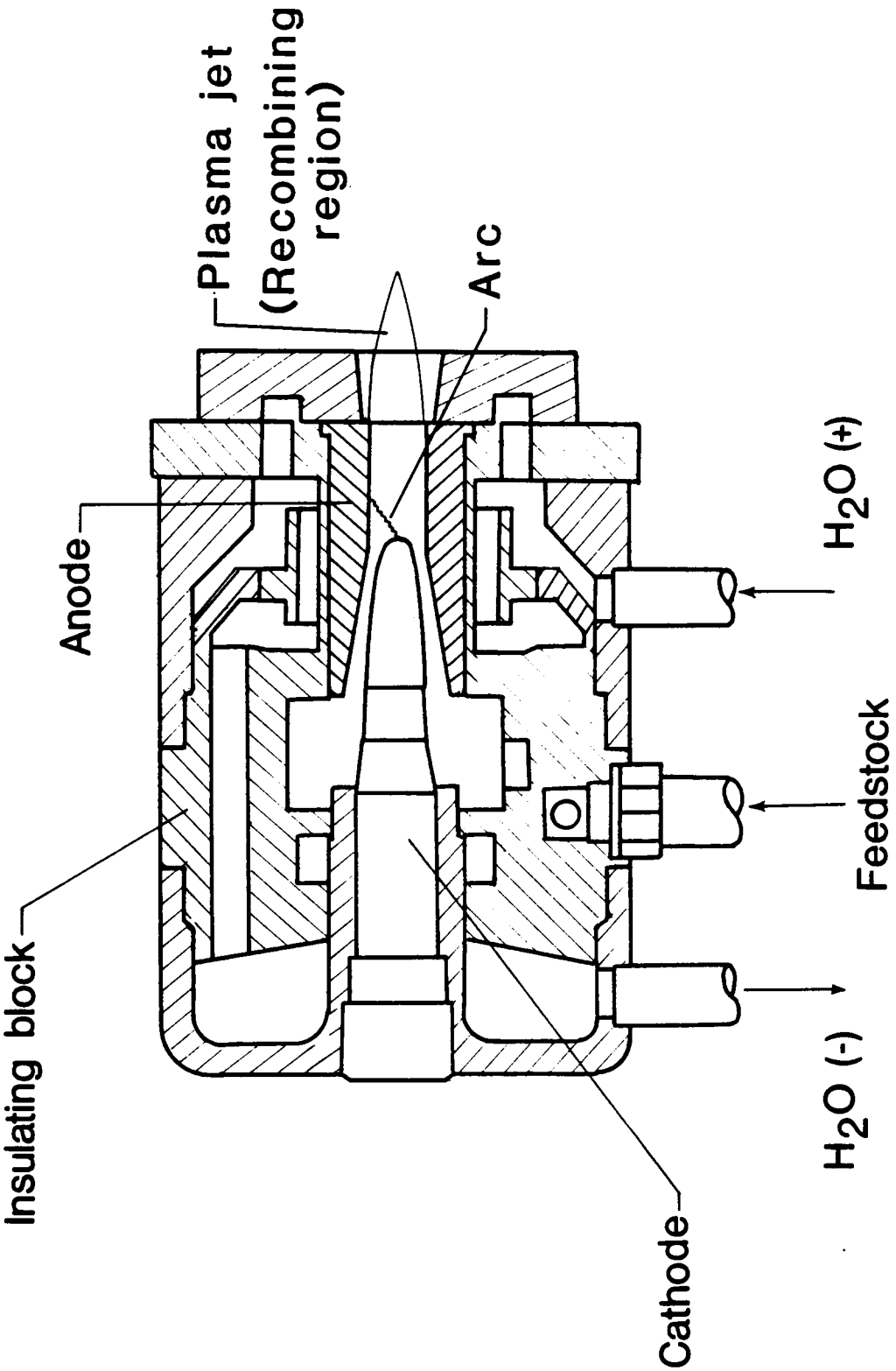

Fig. 6. Schematic of commercial plasma torch.

Cobine,[122] Finkelnburg and Maecker,[123] Pfender,[124] or Hoyaux.[125] As previously stated, the plasma formed in a gaseous electric discharge is composed of ions, electrons and neutral particles. A plasma is electrically neutral on a macroscopic scale. Many types of gaseous electric discharges are possible, for example arc discharges, glow discharges and Townsend discharges. All except the arc discharge are difficult or impossible to maintain in gases at pressures at or above one atmosphere. Since the device used in this research was required to operate at a pressure of approximately 2 atmospheres, an arc discharge was used. Arc discharges are characterized by high currents (> 0.1 amp) and low voltages (< 1000 volts). Either AC or DC power may be used to energize the arc.

A homogeneous plasma is said to be in a state of complete thermodynamic equilibrium (CTE) when one temperature describes all forms of energy distribution:

> the velocity distribution functions for all particles follow a Maxwell-Boltzmann distribution;
>
> the population density of all excited states follows a Boltzmann distribution;
>
> the particle densities are described by the Saha equation;
>
> the electromagnetic radiation field is described by the Planck function (blackbody radiation).

These criteria can never be satisfied in laboratory plasma jets because to do so would require that the plasma be contained in a cavity held at the plasma temperature. For this reason the concept of local thermodynamic equilibrium (LTE) has been introduced, in which the blackbody radiation condition is no longer required. However, LTE does require

that a single temperature can be used in the Boltzmann, Maxwell and Saha equations to describe the population and velocity distributions. The value of electron density required to establish LTE in plasma jets has not been determined definitively (see Ref. 124). For the current investigation, LTE was assumed for plasmas with electron densities in excess of 10^{15} cm^{-3}.

If local thermodynamic equilibrium may be assumed, the composition of a homogeneous plasma is defined by a system of simultaneous nonlinear equations. The equations for a diatomic gas or a mixture of a diatomic and monatomic gas are:

Conservation of mass

$$n_a = \sum_r n_{a,r} \tag{21}$$

where n_a = total number density of particles of species a

$n_{a,r}$ = number density of atoms or ions of species a in ionization level r

Conservation of charge (quasineutrality condition)

$$n_e = \sum_{r,a} r n_{a,r} \tag{22}$$

where n_e = electron number density

and the summation is over all ionization levels, r, of all species, a.

Law of mass action

(a) for ionization

$$\frac{n_{a,r+1} n_e}{n_{a,r}} = \frac{2Z_{a,r+1}}{Z_{a,r}} \frac{(2\pi m_e kT)^{3/2}}{h^3} \exp -\left(\frac{E_{a,r+1} - \Delta E_{a,r+1}}{kT}\right) \tag{23}$$

where $Z_{a,r}$ = partition function of species a in ionization level r

$Z_{a,r+1}$ = partition function of species a in ionization level r+1

$E_{a,r+1}$ = ionization energy for the levels r to r+1 in species a

$\Delta E_{a,r+1}$ = lowering of the ionization energy due to Coulomb interaction of charged particles

(b) for dissociation

$$\frac{n_a^2}{n_{aa}} = \frac{Z_a^2}{Z_{aa}} \frac{(m_a \pi kT)^{3/2}}{h^3} \exp\left(\frac{-u_{aa}}{kT}\right) \tag{24}$$

where n_{aa} = number density of diatomic molecules

u_{aa} = dissociation energy.

The plasma composition may be calculated by either solving this set of simultaneous nonlinear equations or by minimizing the Gibbs free energy for the equilibrium components of the plasma. This situation is comparable to thermochemistry.[126] Both methods require the calculation of partition functions and the determination of the lowering of the ionization energy. Neither method is as easy as it may appear. Patch[127] has calculated the composition of a hydrogen plasma by the method of minimzing the Gibbs free energy. Capitelli et al.[128] has computed the composition of plasmas composed of various mixtures of argon and hydrogen.

4.2 Review of Combustion Enhancement by Plasma Torches

The use of plasma torches in combustion research evolved from work in electrically augmented flames.[129-131] The flameholding potential of a plasma torch was first recognized by Harrison and Weinberg,[118] who

used a plasma torch to stabilize methane-air flames in a flame tube. As previously mentioned, Harrison and Weinberg found that a 700 percent increase in reactant flow rate at blowoff could be realized by adding 10 percent of the total chemical energy to a plasma torch supplied with an argon-nitrogen feedstock. This result was surprising because the 10 percent energy increase would only increase the flame temperature by 209 R. Based on this flame temperature increase, the throughput, as predicted by a perfectly stirred reactor model, could only be increased by 50 percent. This result led the investigators to propose that the observed increase in throughput was not due to a thermal effect but was the result of radicals which were generated by the small electrical input into the plasma torch feedstock.

The ignition capabilities of a plasma torch were first demonstrated by Waterson[132] in his doctoral research on internal combustion engine ignition sources. Waterson used a pulsed plasma device made from a modified spark plug.

Hilliard and Weinberg[133] studied plasma jet ignition of propane-air mixtures flowing in a flame tube. They found that a small plasma torch operated on nitrogen had two beneficial characteristics: operation of the torch could produce flameholding in very lean mixtures and could reduce the amounts of soot and nitrous oxide in the combustion products. A test in the exhaust of an internal combustion engine demonstrated that a plasma torch could reduce NO pollution in practice.

Based on these findings, research into combustion applications of plasma torches has progressed along two paths: one involving continuous plasma torches and one involving pulsed plasma torches. The pulsed

plasma torch has drawn the interest of the automotive industry as an alternative to spark plugs because of the demonstrated ability to ignite lean mixtures and reduce pollution. The incentive provided by this potentially large application has resulted in pulsed plasma torches receiving more attention than continuous plasma torches. A brief review of combustion enhancement research involving both pulsed and continuous plasma torches has been published by Weinberg.[5] Clements[6] has reviewed ignition by pulsed plasma jets. The present review will focus on the use of a plasma torch as a source of radicals for combustion enhancement. The fluid dynamic or turbulence effects of plasma torches will not be discussed in detail.

4.2.1 Pulsed Plasma Torches

Weinberg et al.[134] studied the ignition characteristics of various fuels using as an igniter a pulsed plasma torch the size of a typical spark plug. The design is shown in Fig. 7. The tests were conducted in a bomb containing 5 percent by volume methane in air. Hydrogen, nitrogen, water, methane, or a methane-air mixture were used as torch feedstocks. Methane was the most effective feedstock, producing in usually nonflammable mixtures flame speeds almost equal to those in stoichiometric mixtures. The authors postulated that hydrogen atoms were responsible for the observed increase in flame speed. They further postulated that methane was more effective than hydrogen because methane provided more hydrogen atoms for a plug chamber of a given volume.

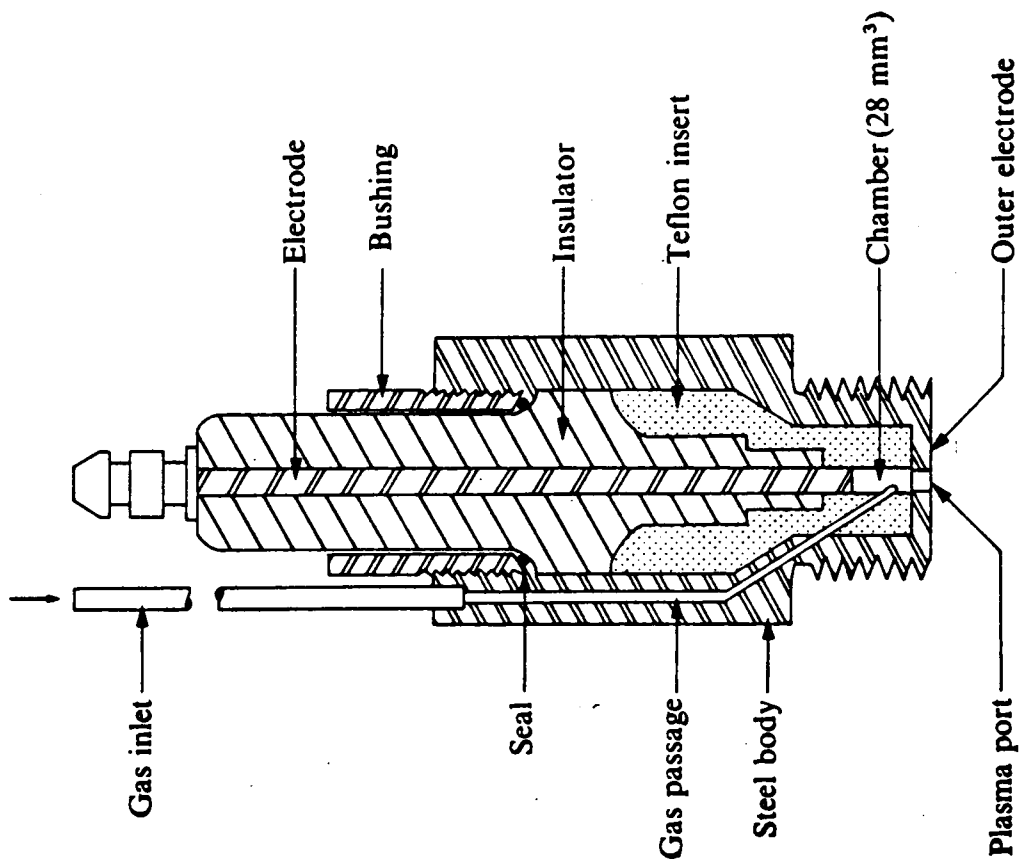

Fig. 7. Schematic of pulsed plasma jet. (From Ref. 134)

Several investigations have focused on the mechanisms responsible for the enhanced ignition and flameholding characteristics of pulsed plasma jets. Orrin, Vince and Weinberg[135] investigated the effects of radiation from a pulsed spark-plug-size plasma torch. They concluded that, at the low energies used in small plasma torches, the emitted radiation had no significant macroscopic effects. However, they noted that it was impossible to determine any localized, microscopic radiation effects which might occur as a plasma is mixed with a combustible mixture.

The same group of investigators studied the fluid mechanical and chemical effects of pulsed plasma jets.[136] Using several different designs of pulsed plasma plugs, the authors found that fuel-air mixtures below the lean flammability limit could be ignited and burned with a flame speed approaching that of a stoichiometric mixture. They also observed that the greatly increased flame speed persisted for milliseconds. Torches fed with liquids including alkanes, alcohols, carboxilic acids, aldehydes, benzene and derivatives, solutions of $LiAlH_4$, water and dichloroethane were just as effective as hydrogen or methane plasmas. The authors postulated that hydrogen, methane and the liquids provided an excess of hydrogen atoms, so that ignition was controlled by other factors. The authors also noted that an argon plasma was a very poor ignition source. An analytical model of plasma-enhanced combustion developed by Westbrook was also presented in this paper. The model was based on chemical kinetics calculations. Plasma injection was modeled by increasing the hydrogen atom concentration above what would be present in equilibrium at the flame temperature. The trends

demonstrated by the results of the calculations were similar to the experimental findings.

Carleton, Vince and Weinberg[137] studied energy and radical losses from pulsed plasma jets. They noted that, when the plasma medium contained hydrogen atoms, the combustion limits of unsaturated hydrocarbons could be extended further than the limits of saturated hydrocarbons. Because the unsaturated hydrocarbons have fewer hydrogen atoms, the authors proposed that hydrogen atoms were responsible for the enhancement. Radical losses to surfaces external to the plasma jet were also studied. The effectiveness of the plasma torch was hindered by the presence of surfaces within 1.2 inches of the torch exit. Therefore, the authors concluded that free radicals were present in the plasma for a minimum of 1.2 inches downstream of the torch.

Klein, Carleton and Weinberg[138] used pulsed plasma torches to investigate ignition stimuli of liquid propellants. Ignition of mixtures containing water and hydroxylammonium nitrate was studied using Schlieren, shadow and streak photography. The plume exiting the torch showed strong temperature variations, indicating the existence of hot pockets of gas. The input energy was too small to cause ignition if it had been uniformly distributed as thermal energy. The authors proposed that ion transport was responsible for ignition.

Clements et al.[139] studied the transport processes in the discharge of a pulsed plasma jet. Nitrogen was used as the feedstock. A Mach-Zehnder interferometer was used to measure the local gas density, from which the temperature was calculated. The velocity was measured by two means: a hot wire anemometer and a Schlieren image of a freon jet

deflected by the exhaust of the plasma torch. The deflection of the freon jet was calibrated using flows of known velocity. A determination of the concentration of nitrogen atoms was made by reacting the exhaust from the plasma torch with oxygen and then measuring the amount of nitric oxide in the products. Nitric oxide is formed by the reaction

$$N + O_2 \rightarrow NO + O \qquad (25)$$

The same experiment was repeated with a matrix of small tubes placed at various distances downstream of the torch in order to estimate the distance that the nitrogen atoms survived downstream of the torch. The purpose of the tubes was to quench any radicals present at that point. From this set of experiments it was determined that the exhaust from the pulsed plasma torch being studied had an average temperature of approximately 700°F, a velocity of 33 ft/s, a concentration of nitrogen atoms above what would be predicted by equilibrium calculations (no numerical values of atomic concentration were given), and the atoms survived for more than one inch downstream of the torch exit. The authors concluded that the free radicals generated by the plasma torch were responsible for ignition, since the measured temperature was much too low for thermal ignition.

Vince, Vovelle and Weinberg[140] studied the effects of a pulsed plasma torch on rich mixtures of ethylene and oxygen. The investigators first used an oxygen feedstock in the pulsed torch, believing that the formation of oxygen atoms was the rate-controlling step for ignition of a rich mixture. Hydrogen was also tested as a feedstock. However, further experiments indicated that a plasma torch fed with a mixture of

ethylene and oxygen created the largest increase in the rich limit of flammability. This result implied that, at least for rich mixtures, neither hydrogen atoms nor oxygen atoms are the most effective radical when used separately. Use of the ethylene-oxygen feedstock also increased the propagation rate and reduced the amount of soot formed. In fact, the increase in propagation rate was inversely proportional to the decrease in soot formation. As had previously been reported by Weinberg et al.[134] and Carleton et al.[137], Vince, Vovelle and Weinberg found that an increase in input power increased the flammability limit but had no effect on propagation rate or the amount of soot formed. The authors also experimented with plasma torches fueled with n-heptane and ethanol.

Warris and Weinberg[141,142] conducted one of the few studies into ignition and flame stabilization by plasma torches in flowing systems. Both continuous and pulsed devices were used. The continuous device will be discussed in the next section. The pulsed plasma torch used in this study was designed around the surface discharge plugs used in gas turbine combustors. The flow system used in these experiments is shown schematically in Fig. 8. The mixing tube was 3.9 inches in diameter and 3.3 feet in length. Gaseous propane was used as the fuel. The velocities of the fuel-air mixture ranged from 16 to 98 ft/s. Ionization probes were used to document the existence and extent of the flame kernel. The plasma torch partially obstructed the premixed freestream, thereby providing a flameholder. The plasma torch was fueled with water, Avtur (jet fuel), or methanol or it was used dry with the propane-air mixture filling the cavity by diffusion. The plasma torch

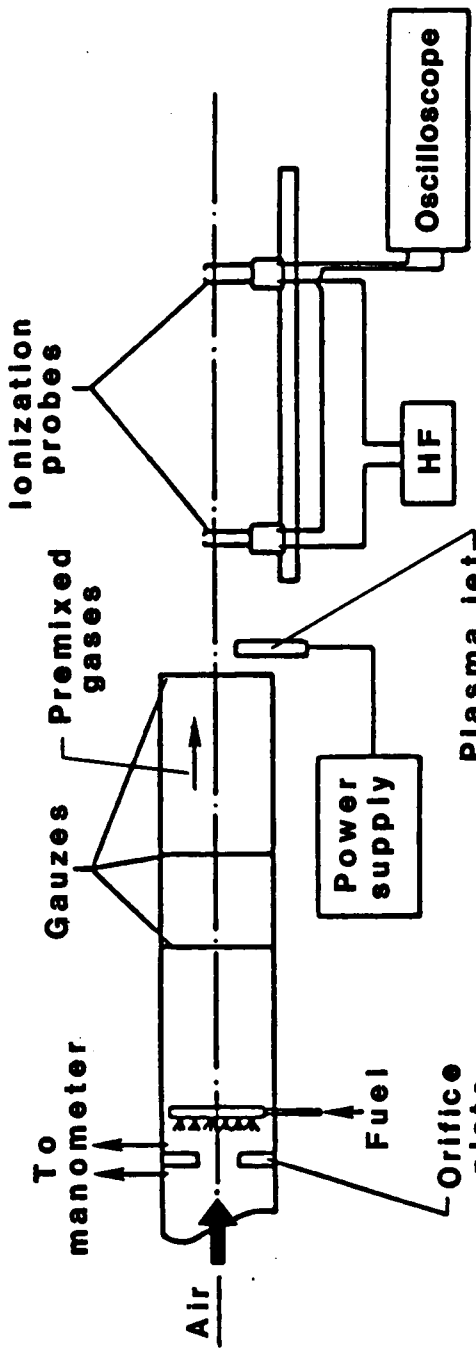

Fig. 8. Schematic of flow apparatus. (From Ref. 142)

ignited fuel-air mixtures which were below the lean limit of flammability for all feedstocks tested. The Avtur feedstock ignited the leanest mixture. The authors attributed the beneficial effects of the plasma to combustion enhancement by radicals.

Boston et al.[143] investigated ignition of lean methane-air mixtures in a bomb equipped with four high speed fans. The fans were used to create turbulence inside the bomb. Five igniters were studied: a conventional spark plug, a surface discharge plug, a plasma torch (without a separate fuel injector, hereafter referred to as a dry plasma torch), a plasma torch fueled with a liquid and a preburner. Propanol, methanol, phenol and water were used to fuel the plasma torch. The results indicated that both wet and dry plasma torches and the preburner were the most effective in a quiescent fuel-air mixture. However, when the fans were used to introduce turbulence, all five igniters had similar rates of flame propagation after the first half millisecond. The authors concluded that the enhancement created by the pulsed plasma torch was due in part to the turbulence created by the jetting action of the effluent.

As was discussed in Section 3, Mittinti and Dabora[8] found that a mixture containing nitrogen dioxide, oxygen and methane ($CH_4 + 6O_2 + NO_2$) was a more effective torch feedstock than methane. They suggested that OH radicals are more effective in reducing the ignition delay than hydrogen atoms. However, a mixture containing only methane and oxygen ($CH_4 + 7O_2$) did not work as well, indicating that the NO_2 had a significant effect.

4.2.2 Continuous Plasma Torches

Continuous plasma torches for combustion applications have been researched and developed only in the last 10 years. Although the research applications for these devices include acetylene production[144] and reduction of soot and other pollutants,[133,140] this review will be limited to the use of plasma torches for combustion enhancement and any findings from other applications which provide an insight into the mechanisms involved.

Jagoda and Weinberg[145] used Schlieren and shadow photography and thermocouples to study the discharge of a magnetically stabilized plasma torch operating with an argon feedstock. The photographs were used to determine the velocity distribution in the plasma jet assuming axial symmetry. Local densities were then calculated from the principle of mass conservation. The results of the calculations indicated that a region existed downstream of the torch where the density actually decreased, indicating a region of heat release by reaction. The authors suggested that this result might have been caused by the recombination of hot pockets of excited or ionized gas, which would appear as a region of heat release by reaction. The region of heat release occurred farther downstream for larger gas flows (higher velocities). However, on a time scale the heat release ocurred at the same time, independent of the gas velocity.

Chan et al.[146] developed a tunable plasma torch capable of operating at power levels from 250 to 1500 W. A cross section of the torch is shown in Fig. 9. The magnetically stabilized torch operated continuously on nitrogen, hydrogen, methane, propane or ethylene. The

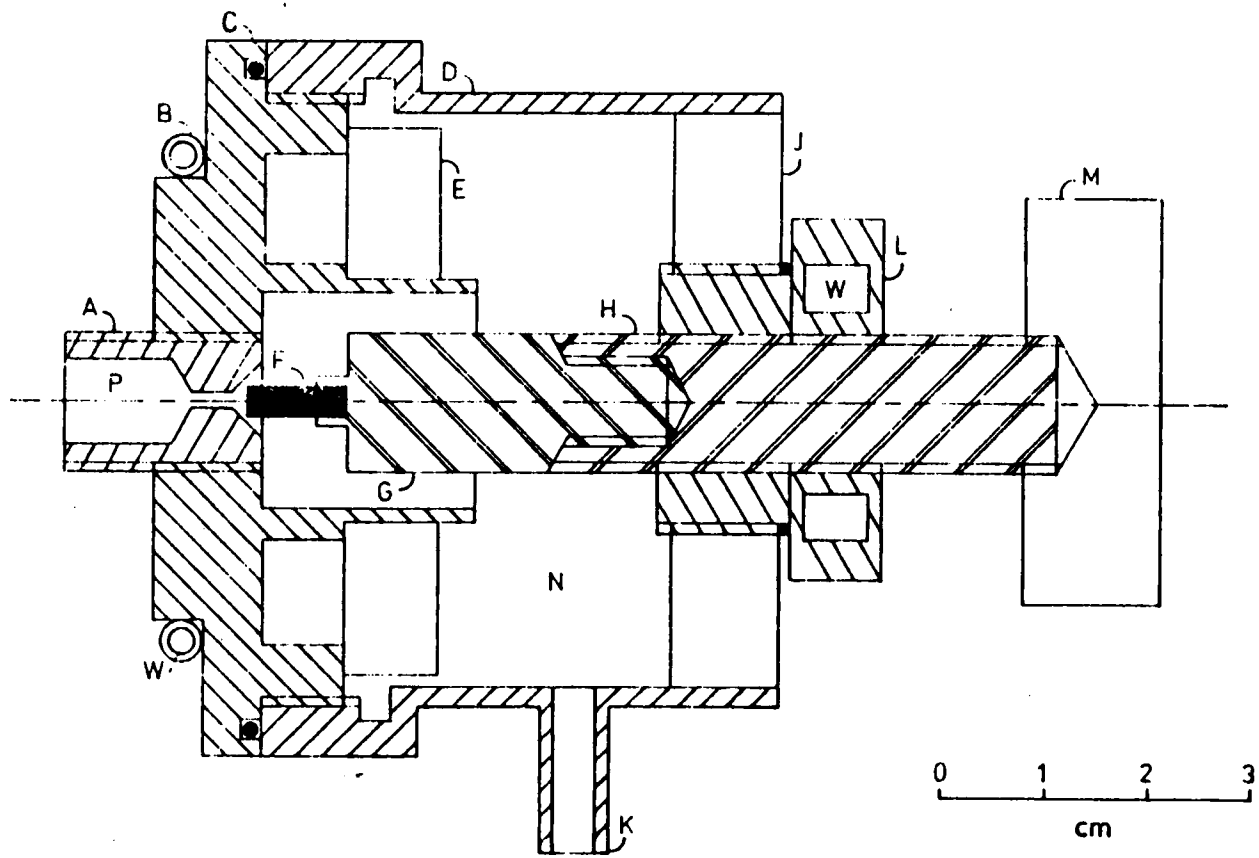

Fig. 9. Schematic of plasma torch.
A, interchangeable anode; B, cooling pipe; C, mild steel magnet support; D, brass outer casing; E, bounded-ferrite annular magnet; F, thoriated (2 percent) tungsten cathode; G, mild steel focusing cathode support; H, arc tuning component; J, Perspex insulating plate; K, feedstock inlet; L, water-cooled tuning component support; M, tuning knob; N, upstream pressure region (p_1); P, downstream pressure region (p_2); W, water cooling. (From Ref. 146)

only reported data were for nitrogen feedstocks. The torch reportedly produced 10^{20} to 10^{21} nitrogen atoms per second, based on a titration experiment involving nitric oxide. The details of the titration were discussed in a paper by Behbahani et al.,[147] a review of which follows.

Behbahani et al.[147] used a titration technique to determine the quantity of nitrogen atoms in the exhaust of the nitrogen-fed plasma torch developed by Chan et al.[146] The titration technique was based on the concept that the NO molecules would react with the nitrogen atoms according to the reaction

$$N + NO \rightarrow N_2 + O \qquad (26)$$

By measuring the amount of NO leaving the reactor, it was possible to deduce the number of nitrogen atoms in the plasma on the basis of one nitrogen atom for each NO molecule removed. The amount of NO leaving the reaction chamber was determined by sampling the exhaust from the reactor exit with an $NO-NO_x$ analyzer. A schematic of the apparatus used in this titration experiment is shown in Fig. 10. The experimental efficiency was defined as the amount of energy required to produce enough nitrogen atoms from dissociation to account for the observed reduction in NO divided by the amount of input electrical energy. The experiments reported in this paper indicated an efficiency of almost 24 percent when the NO was introduced within 0.04 inches of the torch exit. Even when the NO was introduced 0.87 inches downstream of the torch exit, the efficiency was 8 percent, indicating that many of the atoms generated in the arc survived for more than 0.87 inches. The

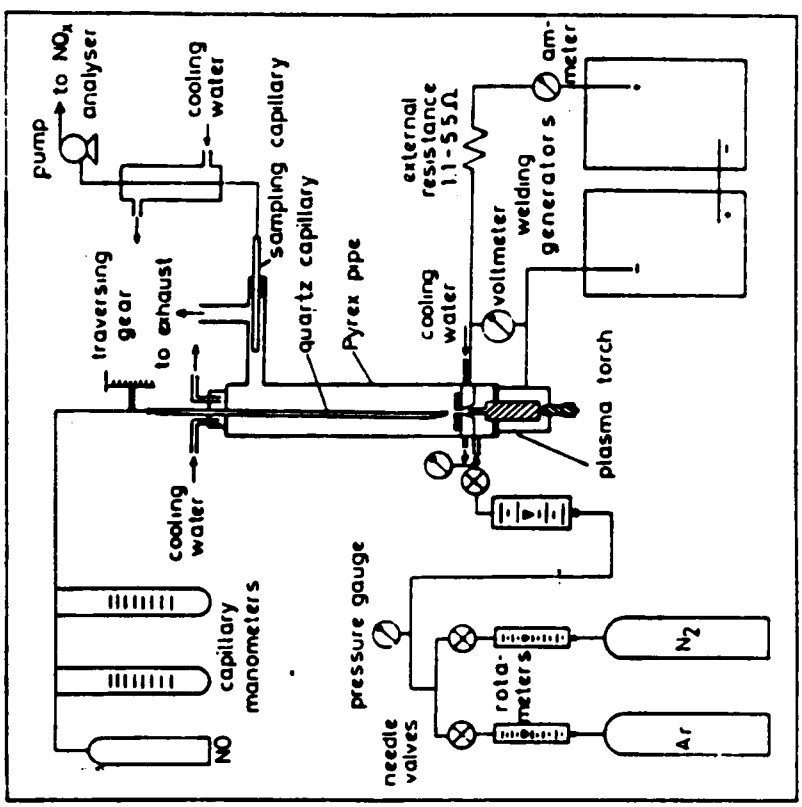

Fig. 10. Apparatus for titration of nitrogen atoms from plasma torch by NO. (From Ref. 147)

authors also considered the possibility of NO removal by excited nitrogen molecules according to the reaction

$$N_2^* + NO \rightarrow N_2 + N + O. \quad (27)$$

However, further experiments indicated that excited nitrogen molecules could not be responsible for the observed results. The authors postulated that less than 1 percent of the torch feedstock actually passed through the arc. This small amount of gas contained almost all of the input energy, causing it to have a very high temperature and therefore a significant amount of dissociation. The authors used ionization probes to test this hypothesis. With these probes the authors demonstrated that the jet from the torch contained hot pockets surrounded by relatively cool gas. The diameter of the pockets was estimated to be less than 0.1 inches. The pockets were hot spots where the atoms could survive without recombination. The investigators suggested that the destruction of the nitrogen atoms was controlled by the diffusion of nitrogen atoms out of these hot pockets.

The torch which was used in the research just described was designed with the intent of heating all of the feedstock. The uniform heating was to be accomplished by magnetically forcing the arc to rotate at a speed such that it supposedly came in contact with all the of gas. However, Behbahani et al.[147] discovered that, despite the arc rotation, most of the energy was contained in tiny hot pockets which were responsible for preserving nitrogen atoms for a considerable time. This finding led Behbahani, Warris and Weinberg[148] to design a torch in which there was no magnet to rotate the arc. The only means of arc

rotation in the new design was the swirl of the gas passing through the torch. The authors postulated that this method of aerodynamically rotating the arc would maintain the arc in contact with the same gas for a longer period of time, thereby enhancing the hot pockets and increasing the efficiency of the torch. The design for the torch was based on a spark plug and is shown in Fig. 11. The torch was operated at power levels of 400 to 1300 W with nitrogen gas flows of 22 to 38 scfh. A titration experiment similar to that of Ref. 147 was conducted. The new torch demostrated efficiencies which were slightly higher than those of the previous design. The atoms generated by the new torch survived for more than one inch. The authors also used ionization probes to study the discharge from the plasma torch. They found that the aerodynamically rotated arc produced a larger number of hot pockets with higher velocities than had been obtained with the magnetically rotated arc. The authors also found that the survival distance of the pockets increased when either the gas flow rate or the power input was increased. The frequency of occurrence of the hot pockets was found to increase only with gas velocity; it was not affected by the amount of input power. The estimated velocity of the hot pockets was ten times the velocity of the bulk gas.

As was mentioned in the section on pulsed plasma torches, Warris and Weinberg[141,142] studied ignition and flameholding in a flowing system using both pulsed and continuous plasma torches. The continuous plasma torch was similar to that used by Behbahani, Warris and Weinberg.[148] The experimental setup has already been shown in Fig. 8. The mean enthalpy of the torch exhaust was 14-19 Btu/mol, but as was

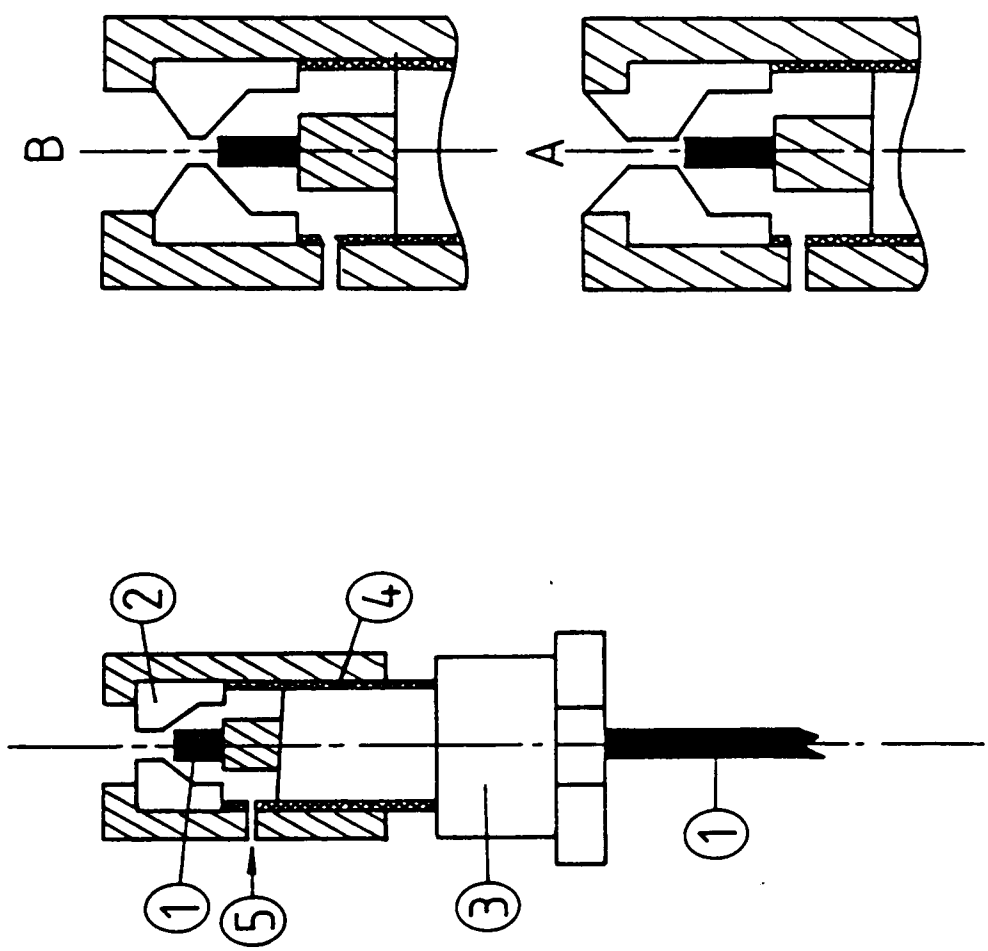

Fig. 11. Schematic of plasma torch with various anode configurations (A and B). 1. Cathode. 2. Anode. 3. Spark plug body. 4. Fine thread for gap adjustment. 5. Tangential gas inlet. (From Ref. 148)

discussed by Behbahani et al.,[147,148] the exhaust was thought to be a combination of hot pockets of reactive species in a relatively cold gas. Nitrogen and argon were the torch feedstocks. The results indicated that an argon plasma was completely ineffective. The authors noted that previous studies which had indicated a small effect from argon had used higher powers than the 1 kW used with this torch. This result was cited by the authors as evidence that this torch operated with a different mechanism, namely that a small portion of the gas was extensively heated while most of the gas remained relatively cool. The nitrogen plasma ignited flowing propane-air mixtures at equivalence ratios below the lean flammability limit for stationary mixtures. Residual flames, those flames not filling the entire flow, occurred at equivalence ratios as low as half the lean limit. The power input was on the order of 0.2 percent of the rate of chemical energy release.

Kimura and Imajo[11] designed and built an arc-heated stirred reactor to investigate the effects of a low-power arc on combustion. The arc voltage was 300 to 900 volts with currents ranging between 0.15 and 0.6 amps. The arc power ranged from 100 to 350 W. Thermocouples were used to measure the temperatures inside the reactor. Samples of the exhaust were analyzed chromatographically. The reactor was a cylinder with electrodes protruding from each end. For a lean propane-air mixture (ϕ = 0.62), the throughput could be increased over 200 percent with electrical inputs of only 4.5 to 6 percent of the chemical energy flux. Propane-air mixtures with an equivalence ratio of 0.43, which is below the lean flammability limit, were reacted with electrical inputs of only 10 percent of the chemical energy flux. The combustion efficency was

estimated to be 80 percent. The authors found that the activization energy for the case with electrical input was reduced by 50 percent from the case without electrical input. Because this low value of activization energy made the reaction virtually independent of temperature, the authors concluded that radicals from the arc were affecting the rate-limiting process of the combustion reaction. A numerical analysis involving perfectly stirred reactors indicated that a heat addition comparable to the energy dissipated in the arc could not support the large increase in throughput which was measured with the arc present.

Plasma torches have been successfully used as both ignition and flameholding sources. In general, the energy input to the plasma torch was insufficient to account for the observed results on a purely thermal basis. The beneficial effects of low-power plasmas have been attributed to the presence of radicals in the torch exhaust, since plasmas containing H, N, OH and O have been demonstrated to be more effective than argon plasmas. However, the mechanisms by which plasma torches enhance combustion are not thoroughly understood at this time.

5. SUMMARY OF PRESENT EXPERIMENT

The present experimental investigation was designed to explore the use of dissociated hydrogen from a continuous-operation plasma jet as an igniter and flameholder for supersonic combustion. All combustion tests were conducted in a Mach 2 flow in the Test Cell #2 facility of the Hypersonic Propulsion Branch of the NASA Langley Research Center. A commercially available plasma torch was used for the initial tests. The torch feedstock was a mixture of argon and hydrogen. Hydrogen was selected because of the importance of hydrogen atoms in hydrogen and hydrocarbon combustion, as was outlined in Sections 3 and 4. The argon was added to stabilize the arc and to reduce the recombination of hydrogen atoms. Argon atoms have a significantly lower efficiency for the three-body hydrogen atom recombination reaction. A limited initial test program was conducted with hydrogen, ethylene, ethane and methane fuels with torch power, air total temperature and fuel equivalence ratio as major variables. The temperature range used in these experiments was chosen to simulate the temperature in a scramjet combustor flying within a realistic flight envelope. However, the static pressure at the entrance to the test section was maintained at approximately atmospheric pressure. Some tests were also conducted to determine the effects of location of the fuel injectors with respect to the plasma torch. All injection was transverse to the airflow. The injection schemes were chosen based on the results of the literature search and the experience of NASA researchers.

Based on the excellent results obtained during the initial tests and the fact that the commercial torch was effective at its lowest stable power (2 kW), a smaller torch was developed. The new torch was designed to operate at power levels of approximately 1 kW with a 1:1 argon-hydrogen mixture. In order to obtain the maximum advantage of the low power plasma torch, a new injector scheme was designed. The fuel injector design consisted of five small upstream pilot fuel injectors, a rearward facing step for recirculation, and three main fuel injectors downstream of the step. The plasma torch was located in the recirculation region immediately downstream of the step. To determine the ignition and flameholding characteristics of the plasma torch used in conjunction with the new injector design, a series of supersonic combustion tests were conducted with hydrogen fuel. Hydrogen was selected exclusively for these tests because of its fast reaction time, high heating value and effectiveness as a heat transfer medium. Because of these characteristics, hydrogen is the ideal fuel for a reusable, non-volume-limited high-speed vehicle. Other igniters, including an argon plasma, a mixture of 20 percent by volume silane in hydrogen, and a surface discharge plug, were also tested for comparison. Shadowgraph pictures were taken to show the shock structure resulting from fuel injection with this injector configuration. Tests were also conducted on a flat plate to demonstrate that the low-power torch could ignite and flamehold without the aid of geometric flameholders. A spectroscopic investigation was conducted to demonstrate the presence of hydrogen atoms in the torch exhaust.

6. PLASMA TORCH APPARATUS AND OPERATING PROCEDURE

6.1 Plasmadyne Torch

One of the plasma torches used in this research was a commercially-available Plasmadyne SG-1B water-cooled flamespraying torch. Figure 6 shows a schematic of the plasma torch cross section. A photograph of the SG-1B torch is shown in Fig. 12. This torch was designed to operate on direct current with feedstocks of argon, hydrogen, nitrogen or mixtures of argon and either hydrogen or nitrogen. The electrodes were replaceable and were available in sets designed for use with one particular gas. In this study the torch was to be used to generate hydrogen atoms, and therefore the electrodes designed for use with hydrogen were employed almost exclusively. The cathode was thoriated tungsten. The anode was copper lined with a molybdenum sleeve. The torch was designed to operate at power levels of up to 80 kW. Two Plasmatron PS20 power supplies connected in series were used to supply 160 open circuit volts to the torch. The power was delivered to the torch through copper tubing, which was also used to carry the cooling water. The arc was initiated by a high frequency voltage inductively coupled to the DC leads. The power supplies were controlled by a Variac. A photograph of the plasma torch control panel is shown in Fig. 13.

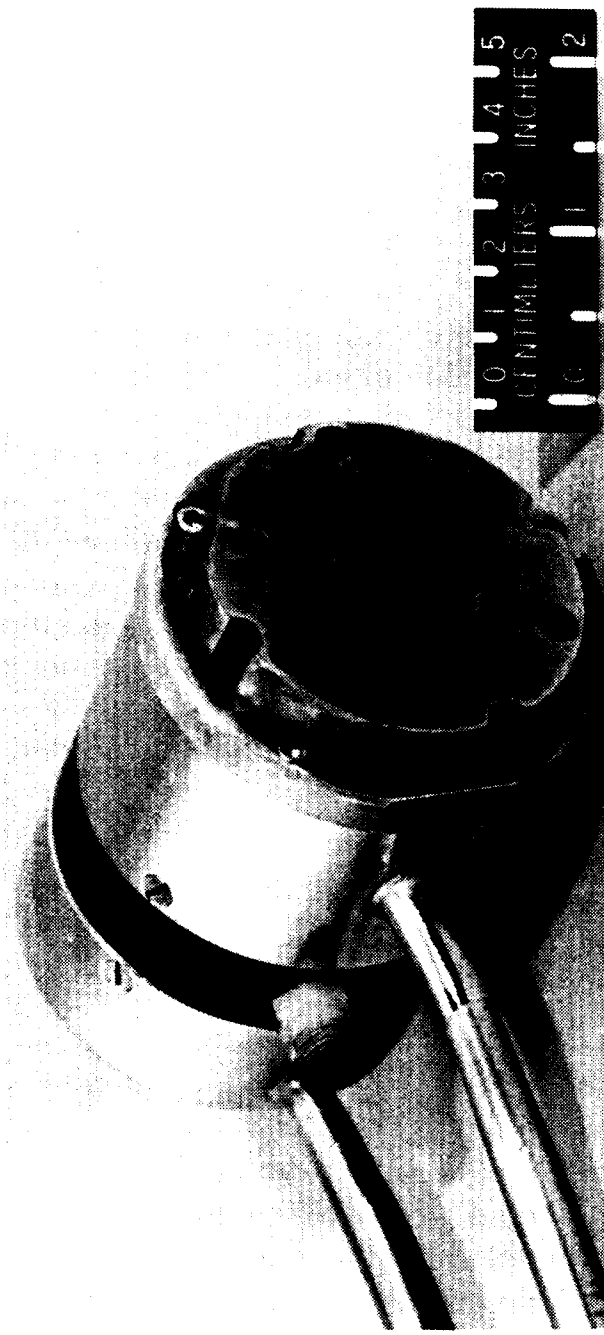

Fig. 12. Photograph of SG-1B plasma torch.

Fig. 13. Photograph of control panel.

6.2 VPI Torch

The second torch used in this research, the VPI plasma torch, was developed expressly for this research by Barbi, O'Brien, and the present author. The details of the development are given in Ref. 149. The purpose of this new torch was twofold. First, the new torch was to operate with a choked exit so that the arc would not be affected by combustion-generated pressure rises in the tunnel test section. This requirement became apparent after the initial tests with the Plasmadyne torch indicated that the pressure rise in the duct as a result of combustion would in some cases extinguish the arc. Second, the torch was designed to demonstrate the ability of a plasma torch to be an effective igniter at power levels of 1 kW or less. A photograph of the torch and a sketch of the cross section are shown in Figs. 14 and 15, respectively. The cathode was a 0.125-inch, 2 percent thoriated tungsten welding rod. The anode was a replaceable insert also made of 2 percent thoriated tungsten. Two Miller SR-150-32 power supplies were used to supply th DC power. These power supplies provided 180 open circuit volts when connected in series and were capable of operating at currents as low as 5 amperes. The arc was initiated with a high frequency voltage. The control of the Miller power supplies was similar to that of the Plasmadyne power supplies.

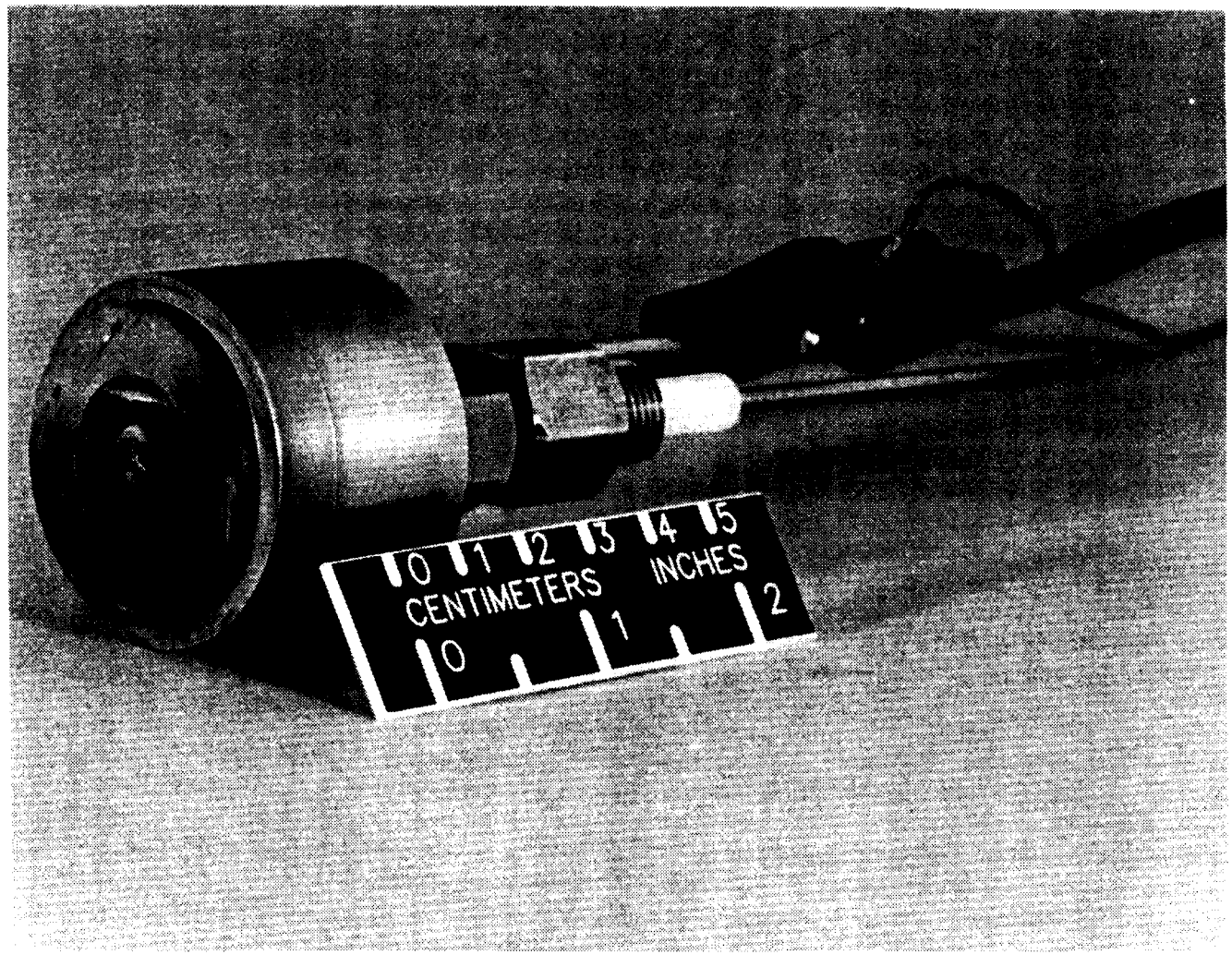

Fig. 14. Photograph of VPI plasma torch.

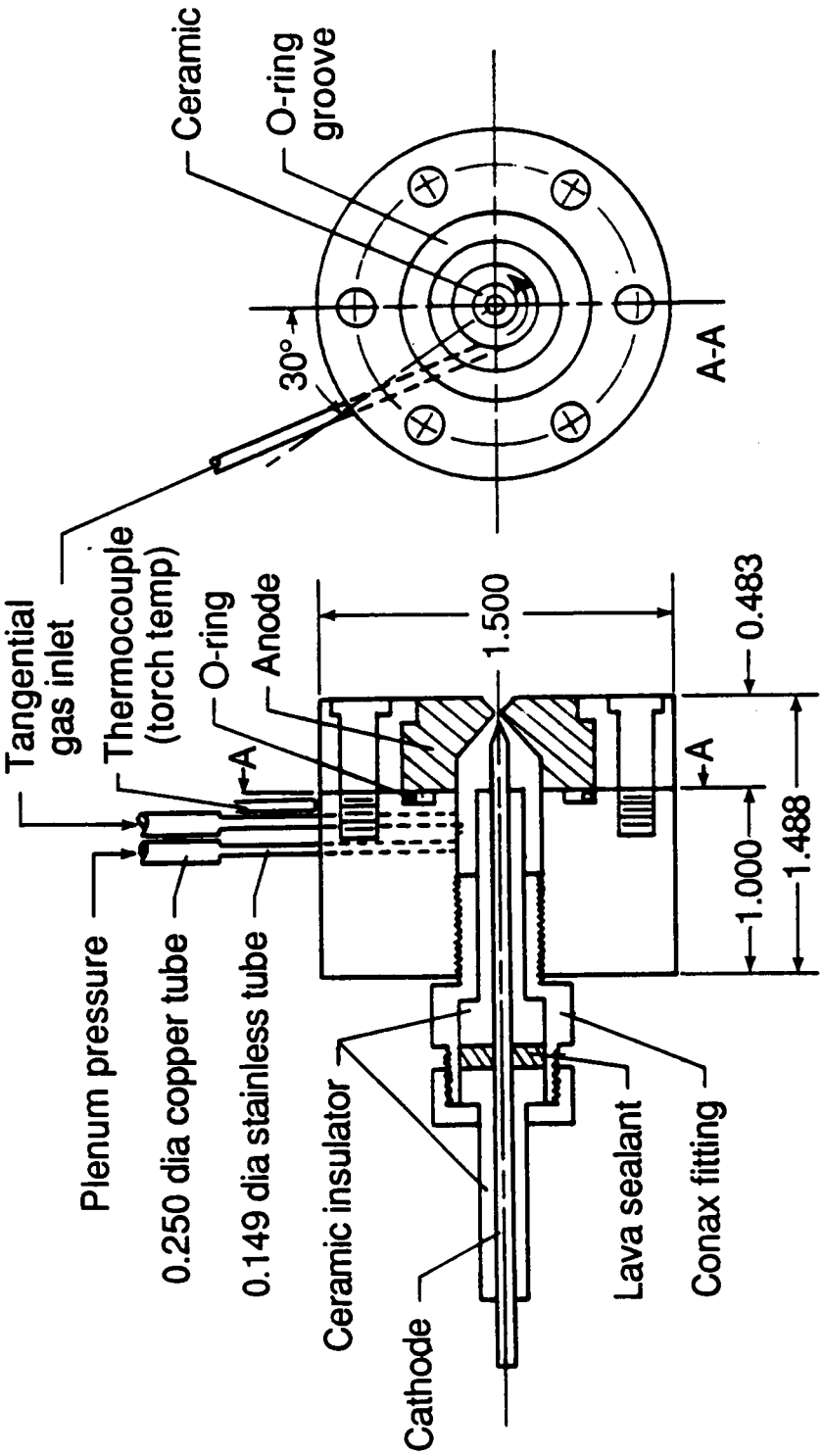

Fig. 15. VPI plasma torch design.

6.3 Plasma Torch Instrumentation

Each plasma torch was instrumented with an analog volt meter and a shunt calibrated for measuring current. Two different shunts were used. A shunt with a resistance of 5×10^{-5} ohms was used during the Plasmadyne torch tests. This shunt was replaced by a 2×10^{-3} ohm shunt for the VPI torch tests. Due to electrical noise problems induced by the presence of the arc, the voltage and current were recorded manually rather than by the data acquisition system (DAS). For the Plasmadyne torch, the cooling water temperature was measured both entering and exiting the torch using platinum resistance temperature probes (PRT's). These devices have a relatively high output of tens of millivolts. The PRT's were chosen after it was found that the electrical noise from the plasma torch significantly affected the low-level signal from thermocouples. The power input to the plasma torches was calculated as the product of the voltage and current. The net power for the Plasmadyne torch was calculated as the difference between the input power and the energy lost to the cooling water.

6.4 Plasma Torch Gas Regulating System

Argon and hydrogen feed stocks for both plasma torches were supplied from high pressure gas cylinders connected to the torch through remotely loaded regulator valves. A schematic of the gas feed system is shown in Fig. 16. The volumetric flowrates of both gases were calculated from the pressures measured upstream of calibrated

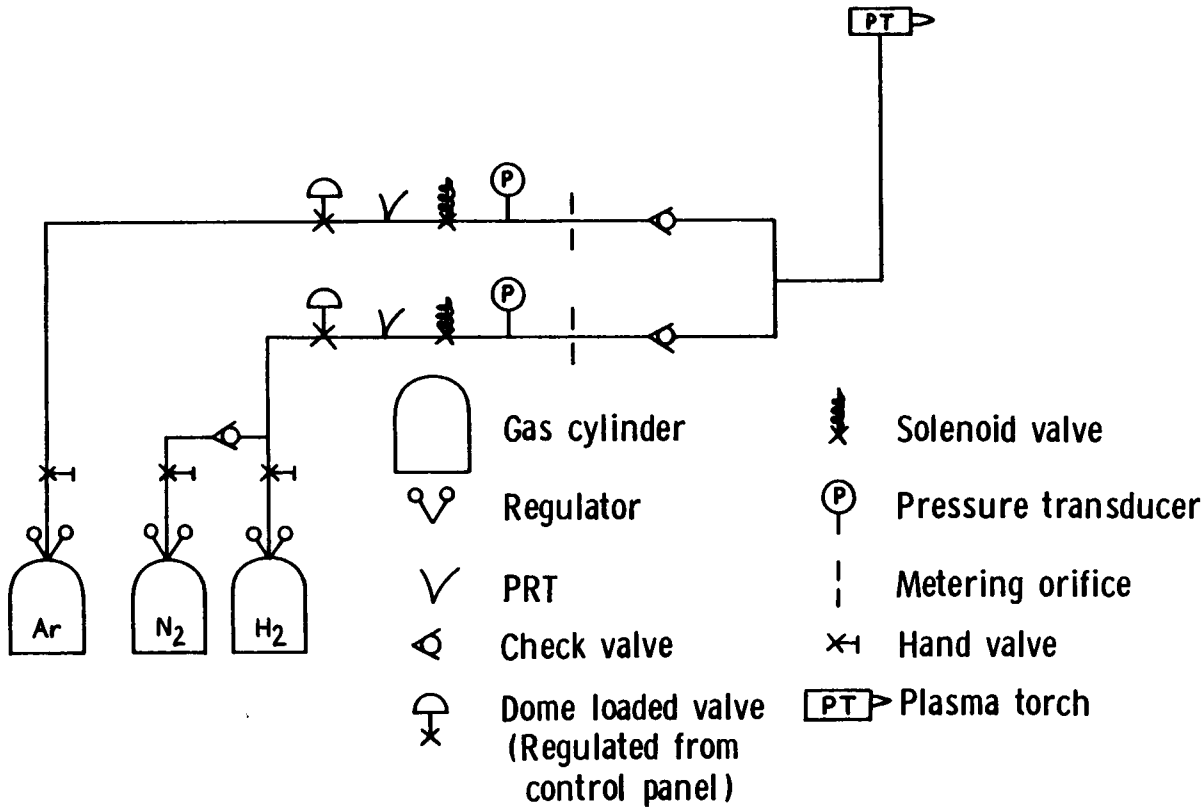

Fig. 16. Schematic of plasma torch gas regulating system.

flow control orifices. The hydrogen and argon orifices were 0.0135 and 0.026 inches in diameter, respectively. Because the VPI torch operated with higher chamber pressures and lower flows than the Plasmadyne torch, the argon orifice was replaced with a 0.0180-inch diameter orifice for the VPI torch tests. This change insured that the orifice would remain choked. The gas temperatures were measured using platinum resistance temperature probes (PRT's). The hydrogen and argon were mixed through a tee fitting. Because of the use of high frequency voltage to initiate the arc, it was necessary to electrically isolate the feedstock tubing from the plasma torch using either a nylon fitting or a short piece of rubber hose. All pressure and temperature data were recorded by the data acquisition system (DAS), which is described in Section 8.2. A discussion of the expected accuracy for all measurements is presented in the Appendix.

6.5 Plasma Torch Operating Procedure

To begin the operation of the Plasmadyne torch, the cooling water flow and argon feedstock flow were begun and the power supplies were energized. The arc was initiated by a short burst of high frequency voltage. A transition to all or part hydrogen was accomplished by increasing the hydrogen flow rate, decreasing the argon flow rate, and increasing the Variac control for the power supplies. This procedure could be accomplished in approximately thirty seconds. The argon-hydrogen ratio was typically adjusted to 1.0 on a volumetric basis. The total feedstock flow rate through the torch was nominally 60 scfh,

or 90.3×10^{-5} lb/s. The maximum flow rate of hydrogen was limited by the voltage limits of the power supply.

The operation of the VPI torch was similar to that of the Plasmadyne torch, except that the cooling water was unnecessary and the argon flow rate did not have to be decreased during the transition. The argon-hydrogen ratio for the VPI torch was also typically 1.0 on a volumetric basis. However, the total feedstock flow rate was nominally 40 scfh, or 60.3×10^{-5} lb/s. A 1:1 volumetric mixture of argon and hydrogen is 95 percent argon on a mass basis. Therefore, the nominal mass flow of hydrogen flowing through the VPI plasma torch was only 30.2×10^{-6} lb/s.

7. PLASMA DIAGNOSTICS

It was desired to conduct diagnostic measurements on the plasma torch exhaust to aid in explaining the observed results of the supersonic combustion tests. The atmospheric pressure plasma jet presents a very severe environment for diagnostics. The author is unaware of any published experimental data for hydrogen or 1:1 argon-hydrogen plasma jets at atmospheric pressure. The only known data for plasma jets with argon-hydrogen feedstocks are for mixtures containing 17 percent hydrogen (by volume)[150] or less.[151,152] Data have been published for wall stabilized hydrogen arcs at atmospheric pressure.[153] The objective of the diagnostic measurements in the current investigation was to verify the presence of hydrogen atoms in the torch exhaust. After a brief review of the diagnostic methods applicable to atmospheric pressure plasma jets, the results of the diagnostic tests will be presented.

7.1 Review of Plasma Diagnostic Techniques

Several different techniques may be employed for measurements in plasmas. These techniques include optical methods, probe methods and microwave methods. Microwave techniques are limited by the plasma frequency cutoff to plasmas for which the electron density is less than 10^{14} cm^{-3}.[152] Since the electron density of atmospheric plasmas is typically greater than 10^{15} cm^{-3},[161-163] microwave methods are not applicable in the current investigation. Of the optical methods,

spectroscopic techniques are the most useful. This review will be limited to spectroscopic and probe techniques. The reader is referred to Refs. 152 and 154 for more information on plasma diagnostics.

Spectroscopy is a very useful tool for plasma diagnostics because it offers good spacial resolution and is nonintrusive. All of the spectroscopic methods to be discussed require the plasma to be optically thin in the wavelength range of interest. All but the Stark broadening technique are based on the existence of LTE in the plasma.

The plasma temperature may be deduced from spectroscopic measurements of the emission coefficients. Three techniques may be used for this measurement: absolute line intensity, a ratio of line intensities from two different spectral lines, or relative line intensities of different ionization stages.[152] All of these methods are based on the existence of LTE in the plasma.

The electron density of a plasma may be determined by spectroscopically measuring the width of an atomic emission line.[154] This technique is based on the Stark effect, in which the wavelength of an emitter is shifted slightly by the presence of an electric field. The charged species in a plasma produce a randomly-oriented electric field which creates random shifts in the wavelength of the atomic emissions. These random shifts result in a broadening of the atomic emission line. The hydrogen beta line due to the second transition in the Balmer series (4861 Å) is especially sensitive to these shifts and is therefore well-suited for measuring electron density. Other mechanisms may also lead to line broadening, including the Doppler effect and pressure effects. For the experimental conditions

of this study, these effects are quite small compared to the Stark effect.[165] The electron density is determined by fitting the experimentally-determined line profiles to theoretical line profiles. The advantage of using the Stark Broadening technique to determine electron density is that LTE does not have to be assumed. This technique will be discussed in more detail later.

Two different types of probes may be used in plasma jets to determine the specific enthalpy of the gas.[152] One type is the calorimetric probe, in which the enthalpy is determined from an energy balance applied to the probe cooling water and the gas sample flowing through the probe. The second type of enthalpy probe is the pneumatic probe. This device uses three sonic orifices: one for the plasma sample, one for a diluent gas which mixes with the plasma sample, and one through which the mixture exits. The enthalpy of the plasma is calculated by applying the principles of mass and energy conservation once the pressure, temperature, and composition of the exiting mixture have been measured.

Another type of probe which can be used in plasmas is the electrostatic probe (Langmuir probe).[154] In this technique, the probe is biased with a DC voltage, and the current flowing from the plasma through the probe is measured. The electron temperature and electron density may be determined from the volt-ampere characteristic. However, the original theory of Langmuir was developed for stationary plasmas at low pressures, where the mean free path is much larger than the probe dimension. The theoretical model must be modified for flowing plasmas at atmospheric pressure.[155-159] Grey and Jacobs[160]

have developed a combined calorimetric-electrostatic probe and demonstrated its use in an argon plasma jet at atmospheric pressure.

7.2 Diagnostic Experiments

The first diagnostic tests in the current investigation were conducted with the SG-1B plasma torch. The electrostatic probe technique was attempted first. A water-cooled probe and a positioning mechanism were designed and fabricated. During the first day of testing, the tip of the probe was paritally melted as a result of the high heat flux from the plasma. A second probe, designed with greater cooling capacity, also failed to survive. Other modifications were tried without success. Sweeping the probe through the flow was considered, but at this point probe techniques were abandoned in favor of nonintrusive spectroscopic techniques.

Of the spectroscopic techniques reviewed earlier, Stark broadening was chosen for use in this investigation because the resulting electron density is not dependent on the existence of LTE in the plasma. The electron density may be determined by comparing the experimental and theoretical profiles of the H_β line. Hydrogen atoms must be present in the plasma if this method is to be employed. The accuracy of this method in measuring the electron density has been estimated at 7 percent.[161] The line width comparison may be made at one point in the profiles, usually the full width at half maximum (FWHM), or the entire line profiles may be compared. The Stark-broadened H_β line may have a very irregular shape, sometimes having

a central dip and asymetries. For these reasons it was decided to compare the entire profiles. Goode and Deavor[162] have developed a computer program for this purpose. This program compares the experimental data with a data base containing Stark-broadened profiles of the H_β line for seven different electron densities as calculated by Vidal et al.[163] A one-parameter least-squares method is then used to determine the electron density which results in the best fit to the theoretical data.

A McPherson Model 225 one-meter scanning monochromator was used to record the shape of the H_β line. This instrument was equipped with a 995.4 mm (39.2 in.) radius of curvature 600 lines/mm (15,240 lines/in.) grating, blazed at 1500 angstroms. The first order reciprocal linear dispersion of the instrument was 17 Å/mm (432 Å/in.) with this grating installed. Prior to the diagnostic tests the monochromator was adjusted as outlined in a procedure supplied by the manufacturer. An EMI 9785B S20 photomultiplier (PM) tube was used as the detector. The PM tube was energized by a Products for Research Model S-504 power supply. The current output of the PM tube was measured by a Keithley 414 micro-microammeter (electrometer). The output from the electrometer was recorded on a Soltec Model 3312 strip chart recorder and on the data acquisition system (DAS). (For a description of the DAS, see Section 8.2). The center of the jet immediately downstream of the torch exit was imaged on the entrance slit of the monochromator through a series of lenses and a quartz optical fiber. The optics are shown schematically in Fig. 17. A piece of ordinary glass was incorprated in the

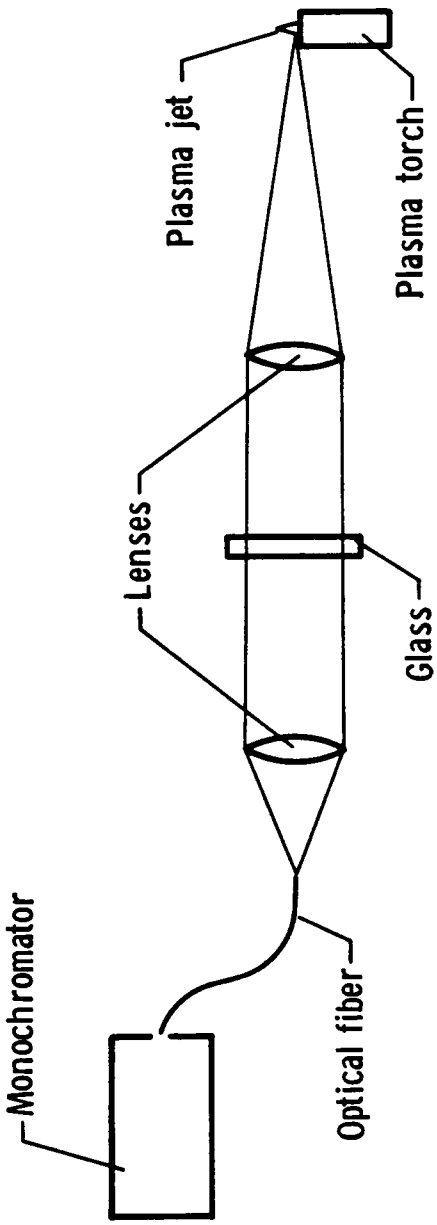

Fig. 17. Schematic of optics for diagnostic tests.

optical path to eliminate the ultraviolet radiation, simplifying the interpretation of the data.

The SG-1B plasma torch was again tested first. Visual observation indicated the exhaust from the torch was pink, signifying the presence of the first transition in the Balmer series of the hydrogen atom (H_α, 6563 Å). Therefore, hydrogen atoms were present. This observation was substantiated by the spectroscopic investigation of the H_β line (4861 Å).

The experimentally-determined electron densities for the Plasmadyne SG-1B plasma torch are shown in Fig. 18 as a function of the net power. Several values of the argon-hydrogen ratio, α, were tested. The power input and the mixture composition were not independent variables. The larger flow rates required higher power inputs to stabilize the arc. The flow rates and powers represented in Fig. 18 were chosen because they produced stable operation. Since almost one minute was required to scan the line width, stability was essential if meaningful data were to be obtained. The combustion tests were conducted at net power levels of 2 to 4 kW, the lowest powers for which the torch would operate. The operation at these low powers was not stable enough to allow repeatable line shapes to be recorded. Therefore, no line width data are available at the lowest power levels, but electron presence is thought to persist.

Assuming local thermodynamic equilibrium, the temperature may be determined from the theoretical data calculated by Capitelli et al.[128] A typical temperature for the data shown in Fig. 18 is approximately 20,000 R. At this temperature essentially all diatomic

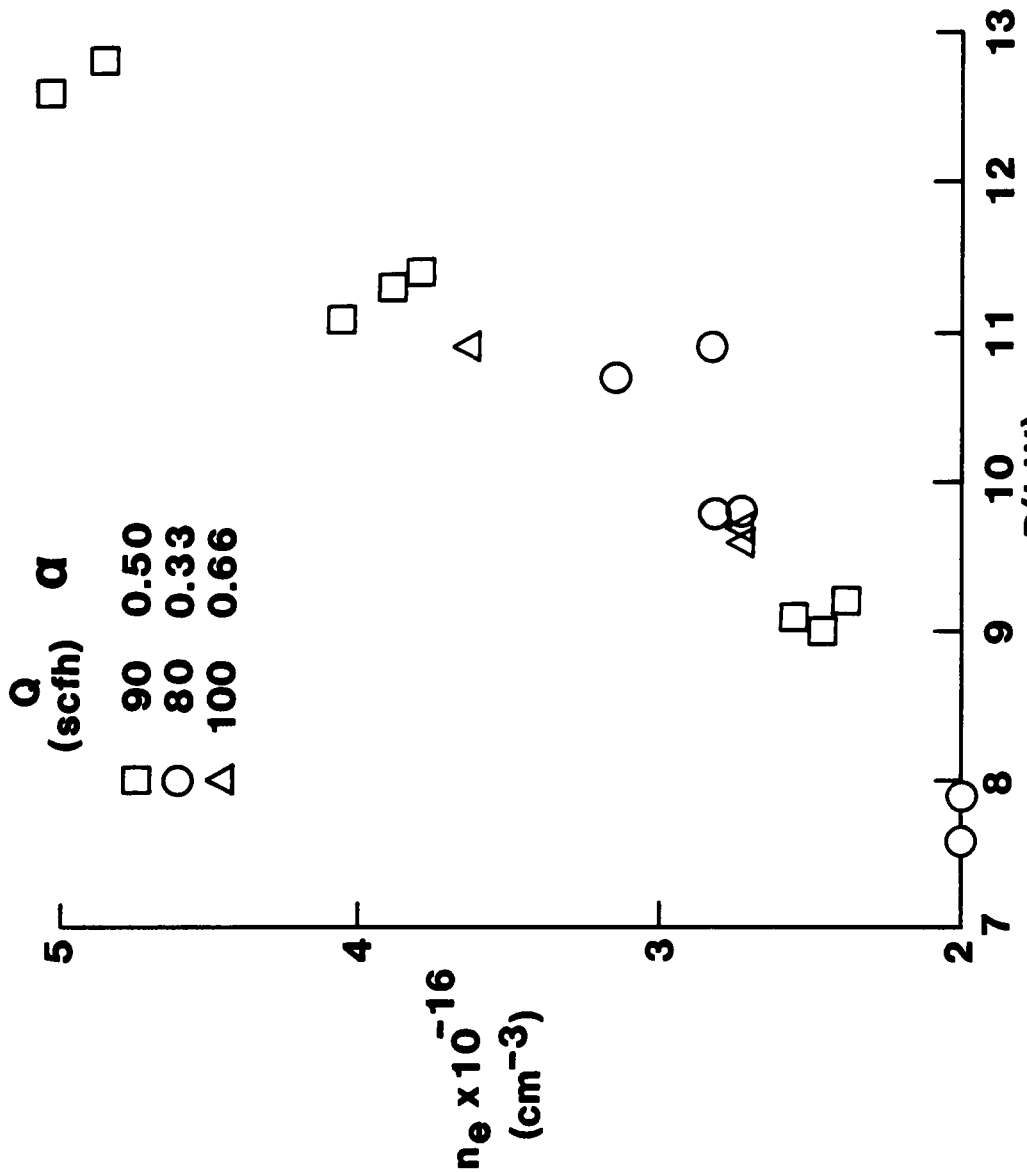

Fig. 18. Electron density vs. net power for SG-1B plasma torch.

hydrogen would be dissociated. However, an input energy of 11 kW would be sufficient to raise 22 percent of the argon-hydrogen flow to that temperature. Therefore, the exhaust is obviously not uniform. Although this technique indicates the presence of hydrogen atoms, the number of hydrogen atoms produced by the torch cannot be quantitatively determined from this measurement.

Due to the inhomogeneity of the plasma, the diagnostic techniques outlined in Section 7.1 cannot be used to quantitatively characterize the torch exhaust. Behbahani et al.[151,152] have reported success in measuring nitrogen atom concentrations in nitrogen plasmas using a titration technique. A similar technique was considered for this work. Hydrogen atom concentration has been measured in low pressure microwave discharges by reacting the atoms with nitric oxide (NO),[164] nitrogen dioxide (NO_2),[165] ozone (O_3),[165] hydrogen chloride (HCl),[166] and nitrosyl chloride (NOCl).[166] However, most of these techniques are not applicable to atmospheric pressure plasma jets. The reaction involving NOCl was considered for use in this investigation, but was abandoned when NOCl could not be obtained commercially. The visual observation of the pink radiation from the H_α line and the spectroscopic detection of the H_β line during the Stark broadening measurements were considered adequate evidence of the presence of hydrogen atoms.

The Stark broadening technique was also used with the VPI plasma torch to provide an upper limit on the temperature of the torch exhaust. The experimentally determined electron densities for the VPI plasma torch are shown in Fig. 19 as a function of the power input.

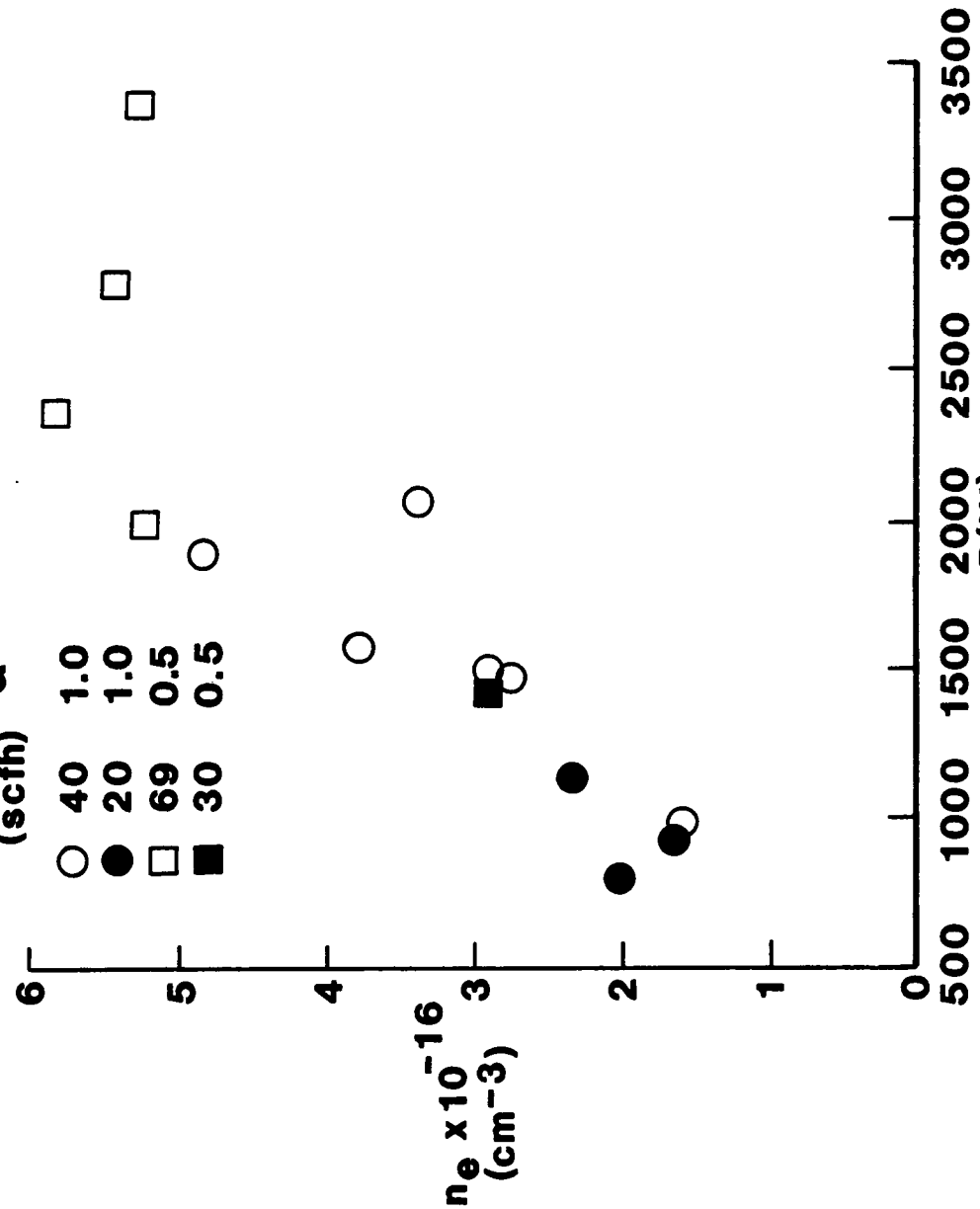

Fig. 19. Electron density vs. input power for VPI plasma torch.

Several values of the argon-hydrogen ratio were tested. The power levels and flow rates encompass the range of values used during the combustion tests. From the theoretical data of Capitelli et al.,[128] the typical temperature for the data shown in Fig. 19 is approximately 20,000 R, assuming the existence of LTE. For a power input of 1 kW, only 11 percent of the gas could be raised to this temperature. Therefore, the exhaust is nonuniform and may be composed of tiny hot pockets immersed in a relatively cool gas. This result is similar to the findings reported in Refs. 147 and 148.

Visual observation of pink radiation from the plasma was used to verify the presence of hydrogen atoms in the VPI torch exhaust. Furthermore, an Optical Multichannel Analyzer (OMA-2) was used with the VPI plasma torch to verify the presence of hydrogen atoms. This device was used because it allowed a large portion of the spectrum (4000 to 6600 Å) to be sampled at one time, stored on diskette, and then compared with another spectrum on one display. The instrument was equipped with a 152.65 lines/mm (3877 lines/in.) flat grating, blazed at 5000 angstroms. The lens arrangement for these tests was identical to that used during the tests with the monochromator. The spectra for three different torch operating conditions are shown in Fig. 20. The three spectra represent three different power levels and two different values of the argon-hydrogen ratio. The four predominant spectral lines which appear in this figure are the first four lines in the Balmer series for the hydrogen atom. These data substantiate the presence of hydrogen atoms in the torch exhaust. Furthermore, the intensity and width of the lines increase for

Curve	Q, scfh	α, Ar/H_2	P, Watts	P/Q, Watts/scfh
1	40.0	1.0	790	19.8
2	40.0	1.0	1258	31.5
3	68.2	0.48	2000	29.3

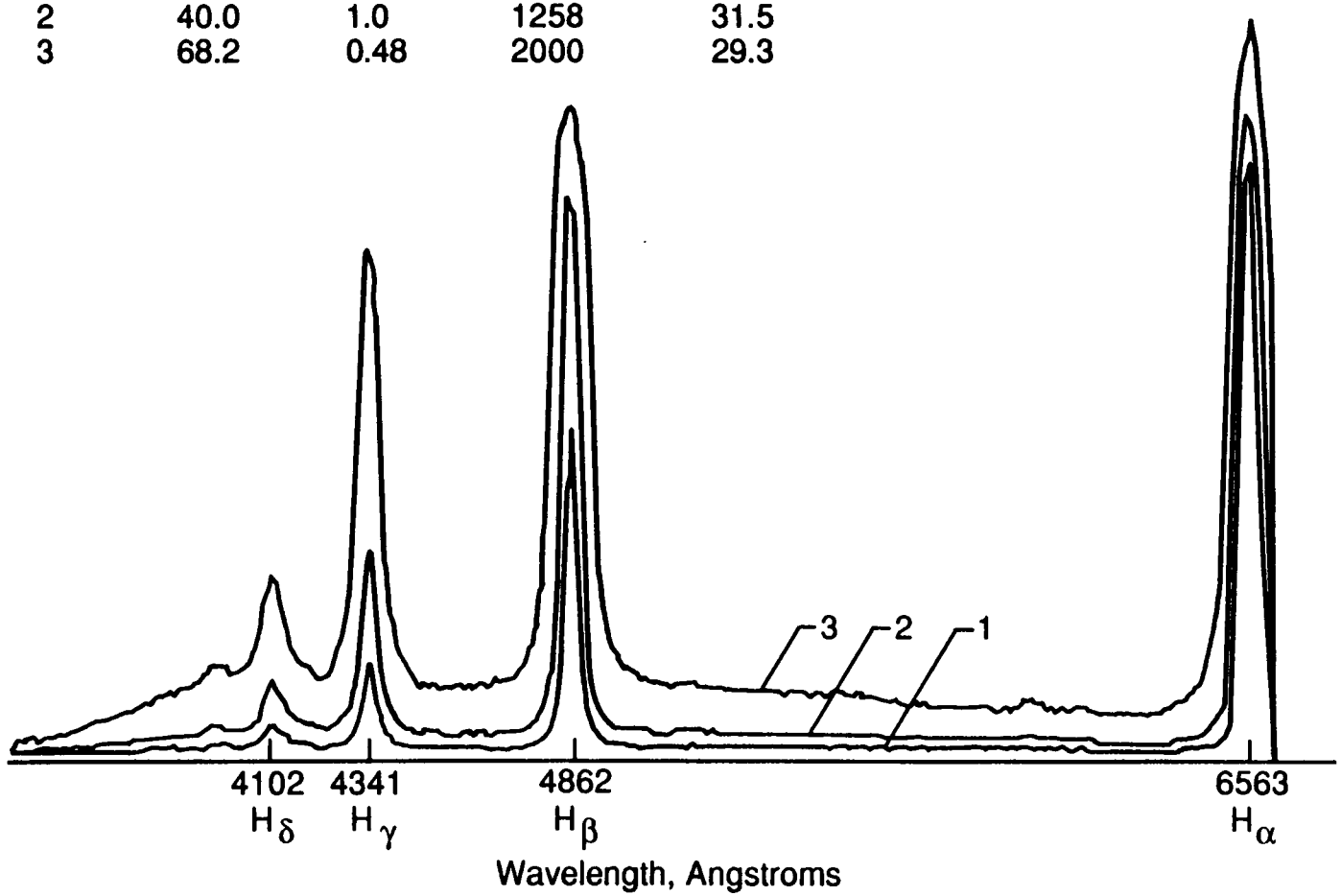

Fig. 20. VPI torch exhaust spectra.

increasing power and hydrogen flow rate, indicating an increase in hydrogen atom density.

From the results of the diagnostic tests it may be concluded that at least a small concentration of hydrogen atoms are present in the exhaust of both the SG-1B and VPI plasma torches. If the supersonic ignition and flameholding theory is applicable, the hydrogen-argon plasma torch should be an effective igniter and flameholder. No definitive measures of individual or comparative torch performance were drawn from the diagnostic work.

8. SUPERSONIC COMBUSTION TEST APPARATUS AND PROCEDURE

8.1 Hardware

To assess the effectiveness of the plasma torch ignition and flameholding concept, supersonic combustion tests were performed. Direct-connect wind tunnel tests were conducted in a hot Mach 2 flow using two configurations. The first configuration used unconfined flow hardware, shown schematically and pictorially in Figs. 21 and 22, respectively. This hardware was designed to allow free optical access from either side in order that cinematography and an OH visualization system could be employed to visualize ignition and flameholding. The flow was bounded only by upper and lower injection blocks. The second configuration used a confined duct to simulate a scramjet combustor. Sidewalls were added to the injector blocks for these tests, and a 48-inch long, diverging duct was bolted downstream of the injector blocks to simulate the expansion section of a scramjet combustor. Two different ducts were used. A 3-degree half angle diverging duct was used during the initial tests with the Plasmadyne torch, while a 2-degree half angle duct was used during the VPI torch tests. The exit of the duct was connected to an air ejector to prevent separation in the expanding duct. This configuration is shown schematically in Fig. 23. The diverging duct was instrumented with static pressure and wall temperature measurements as is shown in Fig. 24. These measurements allowed the combustor performance to be estimated using one dimensional analysis techniques.

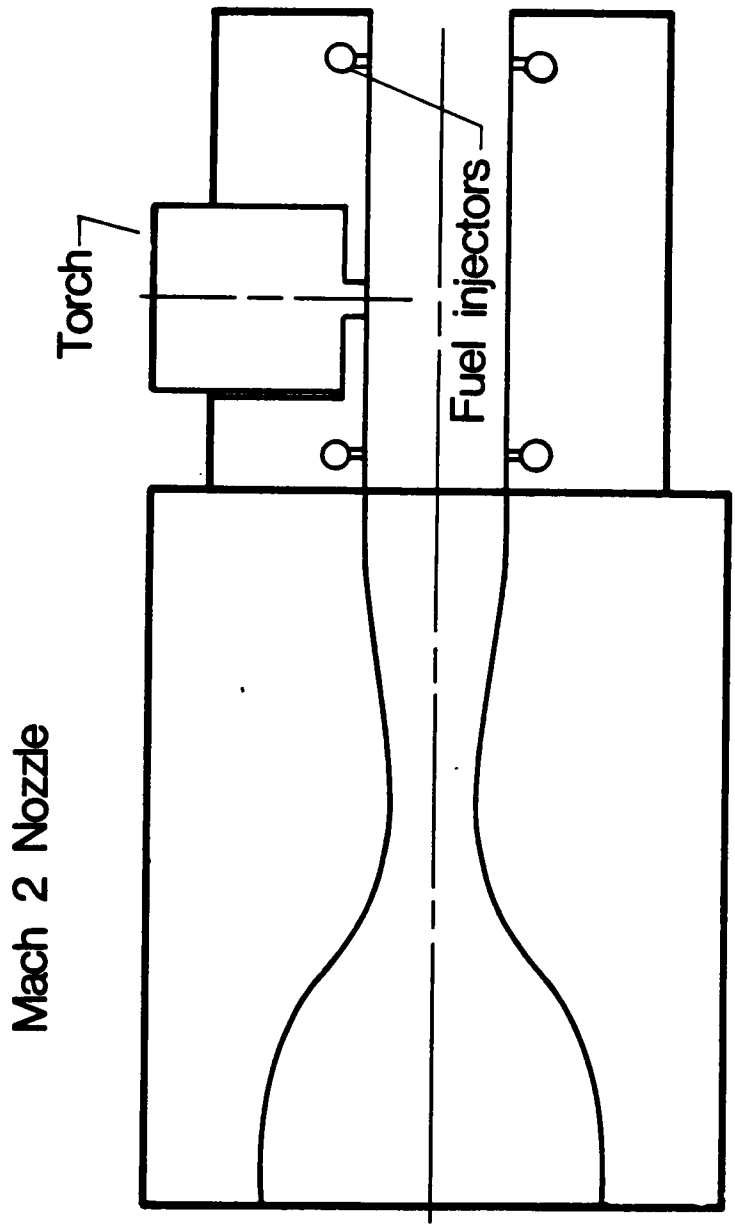

Fig. 21. Schematic of unconfined flow model.

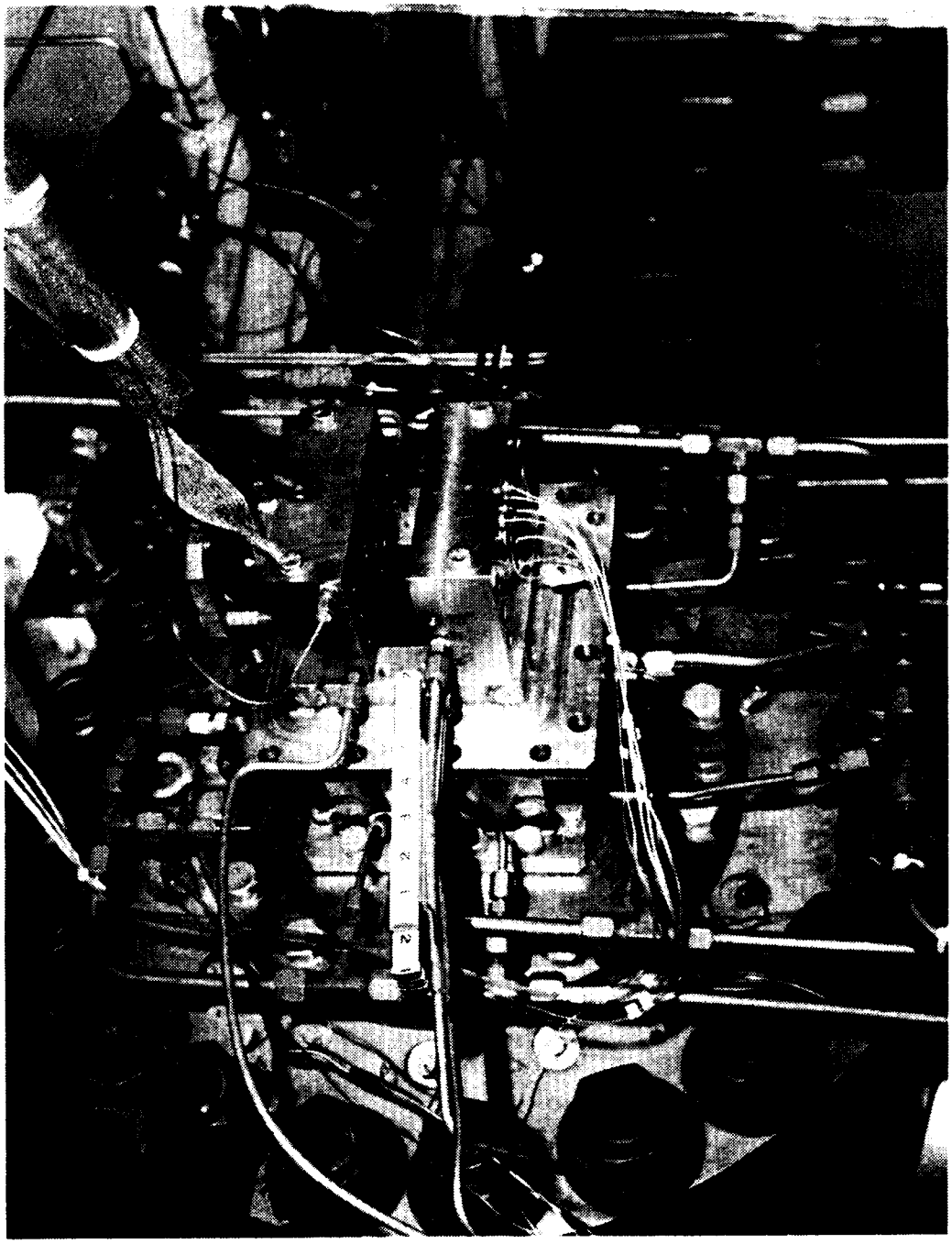

Fig. 22. Photograph of unconfined flow model.

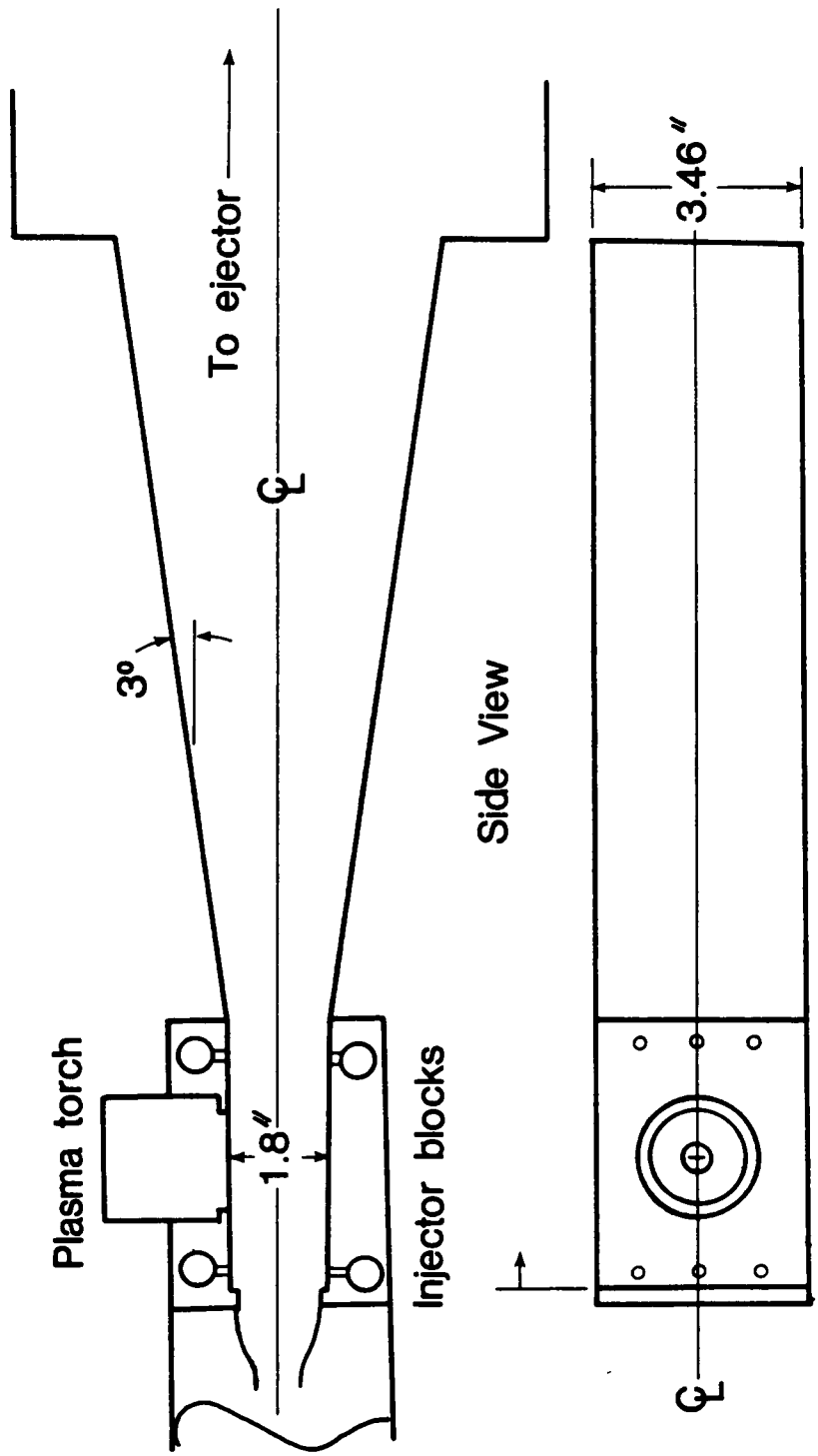

Fig. 23. Schematic of ducted model.

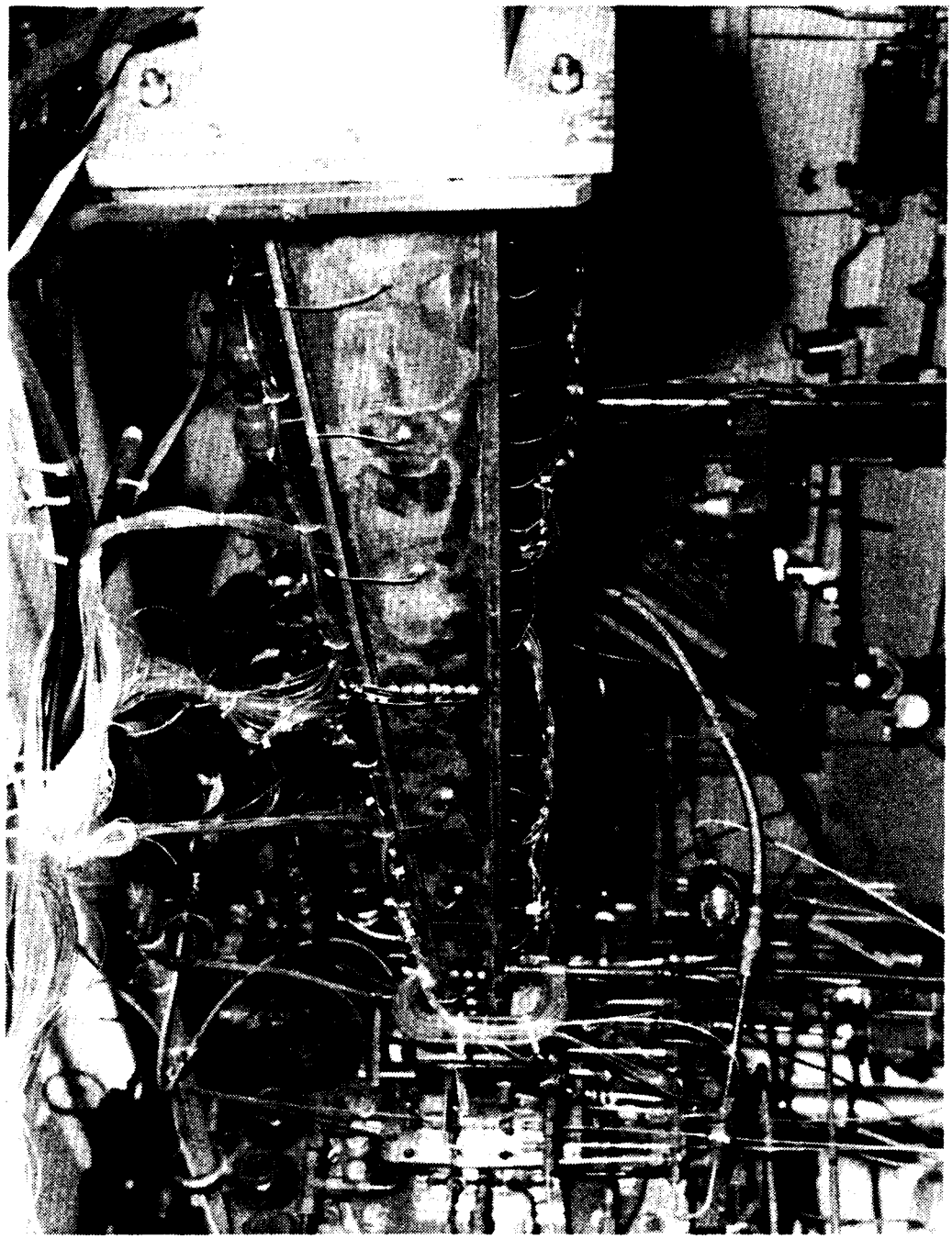

Fig. 24. Photograph of ducted model.

Two sets of injector blocks were used during the initial tests. In both cases the Plasmadyne SG-1B plasma torch was mounted in the upper injector block, as shown in Fig. 21. One set of injector blocks was mounted flush with the facility nozzle and thus simulated injection, combustion and flameholding on a flat plate. A second set incorporated a step (0.150-inch) increase in area just upstream of the fuel injectors to increase the residence time of the fuel and air entrained in the resulting recirculation region. The design of the injector blocks used with the VPI plasma torch was a result of the initial tests with the SG-1B plasma torch, and will therefore be described with the results in Section 9.2.

The test gas which simulates high temperature air was provided by a hydrogen-oxygen-air burner (vitiated heater). The effects of vitiated air on the experiment have been discussed,[92] but the matter is unresolved. The reactant flows to the burner were adjusted so that the combustion products leaving the heater (the vitiated air) had the desired stagnation temperature and contained approximately 21 percent free oxygen by volume. A water-cooled Mach 2 nozzle was mounted on the exit of the heater. The pressure at the exit of the nozzle was controlled by varying the total mass flow through the heater. Typical nozzle exit conditions were a static pressure of 15 psia, a mass flow of 4.5 lb/s, and a total temperature of 1600 R. The total temperature of the burner could be varied between 1100 and 4000 R. The facility could also be operated with ambient temperature air.

8.2 Instrumentation / Data Acquisition

The data from the experimental tests were digitized and recorded in a real-time mode by the data acquisition system (DAS). The main computer in the DAS was a Modcomp IV. A series of Neff amplifiers was used to digitize up to 192 analog signals. An electronically scanned pressure (ESP) measurement system was used to monitor up to 128 pressures on the ducted model. A discussion of the expected accuracy of the data is presented in the Appendix. Raw data were recorded on tape ten times per second. After being converted to engineering units, the data were printed out and stored on disk twice per second. A graphics terminal allowed plots to be made of any given parameter immediately after each test. Each test was begun by starting the run timer, which automatically initiated other timers controlling the opening of valves to allow fuel flow to the model. A Modicon programmable controller could also be used to operate valves, cameras and other equipment.

8.3 Ultraviolet Television

Ignition and the flameholding location were documented, during many of the unconfined flow tests, using an OH visualization system, commonly referred to as the ultraviolet television (UV-TV). Two UV-TV systems were used. A prototype UV-TV, the camera for which is shown in Fig. 25, was used during the Plasmadyne torch tests. This prototype system was equipped with a Westinghouse Model WX4887 ultraviolet

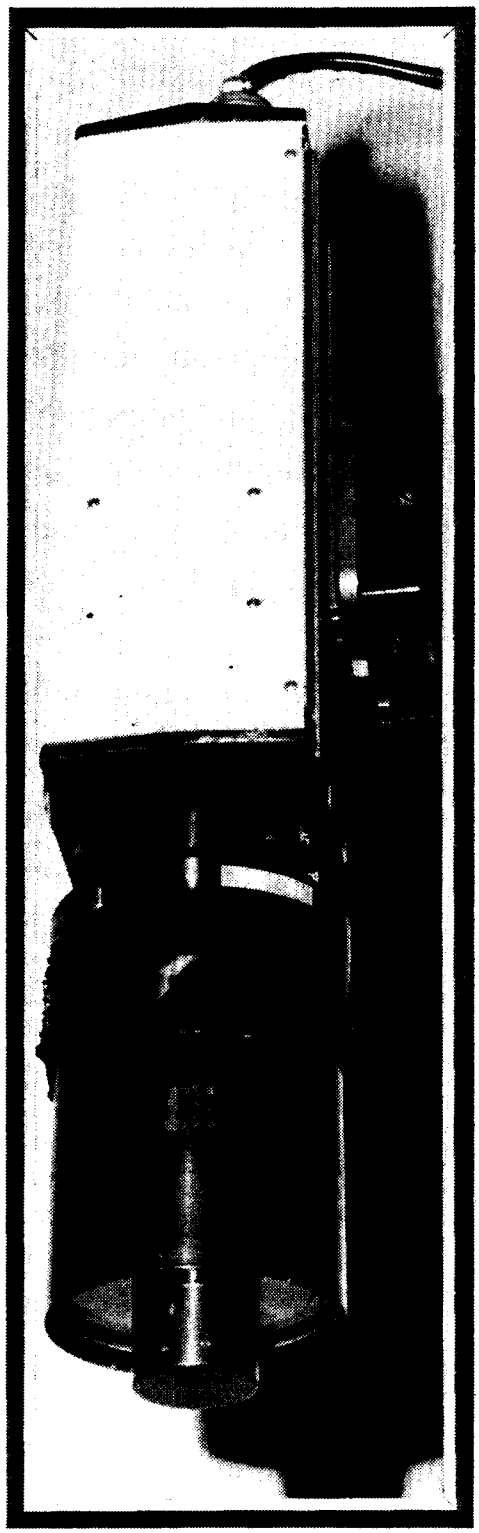

Fig. 25. Photograph of prototype UV-TV camera.

vidicon tube and a 3100 angstrom, 130 angstrom wide (FWHM) bandpass filter with a 71 percent transmission. A 150 mm focal length Schmidt-Chassegrain lens was used to image the flame onto the detector. Any 3100 angstom radiation detected from any resulting flame was assumed to be the natural radiation associated with the generation of OH in the flame. (No external sources were used to excite fluorescence.) Of course, the UV radiation generated by the torch was also visible on the TV.

A two camera system was available for use during the later VPI torch tests. This new system included two Panasonic video recorders and a Model 321 Colorado Video Inc. video analyzer. This analyzer was used to measure the relative intensity of the flame. This intensity measurement was not quantitative in that it could not be used to determine combustion efficiency. However, brighter, more intense radiation was a relative indicator of increased OH emission. One camera was positioned perpendicular to the flow while the other camera was positioned at an oblique angle downstream.

8.4 Combustion Test Procedure

For the Plasmadyne torch, the procedure for the combustion tests was to set the air flow to the desired level, start the torch, transition to the desired argon-hydrogen ratio and power level, and then follow the standard tunnel procedure. The tunnel procedure involved opening valves to allow hydrogen and oxygen to flow into the heater and then generating ignition with a spark initiated torch. The plasma

torch voltage often decreased when the burner was started. For these tests it was necessary to adjust the torch power to the desired level after the burner was operating. Once burner ignition was verified by a temperature measurement, the test was begun by starting the run timer. The operating sequence during a test was controlled by a Modicon programmable controller or by additional timers, as was previously mentioned. In either case the data acquisition system started with the run timer, and the valves controlling the fuel flow to the model were opened after the heater ignition transient. The upstream and downstream injector fuel flows were controlled separately so that it was possible to observe the effects of injection from each location separately. During some runs the plasma torch was extinguished several seconds after the fuel had been ignited to determine if the model would flamehold without the aid of the plasma torch. During other tests the heater temperature was ramped up to increase the velocity in an attempt to blow off the flame while the plasma torch was acting as a flameholder. Both the UV-TV and visual observation of the model were used to determine ignition and the flameholding location during the unconfined flow tests. For the ducted tests the pressure distribution from 26 longitudinal stations was used to detect ignition and flameholding and to infer the combustion efficiency through one dimensional analysis.

9. RESULTS AND DISCUSSION

9.1 Initial Tests

Typical results from the initial tests with the Plasmadyne SG-1B plasma torch are presented and discussed. Both the unconfined and ducted configurations were employed. The UV-TV pictures were the main recorded data for the unconfined flow tests. Although the bottom injector block had pressure taps installed in the wall, during the unconfined flow tests these pressures were not a reliable means to determine ignition on the top wall where the torch was mounted. The data from the initial tests are summarized in Table II.

UV-TV photographs from three unconfined flow tests with methane fuel are shown in Fig. 26. Flow direction is from left to right. The bright overexposed circles in the photographs are the result of UV radiation from the plasma torch. The horizontal line is the cursor positioned at the approximate location of the top wall; the vertical cursor indicates the exit of the Mach 2 nozzle. The bright streak near the bottom of each photograph is the reflection of the torch radiation from the bottom block. The UV-TV was used to determine ignition limits and the location of flameholding. The TV is not quantitative in the sense that it cannot be used to determine combustion efficiency. However, brighter, more extensive radiation is a relative indicator of improved reaction. The extent and density of the bright area emergent from the circular torch radiation was used to judge ignition behavior and flameholding location. Continuous bright

Table II. Summary of data from initial tests with Plasmadyne SG-1B plasma torch.

RUN	BATCH	FUEL	ϕ_{TOT}	T_t (R)	P (kW)	Ignition
36	2	H^2	0.49	3040	2.5	Yes
36	3	H_2	0.49	3040	0	Yes
36	4	C_2H_4	0.36	3040	2.5	Yes
36	7	C_2H_4	0.30	2300	1.8	Yes
36	9	C_2H_4	0.28	3240	2.1	Yes
36	12	C_2H_4	0.25	1600	2.2	No
36	13	C_2H_4	0.21	1630	1.9	Yes
37	4	H_2	0.17	1580	1.9	Yes
37	5	H_2	0.36	1580	1.9	No*
37	6	H_2	0.48	1600	1.7	Yes
37	7	C_2H_2	0.31	1497	2.1	Yes
37	8	C_2H_4	0.16	1540	1.8	Yes
37	9	C_2H_4	0.32	1590	1.6	Yes
37	10	C_2H_4	0.29	1580	1.6	No
37	11	C_2H_4	0.29	1580	1.6	No
37	14	H_2	0.35	1065	2.0	Yes
37	15	H_2	0.15	1060	2.1	No*
37	17	C_2H_4	0.32	1380	4.0	Yes
37	18	C_2H_4	0.29	1380	2.8	Yes
37	19	CH_4	0.29	1400	3.4	No
37	20	CH_4	0.21	1680	3.7	No
37	21	CH_2	0.14	1680	3.7	No
38	3	CH_4	0.28	1650	1.3	No
38	4	CH_4	0.28	1600	1.3	No
38	5	CH_4	0.28	1630	3.0	No
38	8	CH_4	0.28	1860	3.0	No
38	9	CH_4	0.38	3200	3.0	Yes
38	10	CH_4	0.27	2900	3.2	Yes
38	11	CH_4	0.19	3000	1.5	Yes
38	12	CH_4	0.20	2360	1.2	No
39	2	CH_4	0.32	2500	1.1	No
39	3	CH_4	0.15	2400	1.2	No
39	6	CH_4	0.16	2833	2.0	Yes
39	7	CH_4	0.16	2706	1.5	Yes
39	8	C_2H_6	0.20	2817	2.0	Yes
39	9	C_2H_6	0.17	2200	1.7	Yes
39	10	C2H6	0.19	1716	1.6	No

* no upstream fuel injection

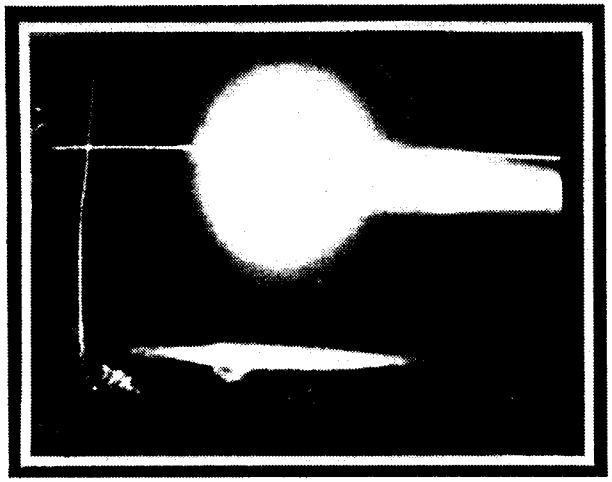

(a) CH_4, T_t = 3200 R, P = 3 kW, Ignition.

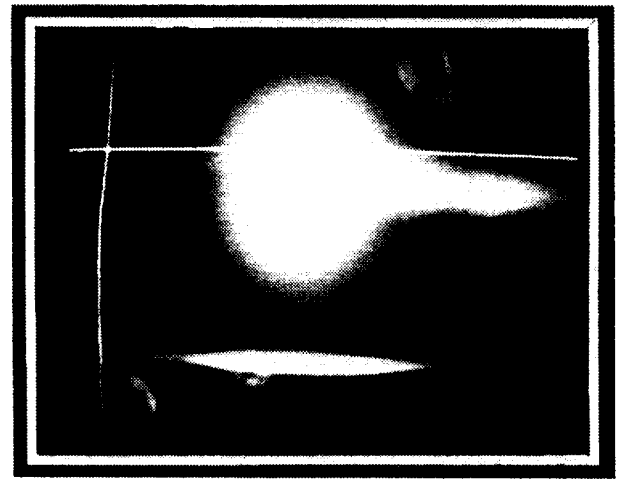

(b) CH_4, T_t = 1860 R, P = 3 kW, No-ignition.

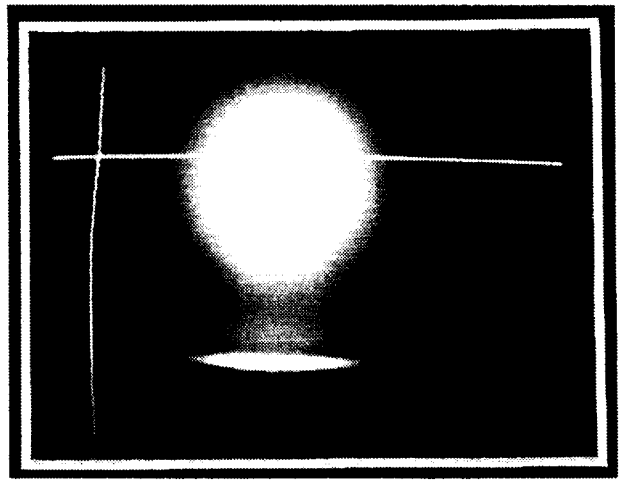

(c) CH_4, T_t = 1400 R, P = 3.4 kW, No-ignition.

Fig. 26. Ignition criteria.

emission past the four-inch long injector block was defined as ignition and flameholding. If the bright emission did not extend to the end of the injector block, ignition may have occurred, but conditions were not favorable for flameholding; these cases were also classified as no-ignition.

Figure 26(a) shows the ignition of methane at a total temperature of 3200 R, an equivalence ratio of 0.34 and a net power of 3 kW. Figure 26(b) shows a photograph from a similar test at a total temperature of 1860 R. In this case the reaction did not extend to the end of the block and thus was defined as no-ignition. (This no-ignition conclusion was also verified by visual observation from the control room located above the test cell.) At 1380 R, only the radiation from the torch was visible (indicating no transport of OH downstream of the plasma torch); see Fig. 26(c).

The effect of plasma torch power on the observed combustion using methane fuel is indicated in Fig. 27. The test conditions for the experiments shown in Figs. 27(a) and 27(b) were similar except that for the test shown in Fig. 27(b) the net power was reduced from 3.2 kW to 1.5 kW. Although a decrease was observed in the overexposure due to torch radiation, no visible difference in the extent of combustion was detected. These results indicate that, at a total temperature of 2900 R, reducing the net torch power by a factor of two had little visible effect on the combustion of methane.

The flameholding performance of the plasma torch is illustrated in Fig. 28 using ethylene (C_2H_4) combustion at a total temperature of 1630 R, an equivalence ratio of 0.21 and a net power level of 1.9 kW.

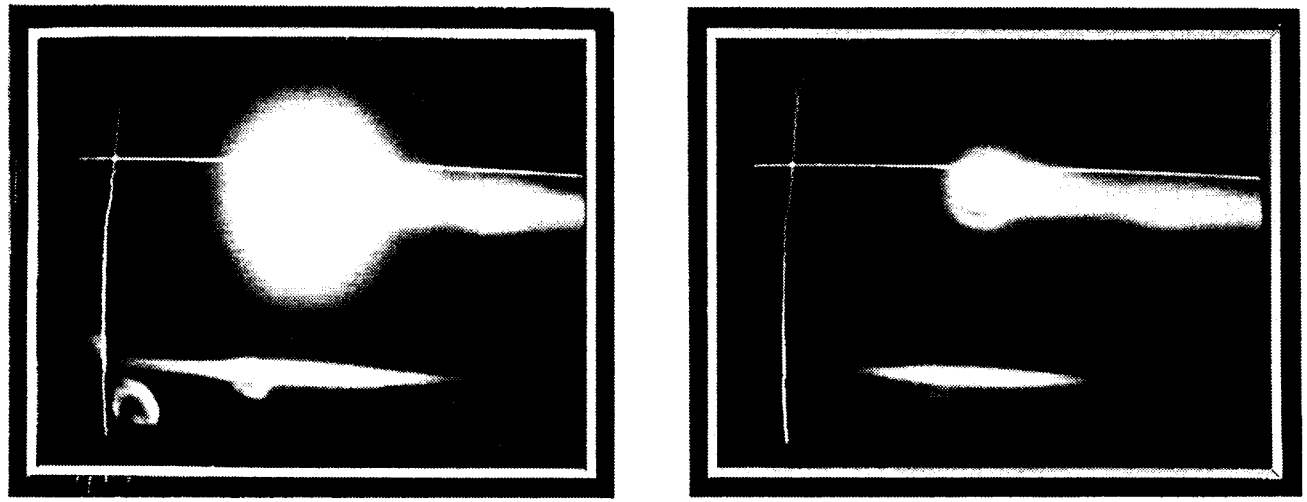

(a) CH_4, T_t = 2900 R, P = 3.2 kW, Ignition. (b) CH_4, T_t = 3000 R, P = 1.5 kW, Ignition.

Fig. 27. Effect of power level.

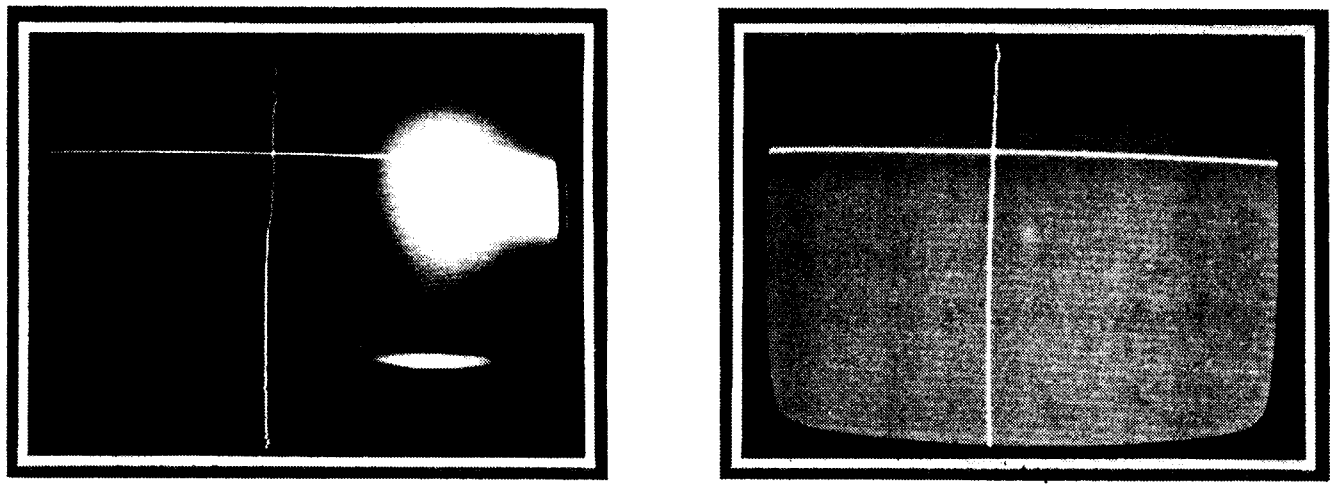

(a) C_2H_4, T_t = 1630 R, P = 1.9 kW, Ignition. (b) C_2H_4, T_t = 1630 R, P = 0 kW, Blow off.

Fig. 28. Torch flameholding.

(The vertical line indicates the end of the nozzle and the beginning of the injector block.) The plasma torch power and hydrogen flow were shut off late in the test and the ethylene flame that had been held by the free radicals generated by the torch was extinguished. (Compare Figs. 28(a) and 28(b).) These results indicate that the concept of a free radical flameholder, as opposed to rearward facing steps, V gutters or other geometric devices, may be promising. During many of the tests, even before the addition of a rearward facing step just downstream of the nozzle, the plasma torch was likewise shown to be an effective flameholder with hydrogen fuel. This was accomplished by shutting off the torch or by increasing the test gas velocity from 2700 to 4800 feet per second (by increasing the heater temperature).

The effects of fuel injection from various locations were investigated using hydrogen fuel. These results are illustrated in Fig. 29. The effect of injection downstream of the plasma torch is illustrated in Fig. 29(a). When hydrogen was injected from the downstream injectors at an equivalence ratio of 0.36, no evidence of combustion was observed. However, when additional fuel at an equivalence ratio of 0.20 was added at the upstream location, vigorous combustion occurred as shown in Fig. 29(b). Apparently the relative location and amount of fuel are critical to effective combustion. Further evidence of this was observed when fuel was added from the bottom wall; no additional combustion was observed. In the limited length of the unconfined flow model, the fuel probably did not penetrate from the bottom wall to mix with the burning fuel being injected from the top wall and being piloted by the torch. This finding is consistent with

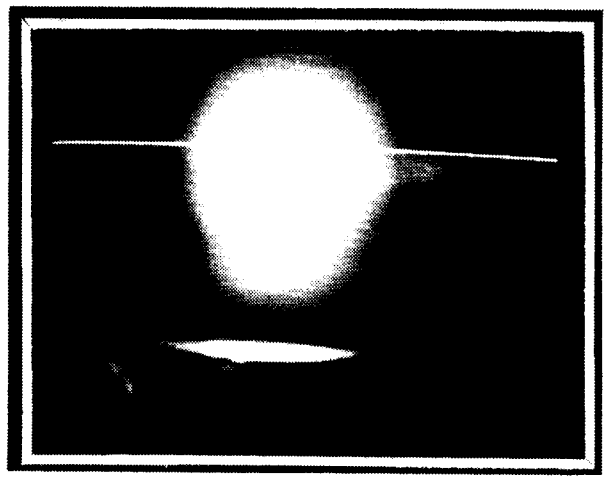

(a) H_2 (downstream), No-ignition. ($\bar{T}_t$ = 1600 R, P = 1.7 kW)

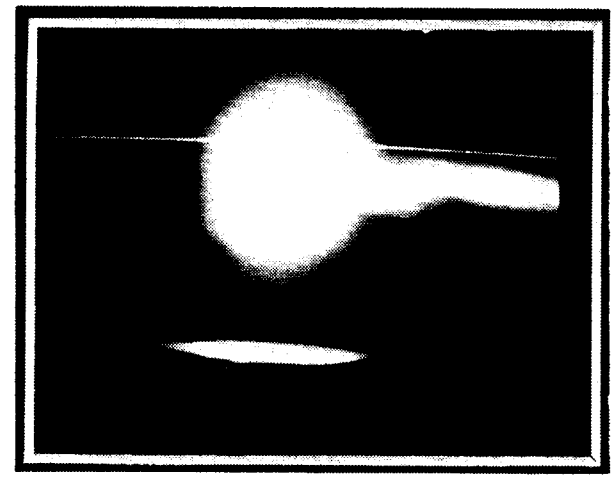

(b) H_2 (upstream and downsteam), Ignition. ($\bar{T}_t$ = 1600 R, P = 1.7 kW)

Fig. 29. Effect of injection location.

previous supersonic combustion test results. (During scramjet engine tests at Mach 7 using silane pilots, improved performance was obtained when the pilot fuel was well-distributed.[13] Piloting from both sides of one strut of a three strut model was not as effective as piloting from all struts. Cross-stream transport of products and free radicals is inhibited in supersonic flows by the large free stream velocities which occur everywhere except near the fuel injectors.)

The fact that some transport can occur near fuel injectors was shown during several tests with ethylene (C_2H_4); combustion was observed to spread upstream to the point of the fuel injector as shown in Fig. 30. The conditions during this test were a total temperature of 1497 R, an equivalence ratio of 0.31 and a net torch power of about 2.0 kW. Surprisingly, such upstream propagation was not observed during hydrogen-fueled tests at similar conditions.

The ignition limits for the plasma torch igniter were explored using the unconfined flow test hardware by operating the heater at various total temperatures and the model at various equivalence ratios. These data are summarized in the several plots of Fig. 31, where the ignition/no-ignition data are plotted as a function of total temperature and injected equivalence ratio for the four fuels used. Closed symbols indicate ignition; open symbols indicate no-ignition. There appeared to be no strong dependence of ignition on equivalence ratio or injector dynamic pressure ratio.

Data for hydrogen fuel are presented in Fig. 31(a). At temperatures as low as 1065 R (the lowest temperature tested), hydrogen appeared to ignite and flamehold. This temperature can be

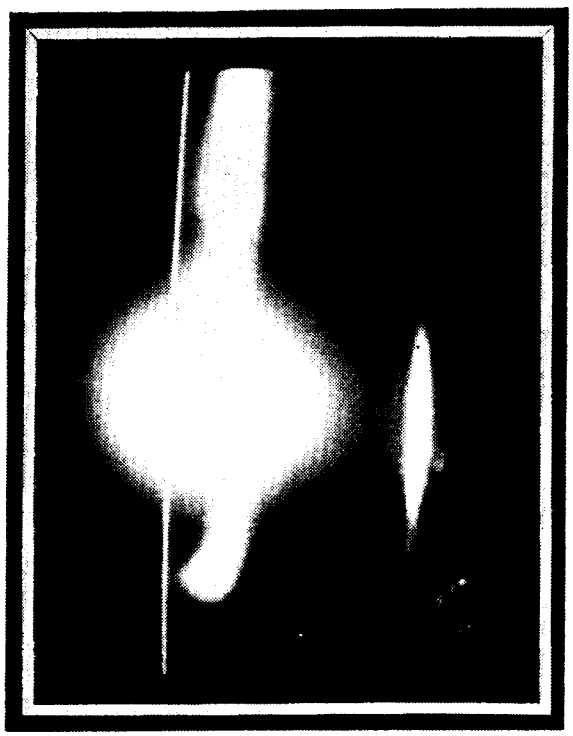

Fig. 30. Ethylene combustion (C_2H_4), T_t = 1497 R, P = 2.1 kW, Ignition.

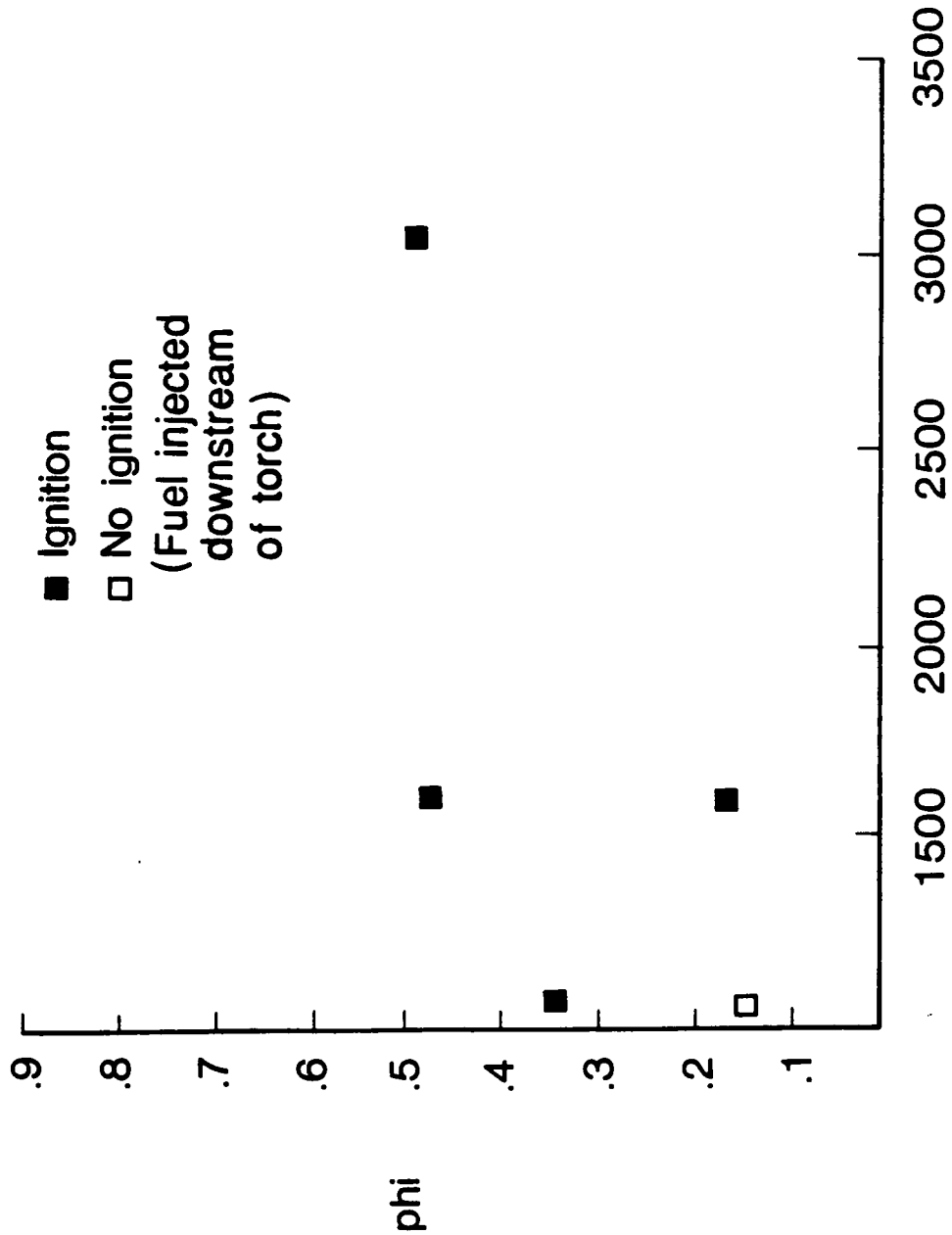

Fig. 31(a). Hydrogen ignition limit with 2kW argon-hydrogen plasma.

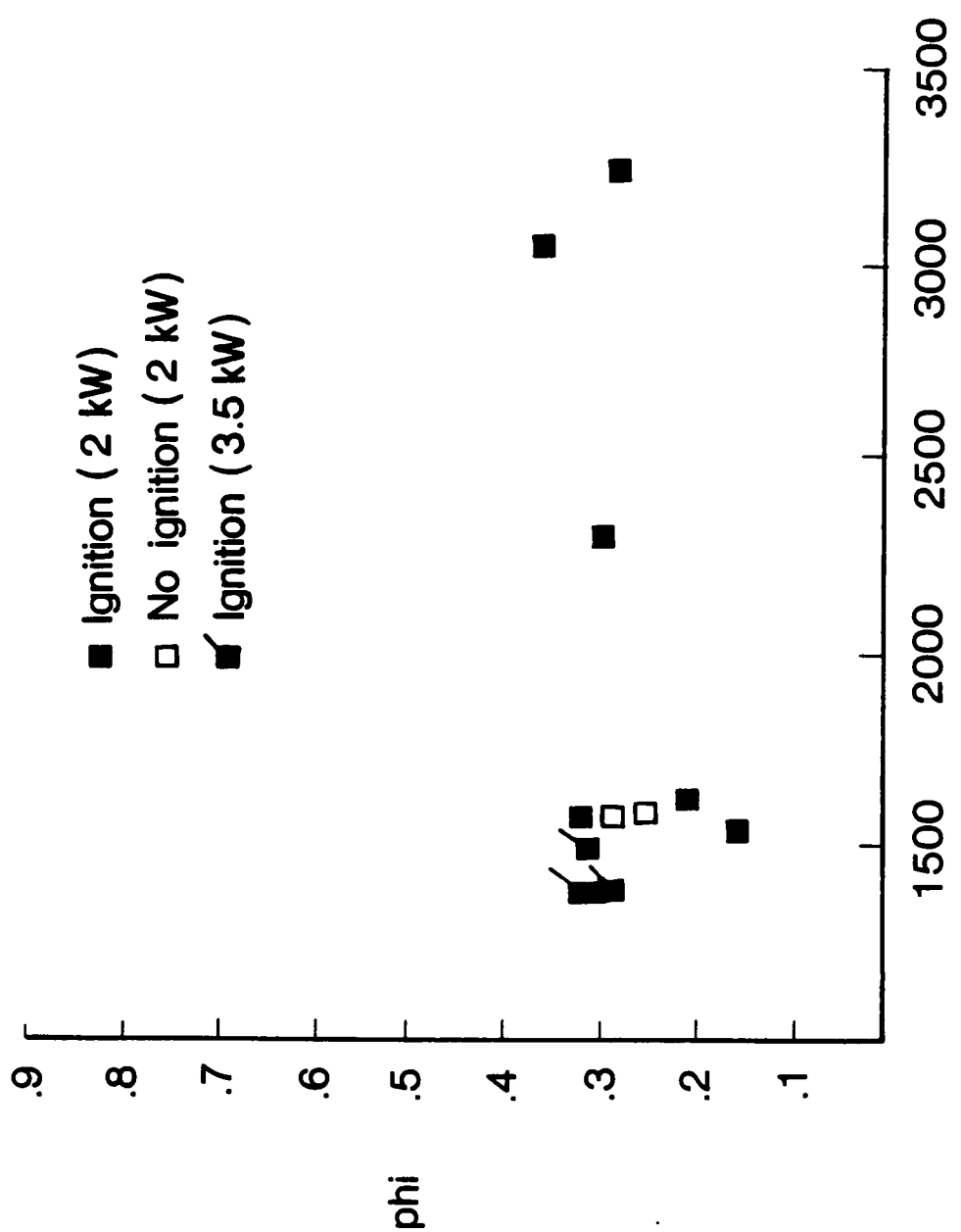

Fig. 31(b). Ethylene ignition limit with 2 kW and 3.5 kW argon-hydrogen plasma.

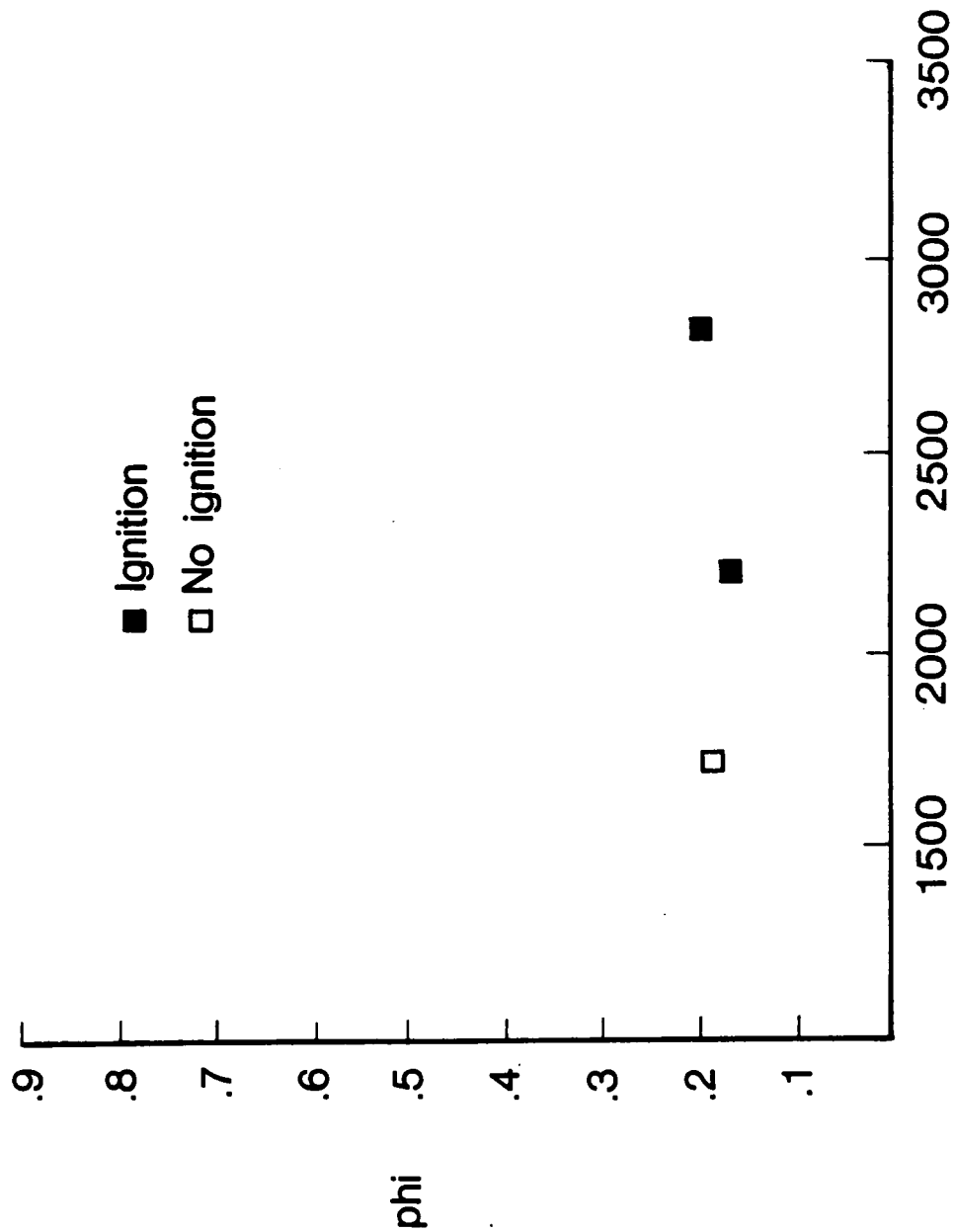

Fig. 31(c). Ethane ignition limit with 2 kW argon-hydrogen plasma.

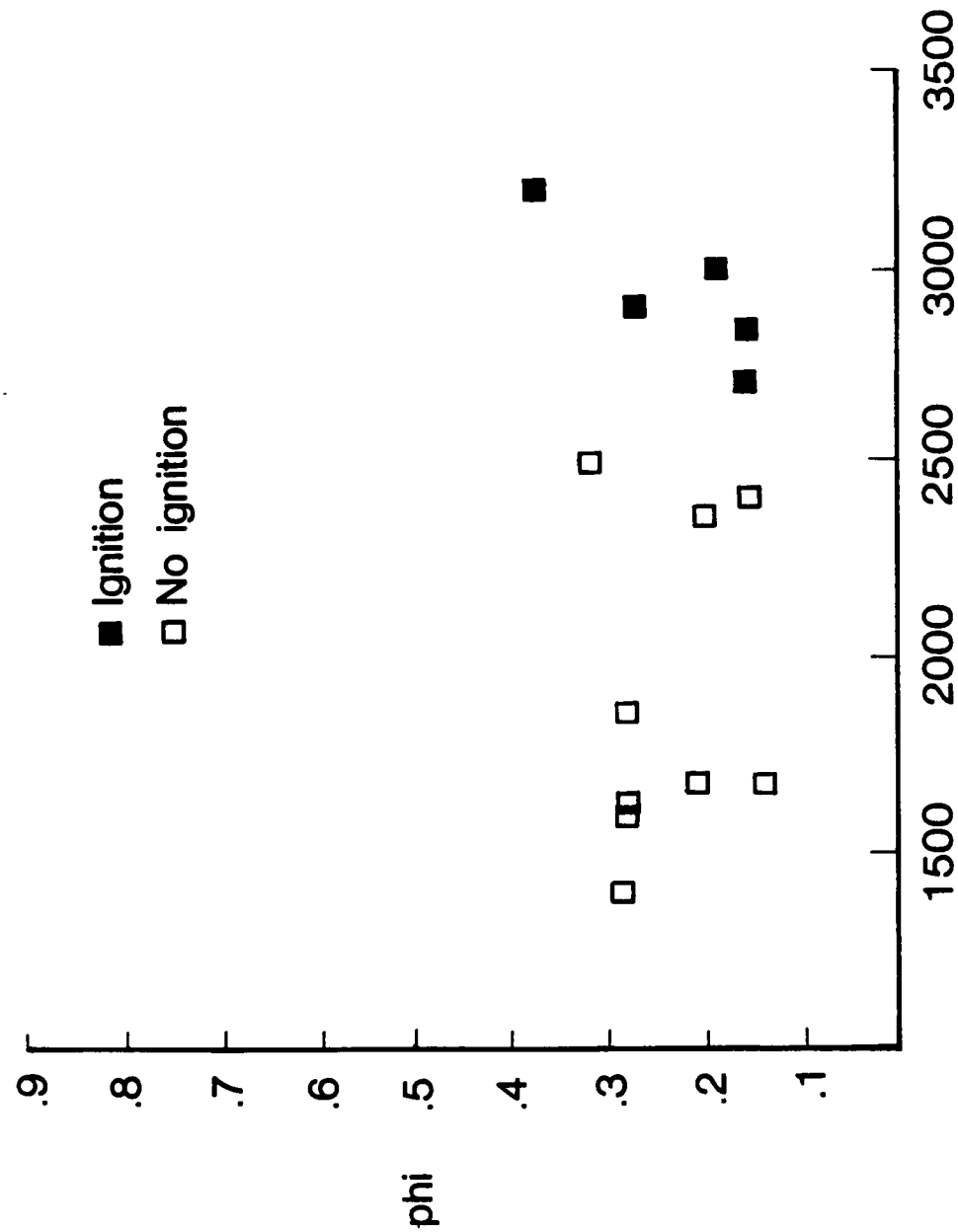

Fig. 31(d). Methane ignition limit with 2 kW argon-hydrogen plasma.

compared with a temperature of 2800 R required for autoignition of hydrogen with this model. Hydrogen flameheld at the plasma torch injection location, and even with the step configuration the flame did not propagate to the upstream fuel injector. The one no-ignition point shown in Fig. 31(a) was for injection downstream of the plasma torch.

The ignition limits for ethylene (C_2H_4) are shown in Fig. 31(b). The scatter around 1500 R indicates that the ignition limit is close to that temperature for 2 kW net torch power. Again, there does not seem to be any sensitivity to equivalence ratio. However, an effect of torch power was found. When the power was increased from 2 kW to approximately 3.5 kW (flagged points), ignition occurred at 1380 R. No tests were run at lower temperatures with this fuel.

Only three tests were conducted with ethane (C_2H_6); the results from these tests are shown in Fig. 31(c). Ethane ignited at a total temperature of 2200 R but failed to ignite at 1717 R with 1.6 kW net torch power. More tests should be conducted with this fuel to determine the dependence of the ignition limits on total temperature and torch power.

Ignition limits for methane (CH_4) are shown in Fig. 31(d). Methane was not ignited at total temperatures below 2700 R. However, above 2700 R, a net power input of 1.5 kW was sufficient for ignition. In the 1700 R temperature range, attempts to ignite methane with up to 4.0 kW were not successful. In an investigation using the same facility and similar hardware, autoignition of methane was not achieved for any temperature tested up to 4000 R.[61]

The minimum ignition total temperatures of the fuels tested using the plasma torch igniter are summarized in Table III. These data follow the same ranking as the unpiloted data reported by Suttrop.[167] It was concluded from these limited tests that the Plasmadyne plasma torch is an effective igniter and flameholder for hydrogen and several gaseous hydrocarbon fuels in the unconfined flow configuration. Based on these promising results, the direct connect expanding duct test hardware was constructed as shown in Fig. 24, and a limited test program was conducted to obtain results in scramjet-like hardware.

Tests with the expanding duct model used three equally spaced fuel injectors upstream and downstream of the plasma torch on the top injector block and three upstream injectors on the bottom block. Figure 32 shows the resulting pressure distribution during a test at a total temperature of 1800 R with hydrogen fuel. The circle symbols represent data for no fuel injection and are given for reference. The square symbols are for ignition and flameholding with the plasma torch operating at 4.2 kW net power. The total upstream equivalence ratio was 0.17; the downstream equivalence ratio was 0.38. The diamond symbols represent data for a similar test where the fuel was initially a pyrophoric mixture of silane and hydrogen. Once combustion was established this mixture was replaced with pure hydrogen.

The nozzle exit pressures just upstream of the step were not affected when the torch was acting as a flameholder. There was a slight pressure rise at the nozzle exit at these conditions for the silane-ignited test with flameholding at the step. For an equivalence ratio of 0.55, approximate combustion efficiency distributions, as

TABLE III - IGNITION LIMITS FOR MACH 2 FLOW

FUEL	MINIMUM IGNITION TOTAL TEMPERATURE (R)	
	PLASMA IGNITION	AUTOIGNITION
HYDROGEN	<1065	2800
ETHYLENE	1500	3240*
ETHANE	2000	3600*
METHANE	2700	>4000*

* These temperatures were determined using a similar geometry, the details of which were reported in Ref. 61.

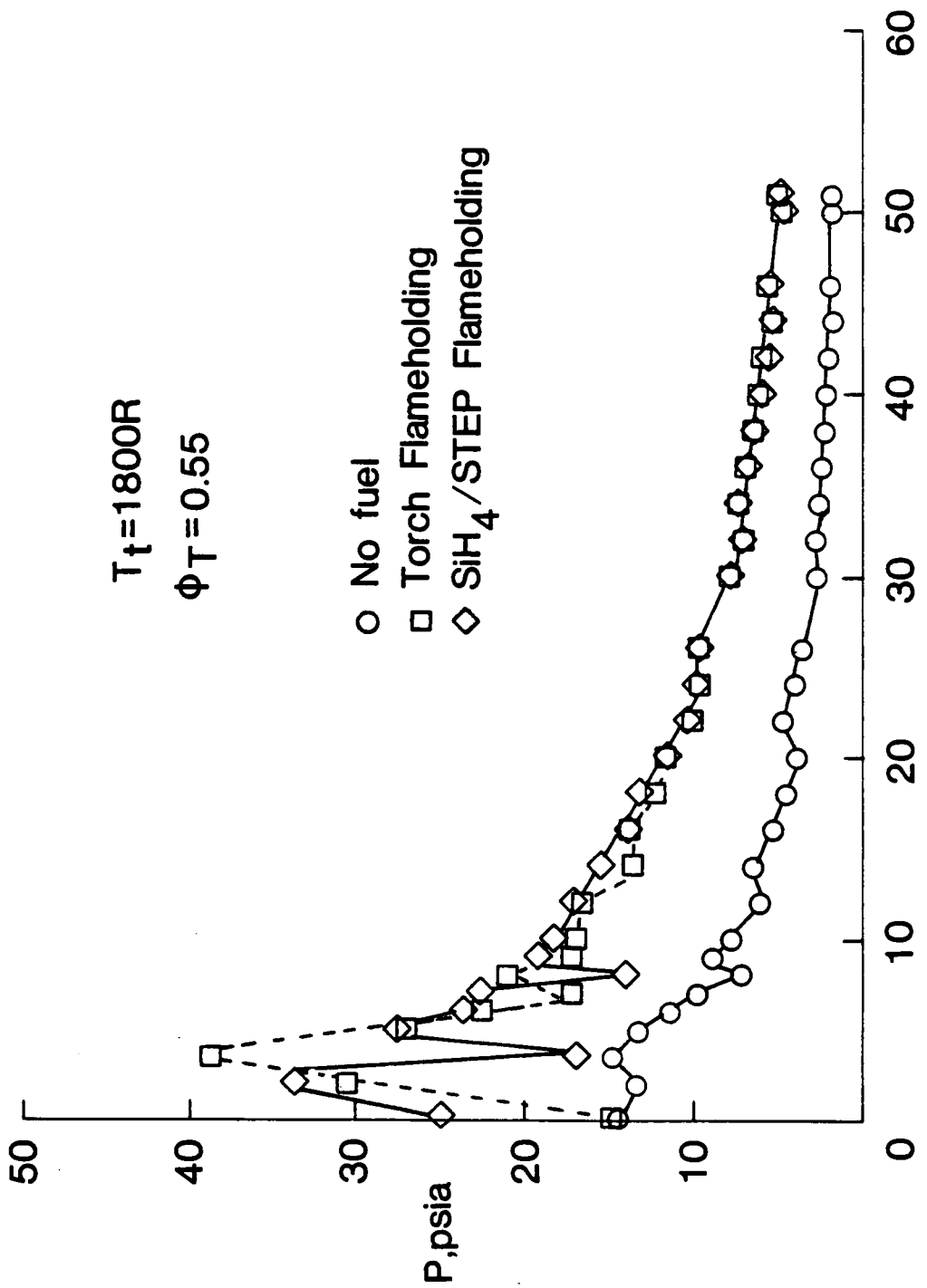

Fig. 32. Pressure distributions - supersonic combustion of hydrogen.

estimated from one dimensional analysis of the pressure data, are shown in Fig. 33. These calculations indicate that about 60 percent of the fuel was burned in the 52-inch length of the combustor. These calculations also indicate that combustion occurred in the all-supersonic combustion mode for this equivalence ratio level and these test conditions. The lateral wall pressures located on the expanding duct 6 inches downstream of the injector blocks were essentially equal and implied no large variations in the flow. It is assumed that poor combustion efficiency resulted from the fuel rich top wall and the possibility that the fuel injected from the bottom wall did not ignite until some distance downstream.

When the equivalence ratio was increased to 0.7, mainly by increasing the downstream fuel from the top wall, the pressure distributions shown in Fig. 34 were obtained. The circle symbols represent data taken during operation of the plasma torch, and the square symbols represent data at the same conditions after the torch was extinguished. Note that in the confined flow tests with a rearward facing step, the model flameheld with the torch off; however, the model was being fueled by both upstream and downstream fuel injectors. Also, note the rise in the upstream pressures when the torch was turned off. These data indicate that the torch acted as a flameholder and prevented the combustion-induced pressure rise from propagating upstream even though the combustor was fueled such that mixed (subsonic-supersonic) mode combustion occurred. One-dimensional analysis indicated that the combustor flow was choked at the end of the constant area section and then expanded to a Mach number of 1.7 at the

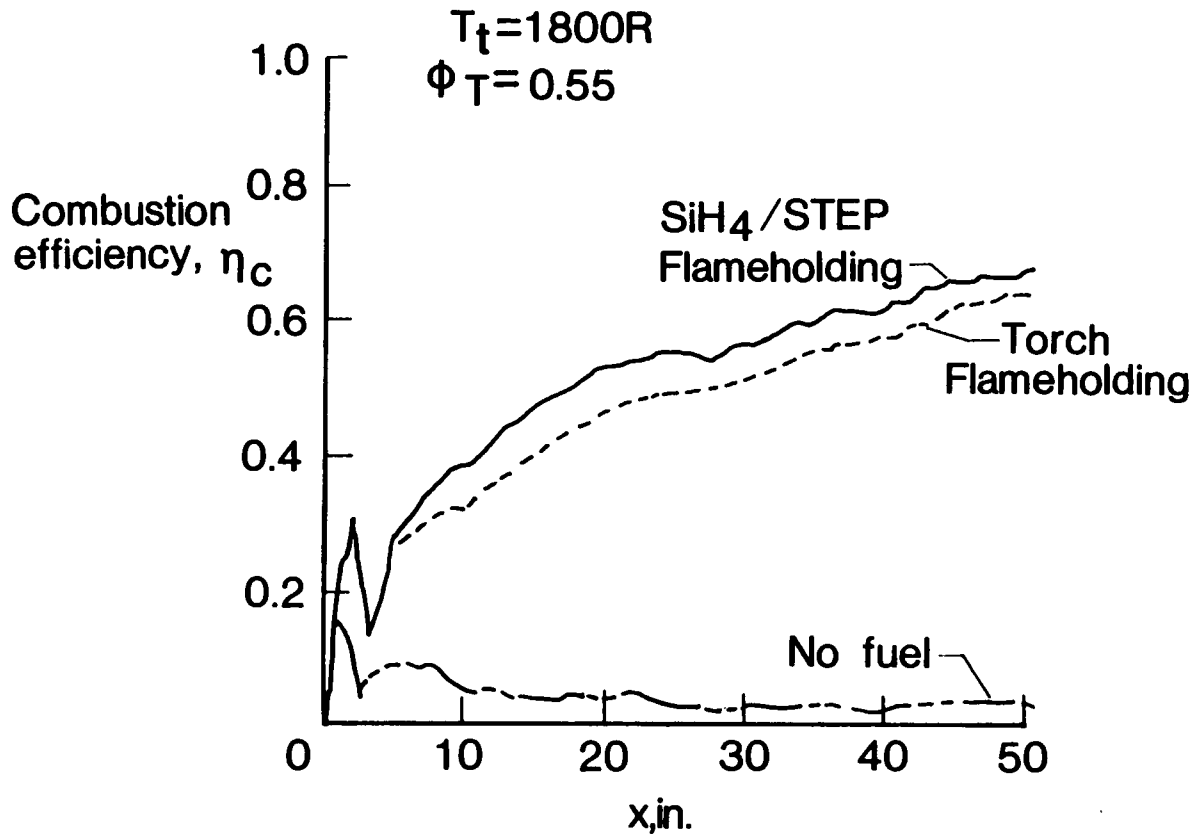

Fig. 33. Combustion efficiencies - supersonic combustion of hydrogen.

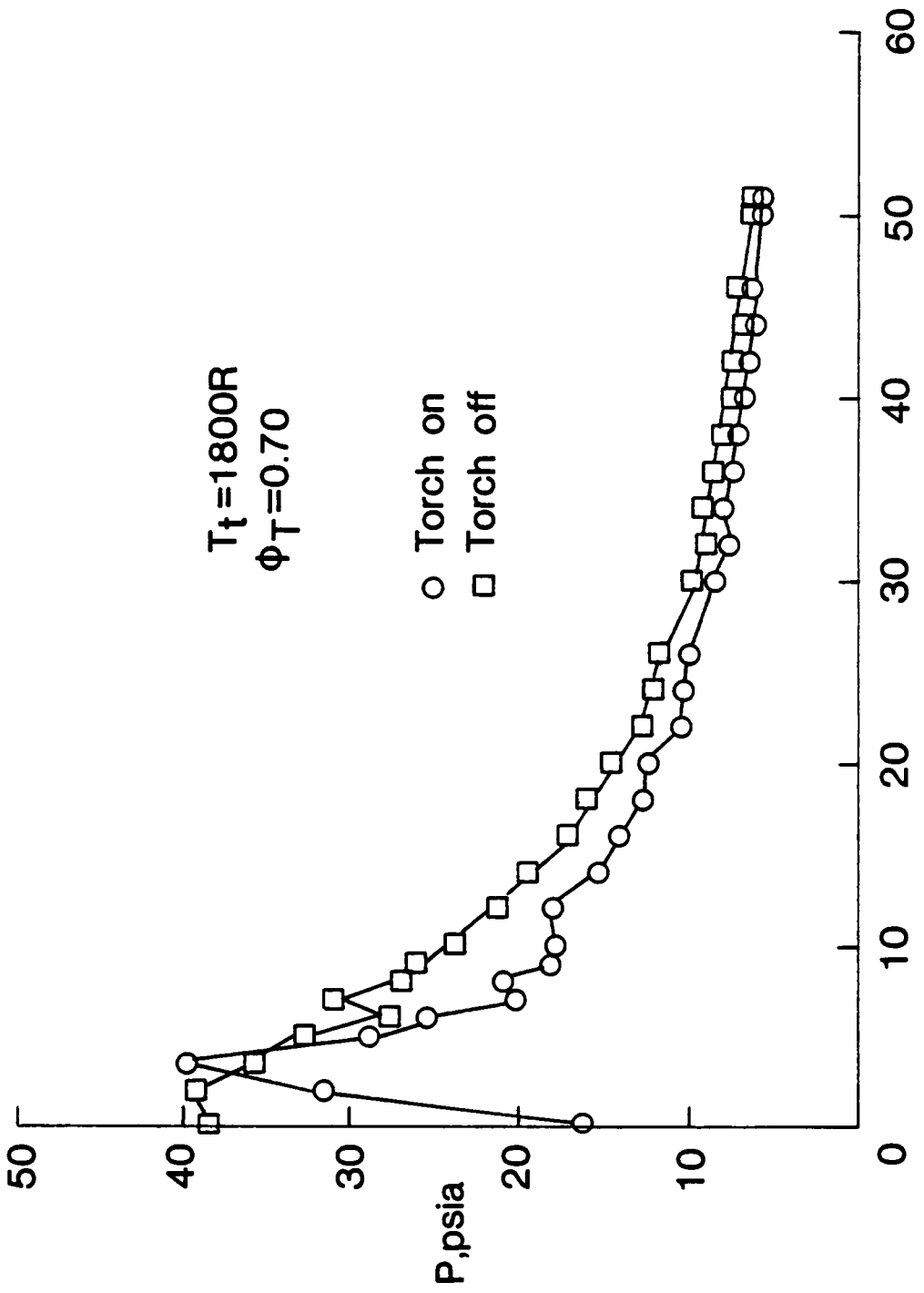

Fig. 34. Pressure distributions - mixed mode combustion of hydrogen.

end of the duct. Approximate combustion efficiencies for these tests are shown in Fig. 35. With the torch on and the flame stabilized by the resulting free radicals, the approximate combustion efficiency was estimated to be about 60 percent. When the torch was turned off, the efficiency rose to about 80 percent, the combustion-induced pressure rise moved upstream, and the flame was held on the step. In fact, the pressure rise extended upstream of the step. Again these efficiencies are probably affected by poor fuel distribution resulting from the particular injection distribution used. Because the torch was able to stabilize the flame and prevent upstream propagation, it may have the potentially beneficial effect of reducing the sensitivity of supersonic combustors to combustor/inlet interactions at high equivalence ratios.

Several tests using hydrocarbon fuels in the expanding duct configuration employing the same injector pattern as was used for the hydrogen (3 upstream and downstream top wall and 3 upstream bottom wall) resulted in poor combustion efficiency. The observation of this poor performance at conditions where the unconfined flow tests had indicated combustion, but with a different injector configuration, implies a strong sensitivity to combustor geometry and/or fuel distribution. Similar tests conducted under NASA contract at General Applied Science Laboratories have shown a strong sensitivity to injector design and location of the silane injection and location of wall expansions. Hydrocarbon fuels performed poorly under conditions which had worked well with hydrogen fuel.[168]

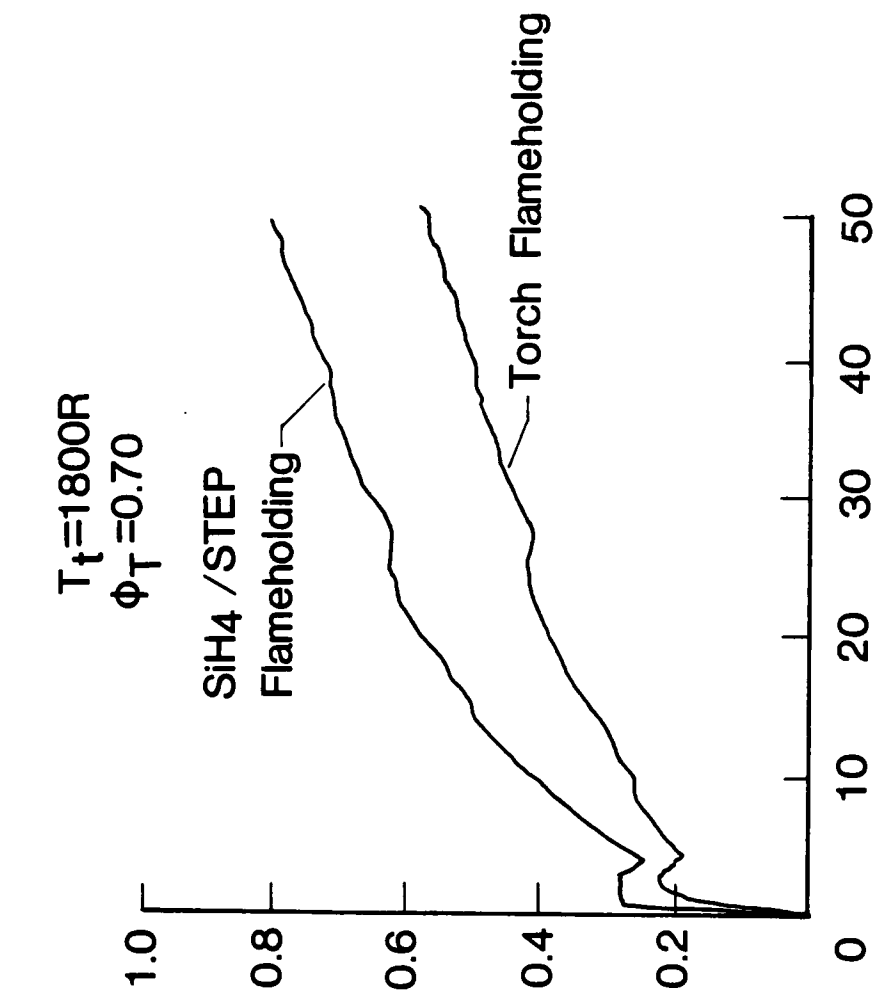

Fig. 35. Combustion efficiencies - mixed mode combustion of hydrogen.

9.2 Design of an Integrated Igniter/Flameholder Configuration

Based on the results of the initial tests, a new injector configuration was developed for use with the low-power plasma torch. The rationale for this design was that the torch should be placed at a location where a minimal amount of ignition energy was required and where any resulting combustion could be used as "leverage" to ignite more fuel. In this type of design the plasma torch could be effective with a minimum power input. The optimum location is obviously the recirculation zone downstream of a rearward facing step, where the increased static temperature and residence time reduce the required ignition energy. However, in order for the torch to be effective with a minimal power input, the recirculation zone must contain a near-stoichiometric mixture. For the "standard" injector design, where all of the fuel injectors are located 3 to 4 step heights downstream of the step, the recirculation region may be excessively rich, depending on the mass flow rate of fuel and the free stream conditions. A possibly better design would incorporate two independently controlled stages of injection, with the upstream injectors fueling the recirculation zone.

For the recirculation region to contain a well-mixed combination of fuel and air, the first fuel injection stage must be located far enough upstream to allow mixing to occur prior to the gases reaching the step. For transverse injection the mixing length is proportional to the injector diameter (see Section 2). Therefore, small orifices should be used in the first stage of fuel injection so that the

injectors do not have to be located far upstream of the step. The penetration of fuel into the crossflow is also proportional to injector diameter; therefore, small holes will not provide much penetration. However, since the purpose of the upstream injectors is to fuel the recirculation zone, penetration is not required or desired.

The second stage or main fuel injectors must be located far enough downstream of the step that the fuel flow will not affect the concentration in the recirculation zone. For Mach 2 flow past a rearward-facing step the reattachment point of the recirculation zone is located approximately 3 to 5 step heights downstream of the step. The separated region ahead of an injector normal to the flow begins approximately 4 to 8 diameters upstream of the injector. Therefore, the distance between the second stage of fuel injectors and the step should be approximately equal to the sum of 4 step heights and 6 injector diameters.

The injector block which resulted from the design concepts outlined above incorporated a 0.150-inch high rearward facing step. This step height was based on experience with the scale of the test section in the facility. (The step height was approximately 10 percent of the height of the duct.) The plasma torch was located 0.30 inches (two step heights) downstream of the step on the centerline of the duct. This location placed the torch approximately in the center of the recirculation region. The primary fuel injection stage consisted of three 0.10-inch diameter holes located 1.16 inches downstream of the step. This diameter was also based on experience with

the scale of the test section. As was discussed in Section 2, previous studies have indicated that for optimum mixing in supersonic flows with transverse injection, the lateral spacing between fuel injectors should be approximately equal to the gap, the distance between opposite walls of fuel injection. The gap for the test section used in these experiments was 1.8 inches, while the width of the test section was 3.46 inches. Therefore, two injectors should provide optimum mixing for this test section. However, by locating a fuel injector in line with the plasma torch it might be possible to enhance any effect of the plasma. Therefore, a three orifice configuration was chosen for the primary fuel injectors.

The pilot fuel injection stage consisted of five 0.05-inch diameter holes located 1.89 inches upstream of the step. The lateral spacing between the holes was 0.50 inches. The hole diameter, spacing and location upstream of the step were interrelated. The axial location for the current design was dictated by the facility hardware. With the injector location fixed, the orifice diameter was chosen so that the mixture near the wall was approximately stoichiometric in the region where the flow passed the recirculation zone. (The mixture composition was estimated by examining concentration profiles from Refs. 37 and 38 for single and multiple injectors.) The lateral spacing was chosen such that the injected hydrogen would fuel the recirculation zone in a fairly uniform manner. A sketch of the injector/flameholder design is presented in Fig. 36, and a photograph of the hardware is shown in Fig. 37. The flow region was only the central portion of the block. The space outside the flow region was

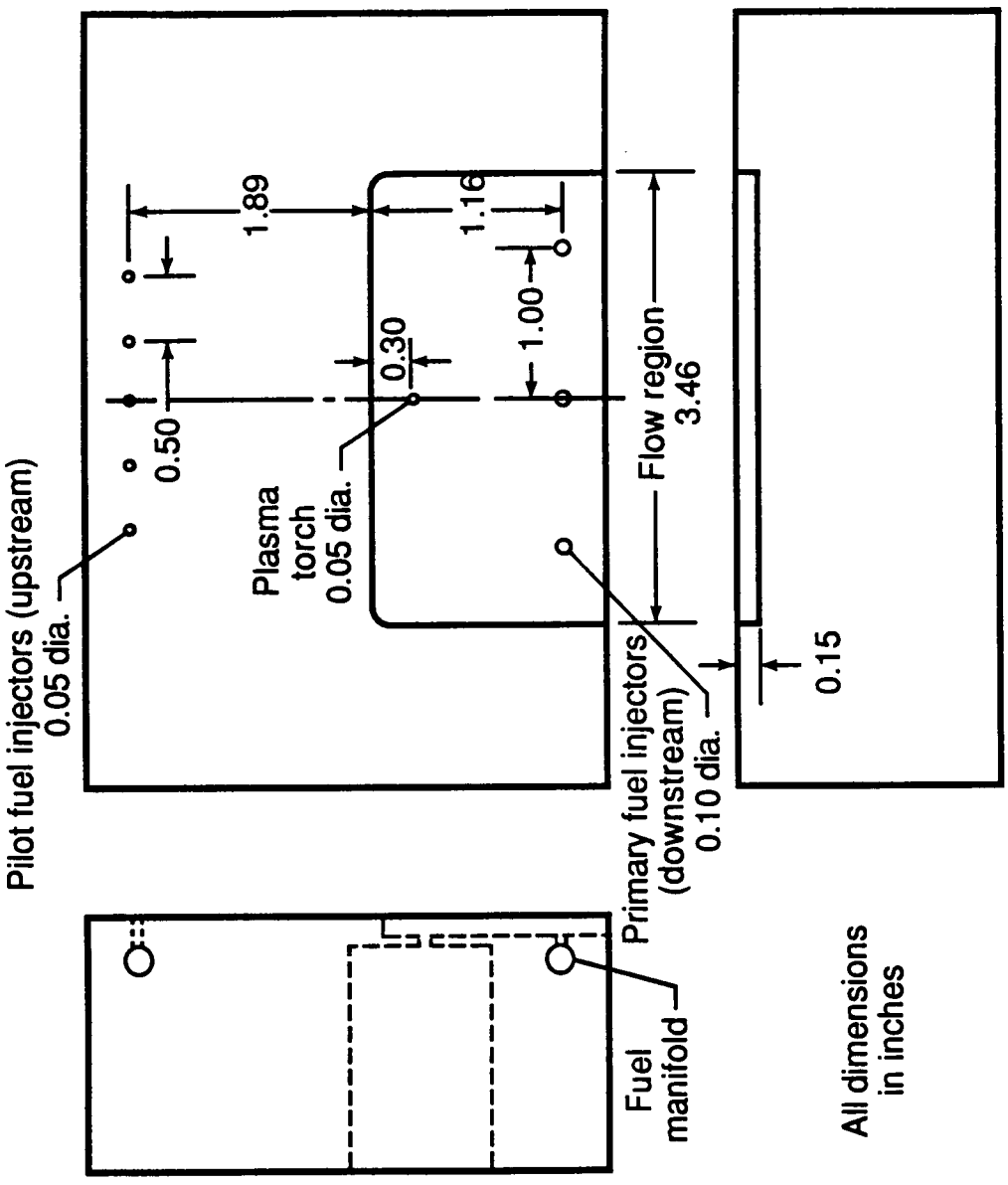

Fig. 36. Injector block.

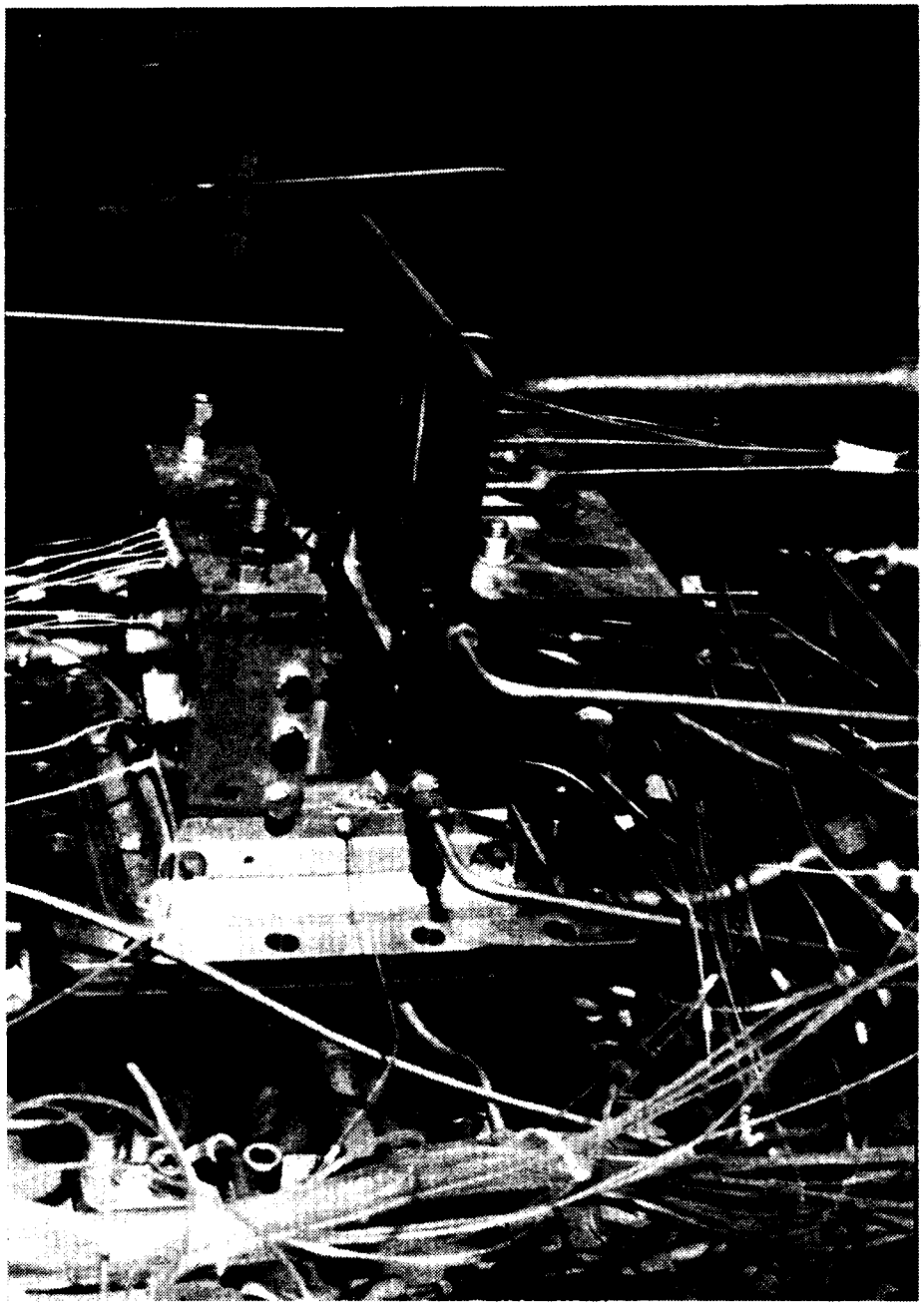

Fig. 37. Photograph of injector block mounted in test section.

for addition of the sidewalls required for ducted tests. The bulk equivalence ratios of the pilot and primary fuel injectors will be referred to as ϕ_1 and ϕ_2, respectively. This injector design, when used with separate controls for the two injection stages, uncouples the ignition and flameholding scheme from the primary fuel injection.

9.3 Integrated Igniter/Flameholder Tests

To determine the ignition and flameholding characteristics of the VPI plasma torch used in conjunction with the previously described injection scheme, both unconfined and ducted tests were conducted. Fuel was injected from the newly-designed injector block, while the opposite side of the test section was not fueled. The test program was divided into two parts. The first part of the test program was designed to explore the effects of torch operating conditions on the ignition and flameholding characteristics of the new injector design as a function of total temperature. The second part of the test program was designed to investigate the characteristics of the injector configuration with igniters other than the plasma torch. In previous experiments using upstream injection, all of the fuel had been added upstream, and at the higher equivalence ratios the recirculation zone became too rich to be an effective flameholder. In the current design with the main fuel injectors located well downstream of the step, the main fuel injection is decoupled from the pilot fuel flow. The use of the pilot fuel was motivated by the desire to obtain the maximum "leverage" from the low-power plasma torch in terms of

generation of free radicals in the recirculation region downstream of the rearward facing step.

9.3.1 Variable Torch Conditions

The effects of torch operating conditions on the ignition and flameholding characteristics of the new injector design were investigated with nominal bulk equivalence ratios for the upstream and downstream injectors of 0.042 and 0.26, respectively. The total fuel mass flow rate was nominally 0.032 lb/s. The burner total temperature and the plasma torch parameters were the primary variables. The data from the unconfined and ducted tests are presented in Tables IV and V, respectively. Results from the unconfined flow tests that show the flameholding location will be presented first followed by results from the combustor tests.

A few typical UV-TV photographs taken from the recorder and video analyzer are presented and discussed. Only pictures from the video camera mounted normal to the flow are presented, since these were used to identify the location of the flame. The model as viewed by this camera is shown in Fig. 38. Note that the upstream fuel injector is not in the field of view. Furthermore, part of the combustion region is hidden from view in the recessed region downstream of the step. A UV-TV photograph from a test with an air total temperature of 1720 R and a torch power of 630 W with a 1:1 argon-hydrogen mixture is shown in Fig. 39(a). The brightness at the torch location is not accurate; it is the result of the high intensity torch radiation being reflected

Table IV. Summary of data from unconfined flow tests with VPI plasma torch.

RUN	BATCH	Q_{AR} (scfh)	Q_{H_2} (scfh)	Q_{TOT} (scfh)	α	V (volts)	I (amps)	P (W)	P/Q_{TOT} (W/scfh)	ϕ_1	ϕ_2	T_t (R)	UV Intensity (% FS) Torch on Inj	Torch on Dn	Torch off Inj	Torch off Dn
14	2	20.0	20.0	40.0	1.00	70	18	1260	31.5	0.043	0.29	1680	.54	.28	-	-
	3	-	-	-	-	-	-	-	-	0.053	0.36	2800	-	-	.98	.45
	4	20.0	20.0	40.0	1.00	70	22	1540	38.5	0.05	0.17	530	-	-	-	-
	5	20.0	20.0	40.0	1.00	70	23	1610	40.3	0.022	0.15	530	-	-	-	-
	6	20.0	0.00	20.0	∞	18	50	900	45.0	0.040	0.27	1650	.32	.11	*	*
16	2	10.0	10.5	20.5	0.95	70	9	630	30.7	0.042	0.27	1720	.50	.21	.45	.20
	3	10.0	10.0	20.0	1.00	60	20	1200	60.0	0.044	0.27	1790	.53	.23	.49	.22
	5	10.0	15.0	25.0	0.67	77	12	920	37.0	0.042	0.26	1820	.52	.22	.50	.22
	6	10.0	5.0	15.0	2.00	50	15	750	50.0	0.042	0.26	1790	.50	.20	.46	.20
	7	-	-	-	-	-	-	-	-	0.056	0.37	2980	-	-	.86	.35
	8	-	-	-	-	-	-	-	-	0.050	0.33	2900	-	-	.92	.45
	9	15.0	15.0	30.0	1.00	69	27	1860	62.1	0.045	0.27	1750	.50	.21	.44	.20
	10	10.0	10.0	20.0	1.00	65	12	780	39.0	0.042	0.26	2150	-	-	.62	.28
	11	10.0	10.0	20.0	1.00	70	16	1120	56.0	0.043	0.26	2170	-	-	.63	.28
	12	-	-	-	-	-	-	-	-	0.043	0.29	2320	-	-	*	*
	16	-	-	-	-	-	-	-	-	0.046	0.31	2620	-	-	.59	.21
	18	-	-	-	-	-	-	-	-	0.047	0.30	2810	-	-	*	*

* no combustion

x no combustion (not repeatable)

Table IV. Concluded.

RUN	BATCH	Q_{AR} (scfh)	Q_{H_2} (scfh)	Q_{TOT} (scfh)	e	V (volts)	I (amps)	P (W)	P/Q_{TOT} (W/scfh)	ϕ_1	ϕ_2	T_t (R)	UV Intensity (% FS) Torch on Inj	Torch on Dn	Torch off Inj	Torch off Dn
17	2	15.0	15.0	30.0	1.00	62	15	930	31.0	0.075	0.28	1750	-	-	X	X
	3	15.0	15.0	30.0	1.00	63	15	950	31.5	0.042	0.27	1800	-	-	-	-
	4	10.0	10.0	20.0	1.00	54	14	760	37.8	0.041	0.27	1500	-	-	-	-
	5	20.0	20.0	40.0	1.00	72	40	1440	36.0	0.044	0.28	1650	-	-	-	-
	6	20.0	20.0	40.0	1.00	73	20	1460	36.5	0.041	0.27	1630	-	-	-	-
	7	20.0	20.0	40.0	1.00	72	20	1440	36.0	0.041	0.27	1620	-	-	-	-
	9	15.0	15.0	30.0	1.00	75	13	980	32.5	0.042	0.28	1680	-	-	-	-
	10	20.0	20.0	40.0	1.00	73	12	1460	36.5	0.042	0.28	1660	-	-	*	*
	12	20.0	20.0	40.0	1.00	74	20	1480	37.0	0.074	0.27	1660	-	-	-	-
18	16	20.0	20.0	40.0	1.00	70	20	1400	35.0	0.039	0.25	1600	-	-	.37	-
	17	20.0	20.0	40.0	1.00	70	20	1400	35.0	0.039	0.27	1610	-	-	-	-
	18	20.0	20.0	40.0	1.00	70	20	1400	35.0	0.039	0.27	1590	-	-	.29	-
	19	20.0	20.0	40.0	1.00	80	20	1600	40.0	0.040	0.27	1600	-	-	*	*
	20	20.0	20.0	40.0	1.00	74	20	1480	37.0	0.040	0.27	1620	-	-	*	*

Table V. Summary of data from ducted tests with VPI plasma torch.

RUN	BATCH	Q_{AR} (scfh)	Q_{H_2} (scfh)	Q_{TOT} (scfh)	α	V (volts)	I (amps)	P (W)	P/Q_{TOT} (W/scfh)	ϕ_1	ϕ_2	T_t (R)	η_c on[1]	η_c gases[2]	η_c off[3]
20	2	20.0	20.0	40.0	1.00	75	10	750	18.8	0.042	0.27	1740	-	-	-
	3	20.0	20.0	40.0	1.00	78	10	780	19.5	0.041	0.26	1730	0.43	0.43	-
	4	20.0	20.0	40.0	1.00	70	20	1400	35.0	0.042	0.27	1790	0.48	0.45	-
	5	20.0	20.0	40.0	1.00	64	24	1540	38.4	0.042	0.27	1780	0.48	-	0.54
	7	21.9	46.8	68.6	0.46	80	31	2480	36.2	0.045	0.27	1800	-	-	x
	8	22.0	47.1	69.1	0.47	81	32	2590	37.5	0.044	0.27	1800	0.45	-	0.54
	9	22.0	47.5	69.5	0.46	79	30	2370	34.1	0.042	0.26	1790	0.48	0.48	-
	10	22.1	47.2	69.3	0.47	80	31	2480	35.8	0.042	0.27	1800	0.47	-	0.55
	11	20.0	20.0	40.0	1.00	80	11	880	22.0	0.094	0.28	1850	0.47	-	0.47
	12	20.0	20.0	40.0	1.00	80	10	800	22.0	0.079	0.29	1840	0.45	-	0.45
	13	20.0	20.0	40.0	1.00	80	10	800	20.0	0.130	0.26	1800	0.53	-	0.53
	14	20.0	20.0	40.0	1.00	80	10	800	20.0	0.021	0.27	1820	0.46	-	0.57
	15	20.0	20.0	40.0	1.00	80	10	800	20.0	-	0.28	1880	*	-	0
	16	20.0	20.0	40.0	1.00	76	12	910	22.0	0.052	0.28	1930	0.49	-	-
	17	20.0	20.0	40.0	1.00	75	11	830	20.6	0.036	0.22	1400	+	0.62	0.62
	18	22.3	30.0	52.3	0.74	75	20	1500	28.7	0.039	0.26	1450	0.57	-	0.60

* no combustion

x no combustion (not repeatable)

\+ torch blown out by combustion-generated pressure rise

on[1] combustion efficiency with torch operating

gases[2] combustion efficiency with torch power off but feedstock still flowing

off[3] combustion efficiency with torch power and feedstock flow off

Table V. Concluded.

RUN	BATCH	Q_{AR} (scfh)	Q_{H_2} (scfh)	Q_{TOT} (scfh)	e	V (volts)	I (amps)	P (W)	P/Q_{TOT} (W/scfh)	ϕ_1	ϕ_2	T_t (R)	η_c on[1]	η_c gases[2]	η_c off[3]
21	2	20.0	20.0	4.0	1.0	75	10	750	18.1	0.021	0.085	1840	0.53	-	*
	3	22.1	0.00	22.1	∞	20	38	760	34.4	0.040	0.28	1750	0.56	-	0.56
	4	22.0	0.00	22.0	∞	20	38	760	34.4	0.043	0.27	1800	0.56	-	0.56
	5	20.0	20.0	40.0	1.0	84	10	840	21.0	0.14	0.27	1790	+	0.53	0.53
	6	20.0	20.0	40.0	1.0	74	10	740	18.5	0.042	0.27	2190	0.59	-	0.59
	7	20.0	20.0	40.0	1.0	84	10	840	21.0	0.14	0.28	2200	0.53	-	0.53
	8	22.0	0.00	22.0	∞	20	37	740	33.6	0.039	0.27	1460	*	-	-
	9	22.0	0.00	22.0	∞	20	38	760	34.5	0.039	0.27	1460	*	-	-
	13	22.0	0.00	22.0	∞	20	38	760	34.5	0.038	0.27	1610	0.43	-	0.43
22	2	20.0	20.0	40.0	1.0	85	13	1110	27.6	0.038	0.24	1590	0.51	-	-
	3	20.0	20.0	40.0	1.0	70	14	980	24.5	0.040	0.26	1610	10.44	-	x
	4	20.0	20.0	40.0	1.0	65	15	980	24.4	0.039	0.25	1610	0.44	0.59	-
	5	20.0	20.0	40.0	1.0	80	11	880	22.0	0.048	0.30	2430	0.55	-	0.55
	6	-	-	-	-	-	-	-	-	0.041	0.29	2490	-	-	*
	7	-	-	-	-	-	-	-	-	0.040	0.29	2700	-	-	0.60
	10	20.0	20.0	40.0	1.0	80	12	960	24.0	0.041	0.29	2670	0.54	-	0.54
	11	-	-	-	-	-	-	-	-	0.043	0.29	2700	-	-	0.63
	13	-	-	-	-	-	-	-	-	0.043	0.33	3080	-	-	0.51
	14	-	-	-	-	-	-	-	-	0.043	0.27	3060	-	-	0.60
	15	-	-	-	-	-	-	-	-	0.044	0.28	3150	-	-	0.55
										-	0.28	3150		-	0.66
	16	-	-	-	-	-	-	-	-	0.044	0.28	2520	-	-	*
	17	-	-	-	-	-	-	-	-	0.046	0.30	2670	-	-	0.62
	18	-	-	-	-	-	-	-	-	0.045	0.28	2640	-	-	0.67

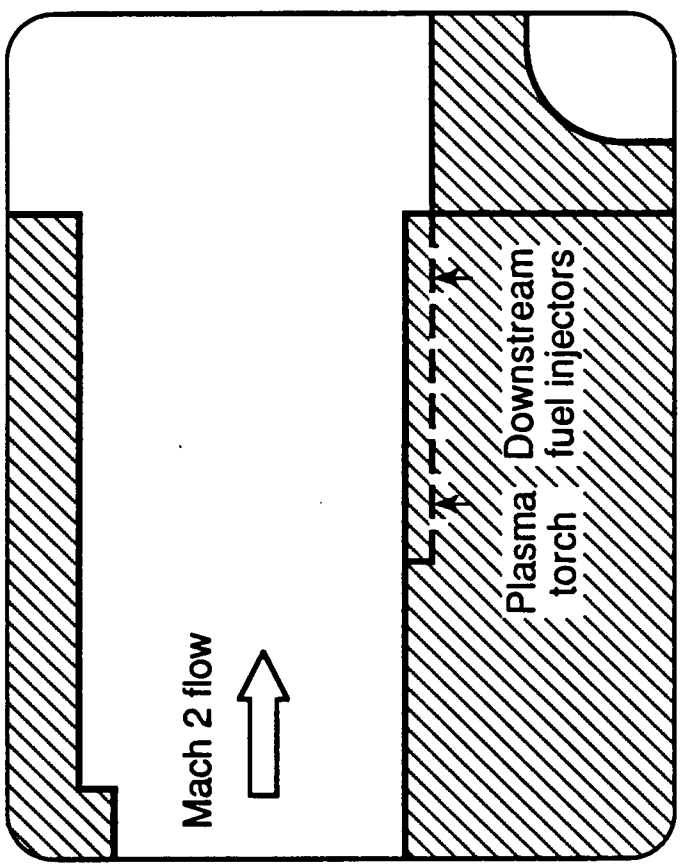

Fig. 38. Unducted model as viewed by UV-TV.

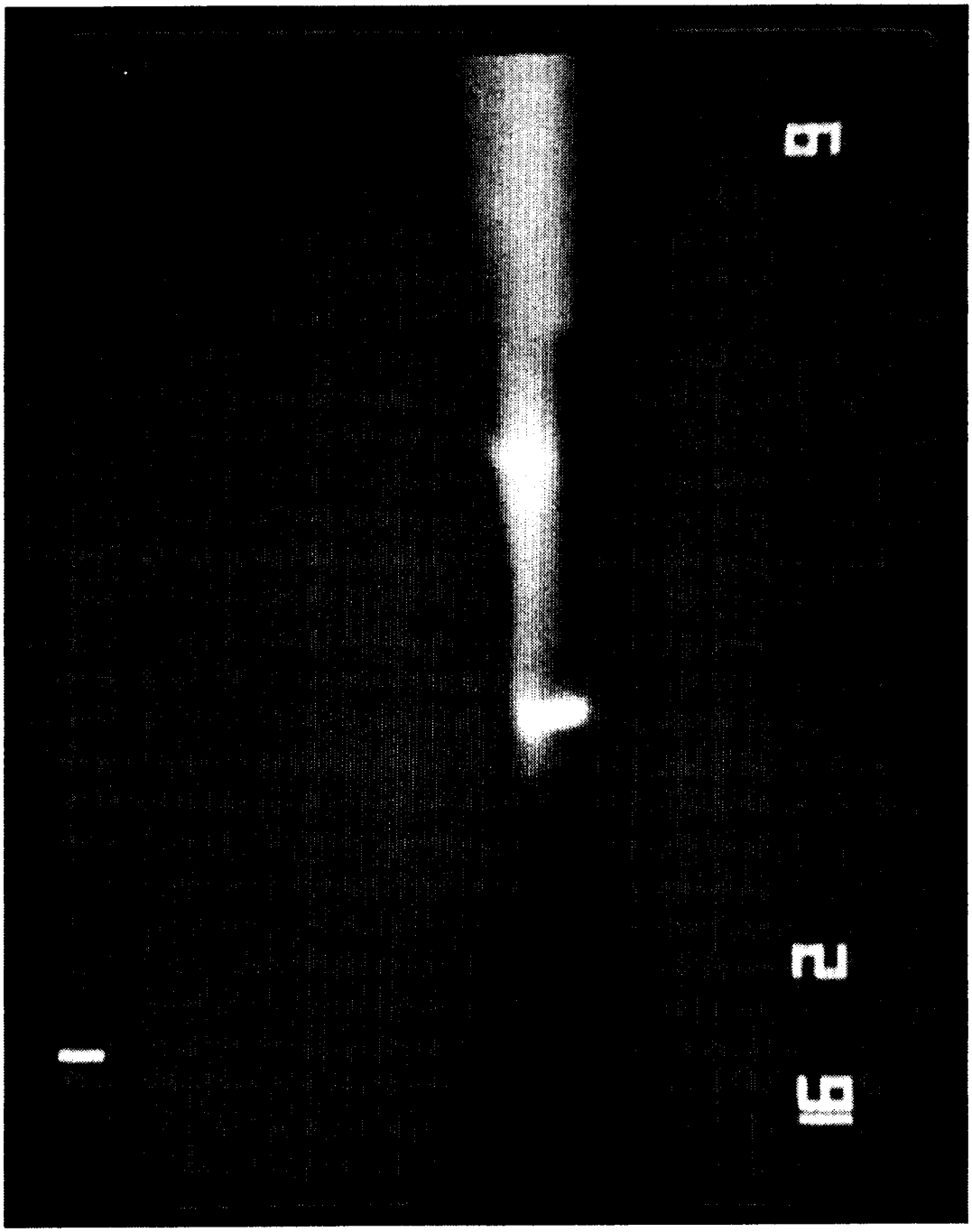

Fig. 39(a). UV-TV photograph (argon-hydrogen plasma).
(T_t = 1720 R, P = 630 W, Q = 20.5 scfh, α = 0.95)

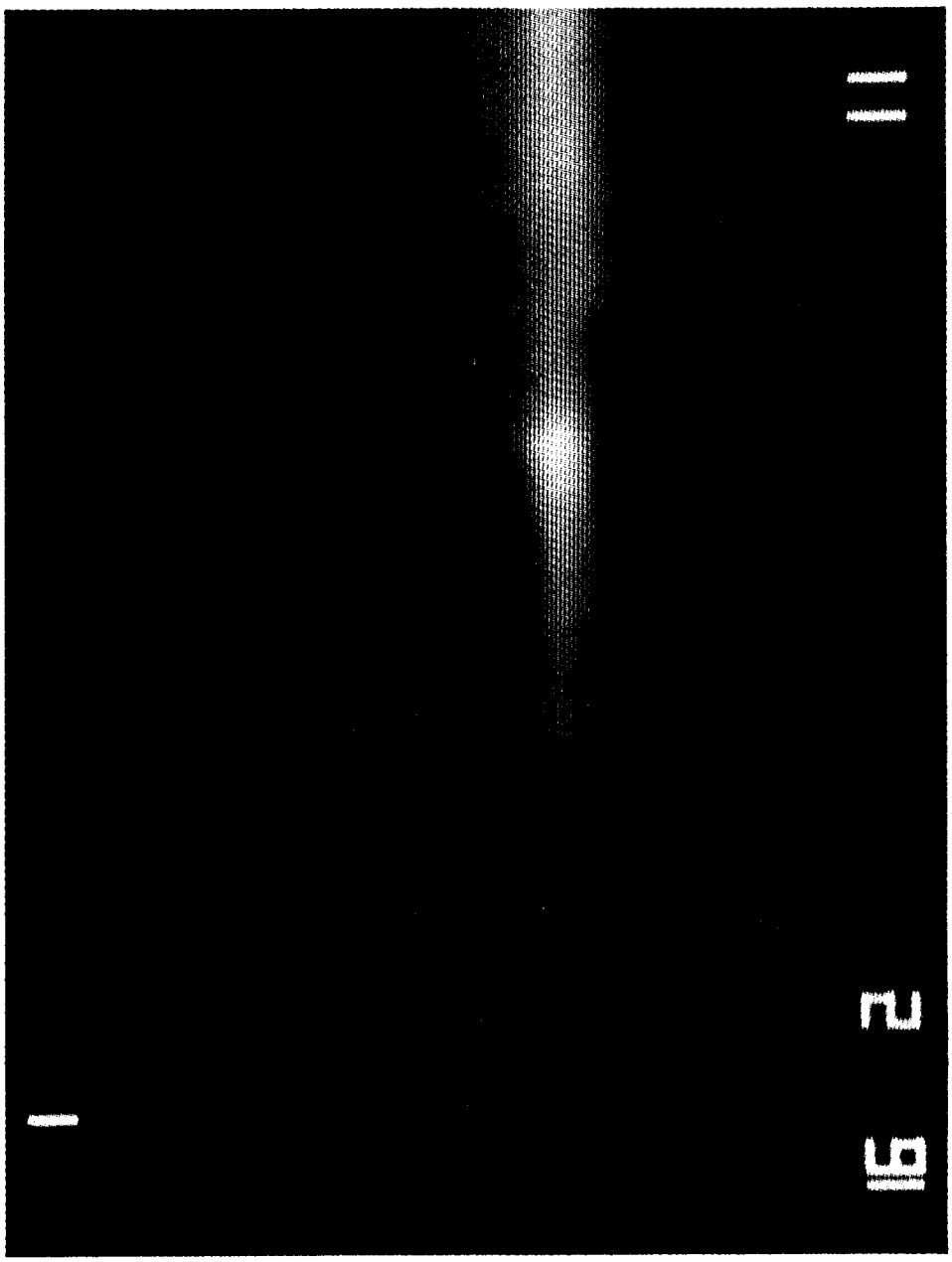

Fig. 39(b). UV-TV photograph (after torch turned off).
(T_t = 1720 R, P = 0 W, Q = 0 scfh)

prior to detection by the camera. Radiation (combustion) was observed in the step region and well downstream of the primary fuel injectors. Figure 39(b) shows a similar test during which the plasma torch was extinguished after ignition was established. The flame was still held in the recirculation zone. These photographs suggest that, once ignition was established, the excess free radicals supplied externally by the torch did not significantly increase the free radical pool generated by the reaction of the pilot fuel in the recirculation zone.

A video analyzer was used to make relative measurements of the intensity of the video images in order that the signal levels could be compared. A photograph with the video analyzer located at the primary fuel injection station is shown in Figure 40. Analysis of the images showed little variation in intensity for a wide varity of plasma torch operating conditions (P from 630 to 1860 W, α from 0.5 to 2.0, and Q from 15 to 60 scfh). However, when all argon was used for the torch feedstock ($\alpha = \infty$), the measured intensity was only half of that recorded during the tests with the argon-hydrogen feedstock. The UV-TV picture from this test is shown in Fig. 41. The faint circle appearing in the picture is the result of spherical aberration of the torch radiation. Unlike the combustion ignited by the argon-hydrogen plasma, the weak flame ignited by the argon plasma blew off immediately when the torch was turned off. The minimum total temperature for autoignition with this configuration was 2720 R. Figure 42 shows the UV-TV photograph for an autoignition test. Note that although the intensity is greater, the flame did not appear to spread as far upstream as it did when the plasma torch was used as an igniter.

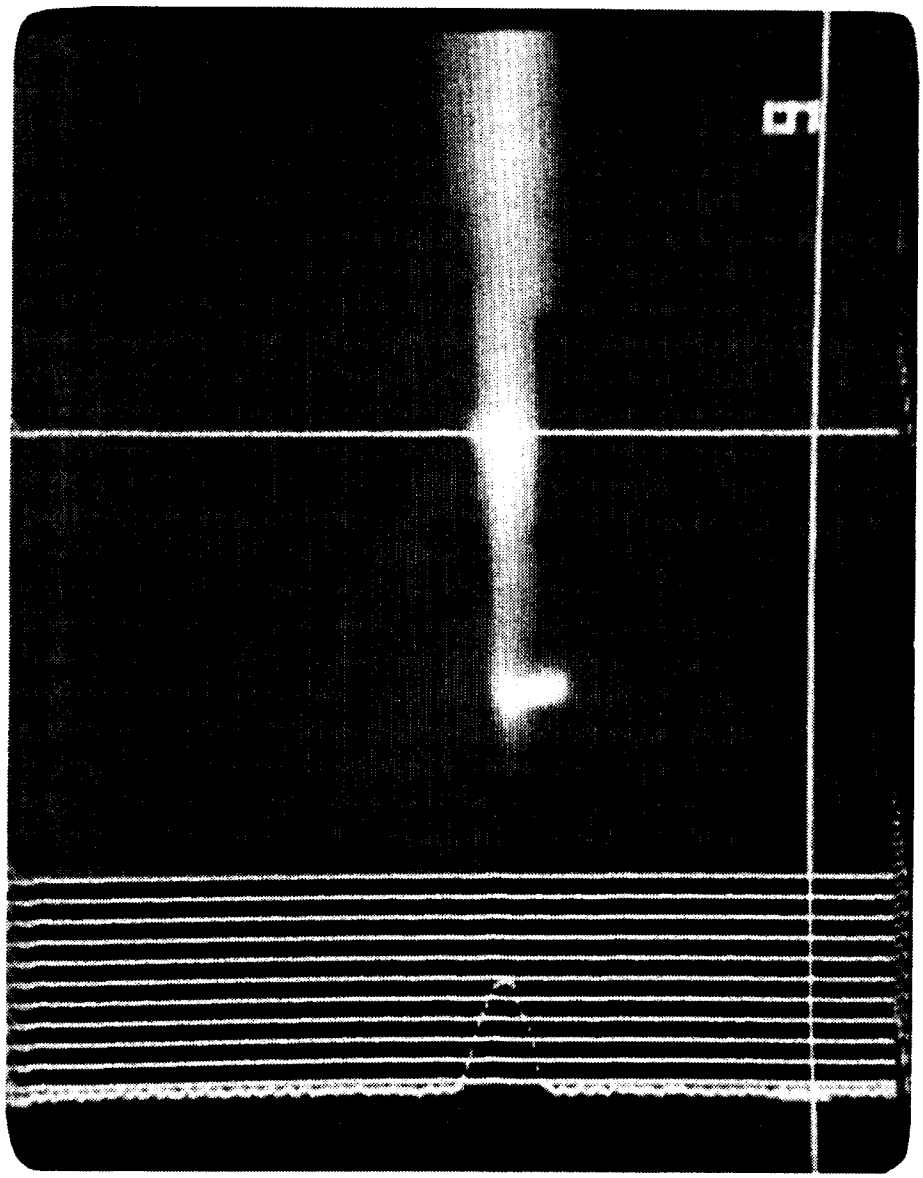

Fig. 40. UV-TV photograph (with video analyzer).
(T_t = 1720 R, P = 630 W, Q = 20.5 scfh, α = 0.95)

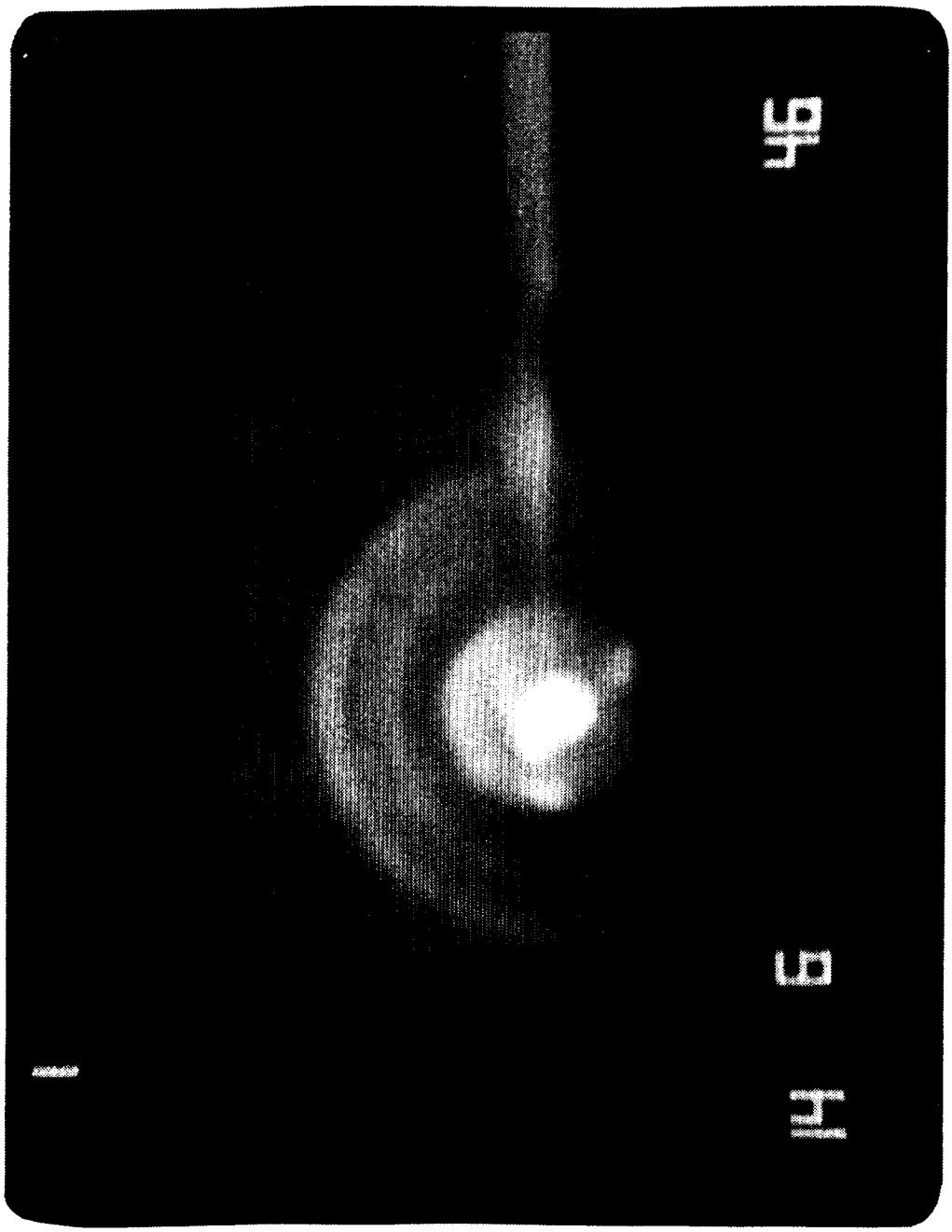

Fig. 41. UV-TV photograph (argon plasma).
(T_t = 1650 K, P = 900 W, Q = 20.0 scfh, $\alpha = \infty$)

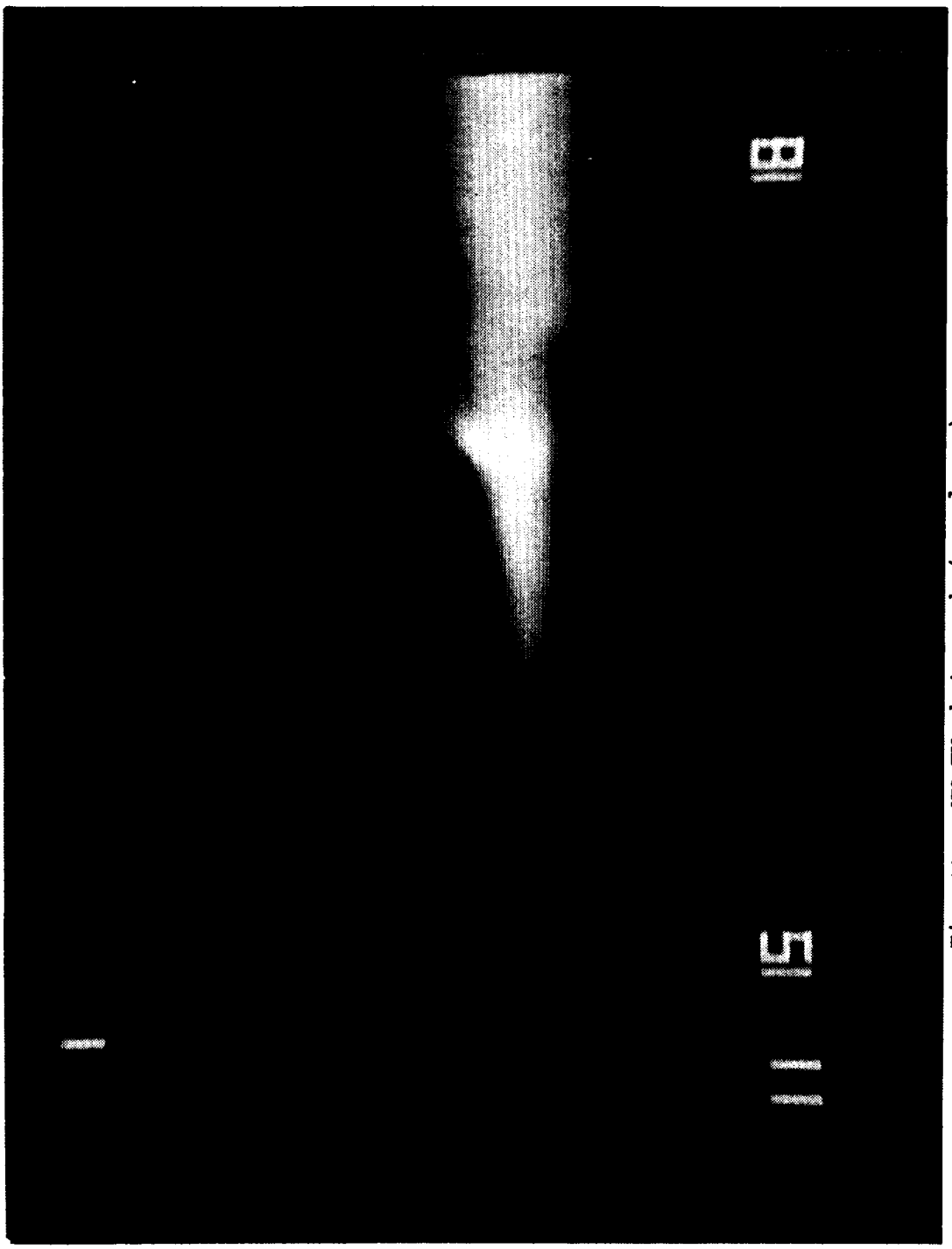

Fig. 42. UV-TV photograph (no plasma).
(Autoignition, T_t = 2720 R)

Based on the promising performance of the low-power argon-hydrogen plasma torch as an igniter for the unconfined flow tests, the duct was installed and tests were conducted in the simulated scramjet combustor. A series of tests was conducted at a simulated flight Mach number of approximately 4 (T_t = 1600 to 1800 R). Since this temperature is well below the autoignition temperature for hydrogen in this configuration , some form of external ignition source was required. The pressure distributions from the ducted tests were used to assess the performance and estimate the combustion efficiency at the end of the duct as a function of total temperature and plasma torch parameters. Figure 43 shows the pressure distributions for three different torch operating conditions. (The pressures shown are pressure ratios, i.e. the local measured wall static pressure divided by the static pressure at the exit of the facility nozzle.) The power was varied from 780 to 2590 W. For two of the tests the total flow was 40 scfh and the argon-hydrogen ratio was 1.0, and for the third test at the higher power the flow rate was increased to 69.1 scfh and the argon-hydrogen ratio was 0.47. The fourth data set presented in the figure is the pressure distribution with no fuel to the model and is shown for reference. (A similar no-fuel pressure distribution is also shown in Figs. 44-47.) The estimated combustion efficiencies were approximately 45 +/- 3 percent and were independent of the torch operating conditions. Using the mixing efficiency equation presented in Section 2, the maximum mixing efficiency for this short duct configuration is approximately 66 percent. Therefore, all of the

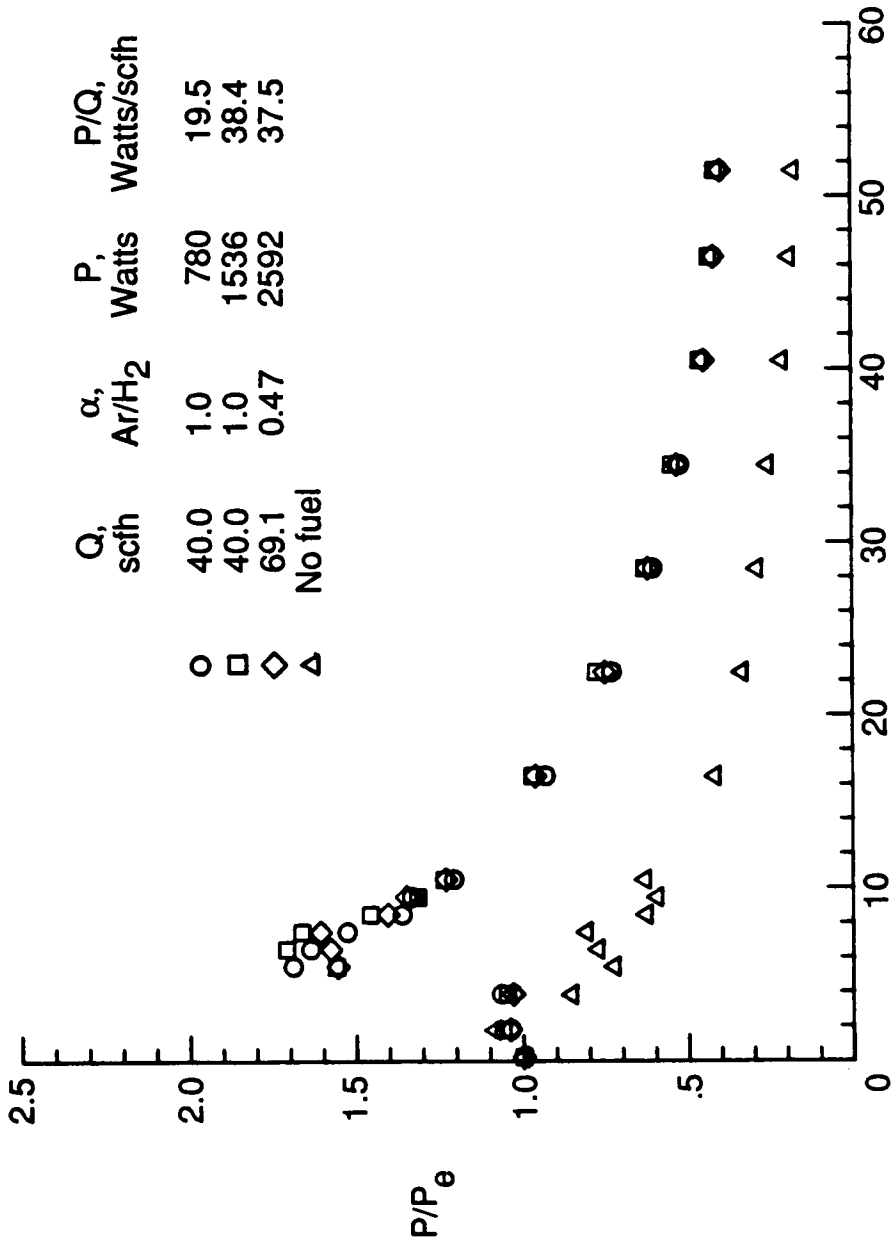

Fig. 43. Pressure distributions: Ar/H_2 plasma. (T_t = 1760 R, ϕ = 0.31)

combustion efficiencies presented in this section should be referenced to 66 percent, not 100 percent.

Not only was the performance independent of the torch operating conditions, turning the torch power and feedstock flow off had no effect on performance once ignition had been established. Figure 44 shows the pressure distributions from a test in which the torch was extinguished after ignition had been established. The distribution did not change significantly when the torch was extinguished. The estimated combustion efficiencies were 55 percent. In a few tests with burner temperatures of 1800 R or less, the calculated efficiency changed when the torch feedstock flow was turned off. The reason for this change is not understood.

The burner total temperature was reduced to a nominal temperature of 1425 R and tests were conducted with torch powers from 825 to 1500 W. The pressure distributions from two of these tests are shown in Fig. 45. The low-power argon-hydrogen plasma was effective in igniting the flow even at this reduced temperature. The estimated combustion efficiencies were approximately 60 percent and again were independent of the torch operating conditions. Since this was about the lower temperature limit for burner operation with hydrogen combustion, the burner was not turned on and a run was made with ambient temperature air (T_t = 530 R) expanded to Mach 2. A reaction occurred, but the pressure rise in the combustor was large enough to separate the flow forward into the facility nozzle, preventing the calculation of combustion efficiency. While it is unclear to what extent combustion would have occurred without the flow separation, the argon-

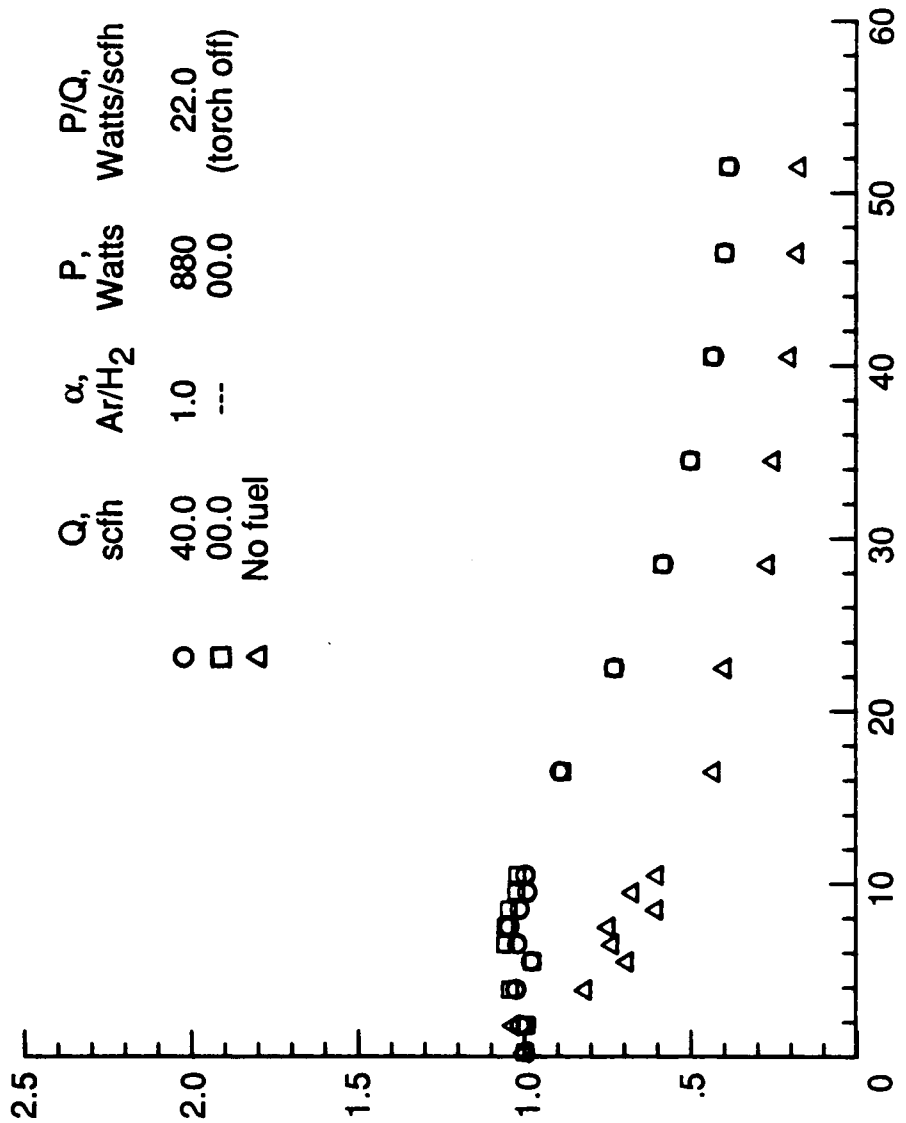

Fig. 44. Pressure distributions: Ar/H_2 torch on and off. (T_t = 2430 R, ϕ = 0.35)

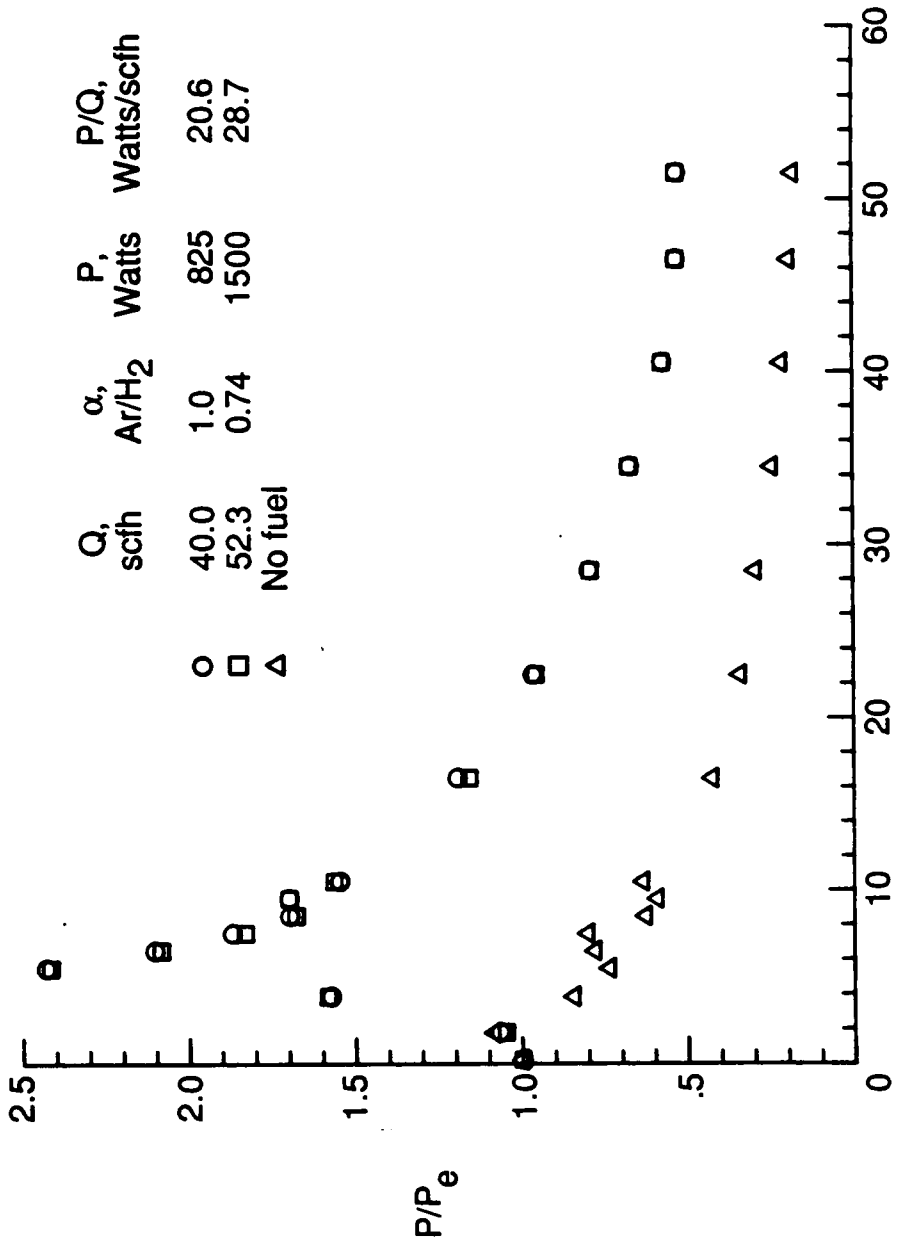

Fig. 45. Pressure distributions: Ar/H_2 plasma. (T_t = 1425 R, ϕ = 0.28)

hydrogen plasma obviously initiated a reaction even at this very low temperature. Additional tests were also conducted at higher temperatures approaching the autoignition limit, and the torch was still found to be effective. From these tests two conclusions were drawn: (1) the injector configuration with the upstream pilot fuel injection and the argon-hydrogen plasma igniter is a very effective combination for operation of a supersonic combustor over a wide total temperature range, and (2) variation of the plasma torch operating conditions over a wide range had no effect on combustor performance.

Tests were conducted with all argon as the torch feedstock to demonstrate that the experimental results were a consequence of operating the torch on hydrogen, regardless of the mechanism of augmentation. Pressure distributions with the argon and argon-hydrogen plasmas are compared in Fig. 46 for an air total temperature of 1400 R. At this low temperature with a nominal power of 800 W the argon plasma was not an effective igniter. However, when the temperature was increased to 1610 R with a similar power input, the argon plasma produced ignition and vigorous combustion. The pressure distributions from tests with the argon and argon-hydrogen plasmas at 1610 R are compared in Fig. 47. The estimated combustion efficiencies were 43 percent.

From these tests it was concluded that hydrogen atoms were responsible for ignition during the low temperature tests. However, during tests at temperatures above 1600 R, the injector configuration was such that the thermal or radiative effect of the argon plasma was sufficient to cause ignition.

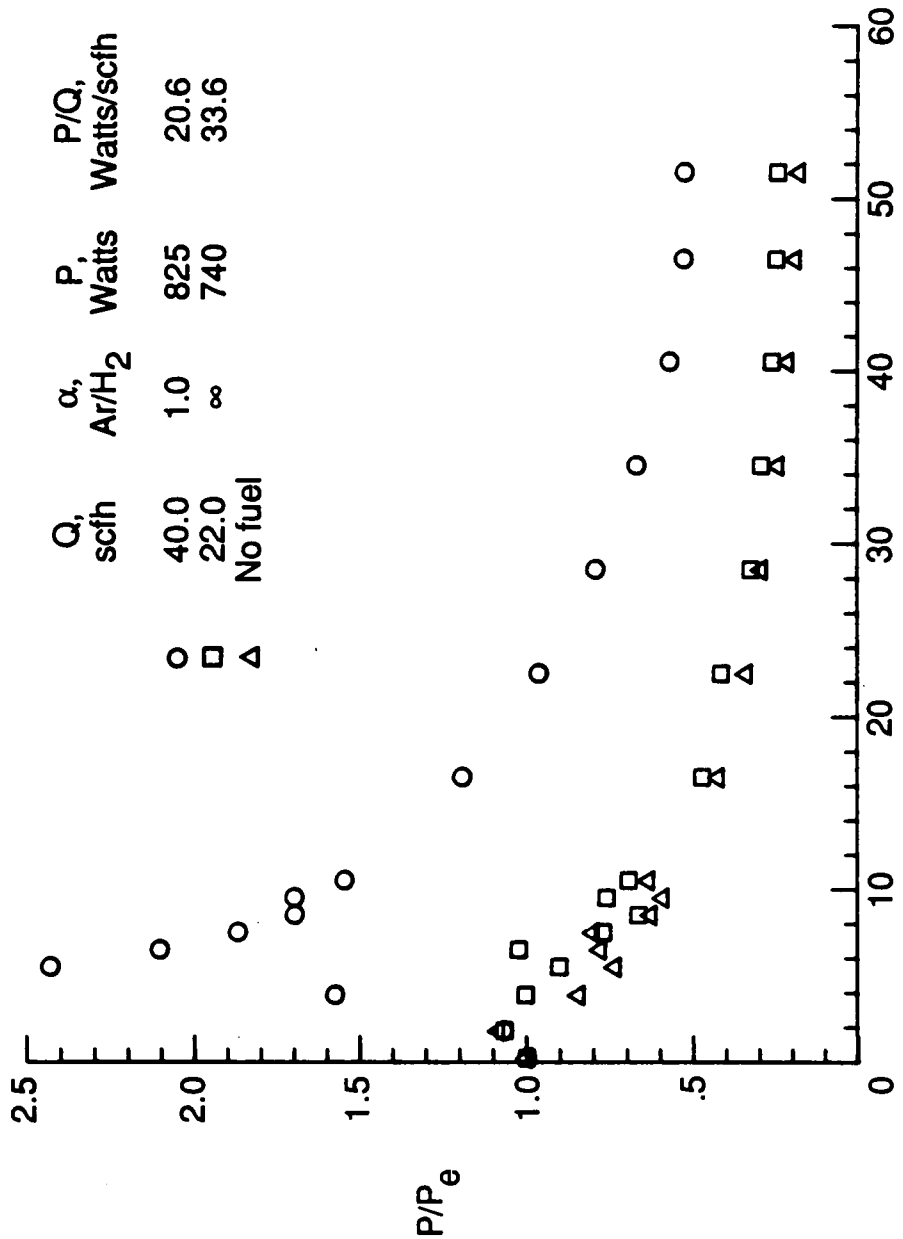

Fig. 46. Pressure distributions: Ar/H_2 and Ar plasmas. (T_t = 1400 R, ϕ = 0.28)

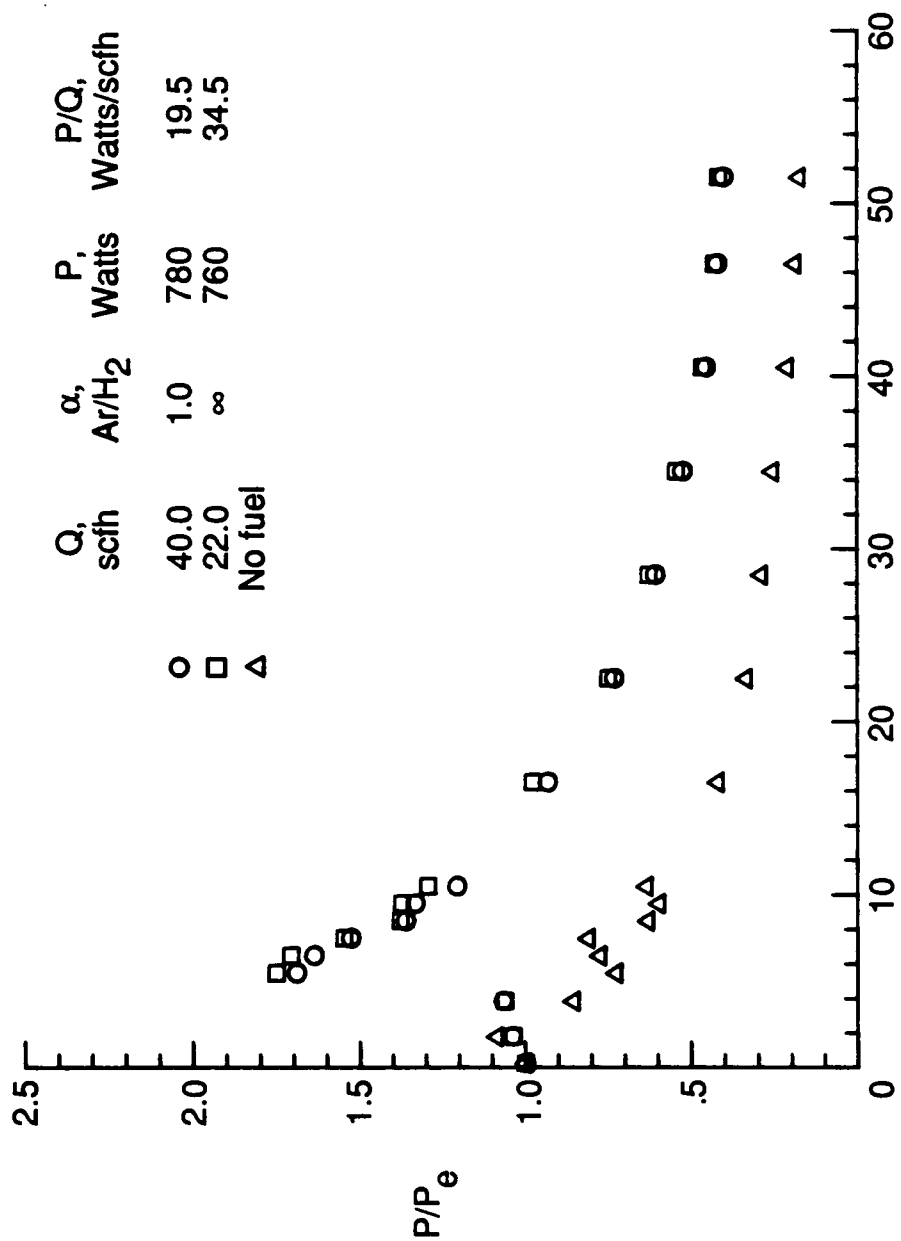

Fig. 47. Pressure distributions: Ar/H_2 and Ar plasmas. (T_t = 1610 R, ϕ = 0.30)

9.3.2 Characteristics of Integrated Igniter/Flameholder Configuration

The characteristics of the igniter/flameholder configuration were studied as part of the experimental program. This part of the investigation involved visual and UV-TV observations of the flameholding location, shadowgraph pictures of the flowfield and the determination of the effect of upstream and downstream equivalence ratio. Besides the plasma torch, a surface discharge plug and a 20/80 mixture of silane-hydrogen were evaluated as igniters for this configuration.

Visual observations during unconfined autoignition tests revealed some interesting phenomena about this igniter/flameholder configuration. Recall that the upstream pilot fuel injection began several seconds before the primary fuel flow, allowing separate observation of the pilot fuel combustion and combined pilot and primary fuel combustion. For autoignition tests with total temperatures between 2700 and 3000 R, the hydrogen injected through the upstream pilot fuel injectors burned in an unstabilized flame approximately 4 inches downstream of the step (see Fig. 48). When fuel was introduced through the primary fuel injectors, the disturbance created by the injection caused the flame to anchor in the region between the step and the downstream fuel injectors (see Fig. 49). For a total temperature of 3200 R, the combustion of the hydrogen pilot fuel was stabilized in the region of the recirculation zone (see Fig 50). The intensity of the radiation from the recirculation region increased when fuel was introduced through the primary fuel injectors (see Fig. 51). For pilot fuel injection with temperatures in excess of 3500 R, some

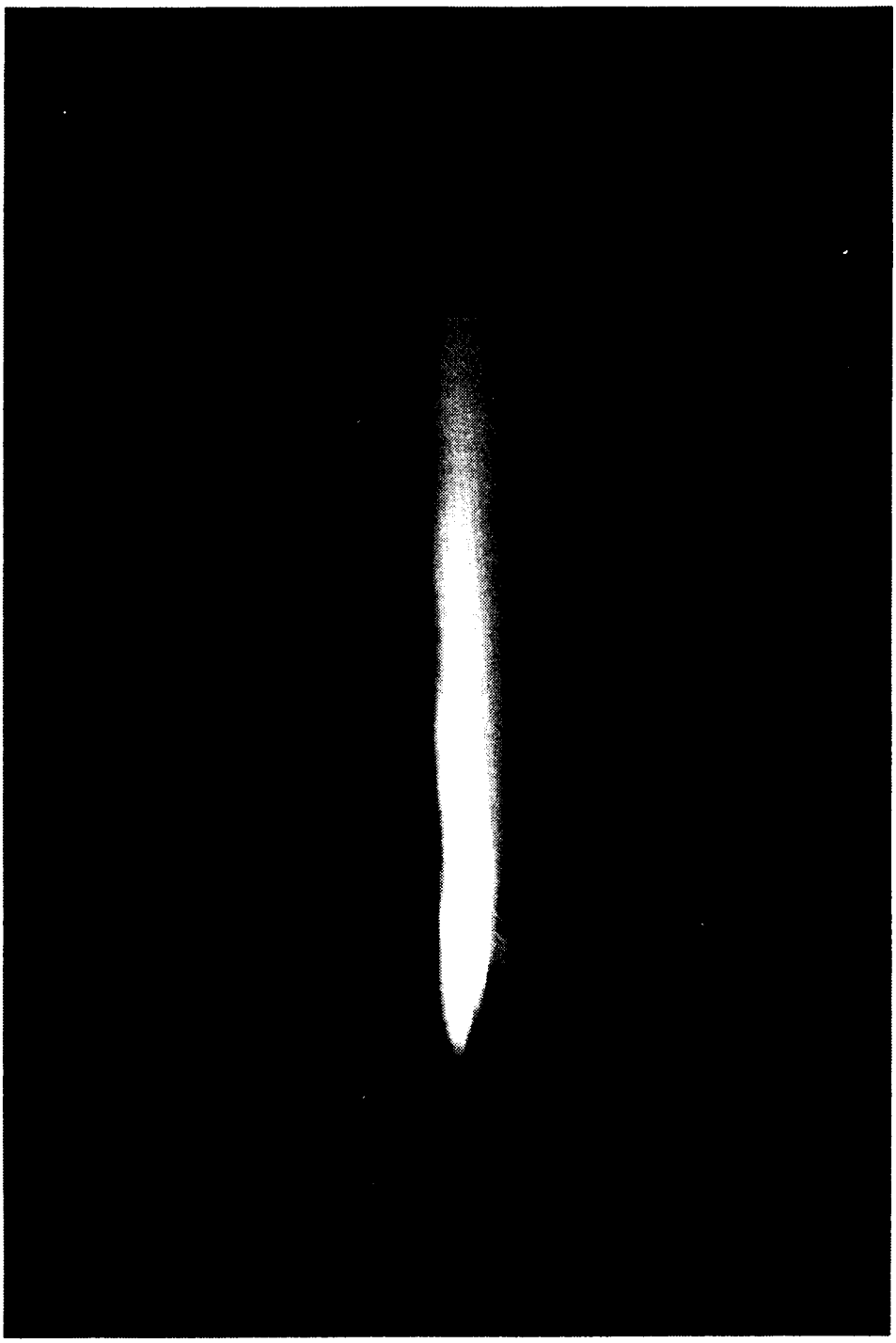

Fig. 48. Photograph of autoignition, pilot fuel injection only. (T_t = 2850 R, ϕ_1 = 0.052)

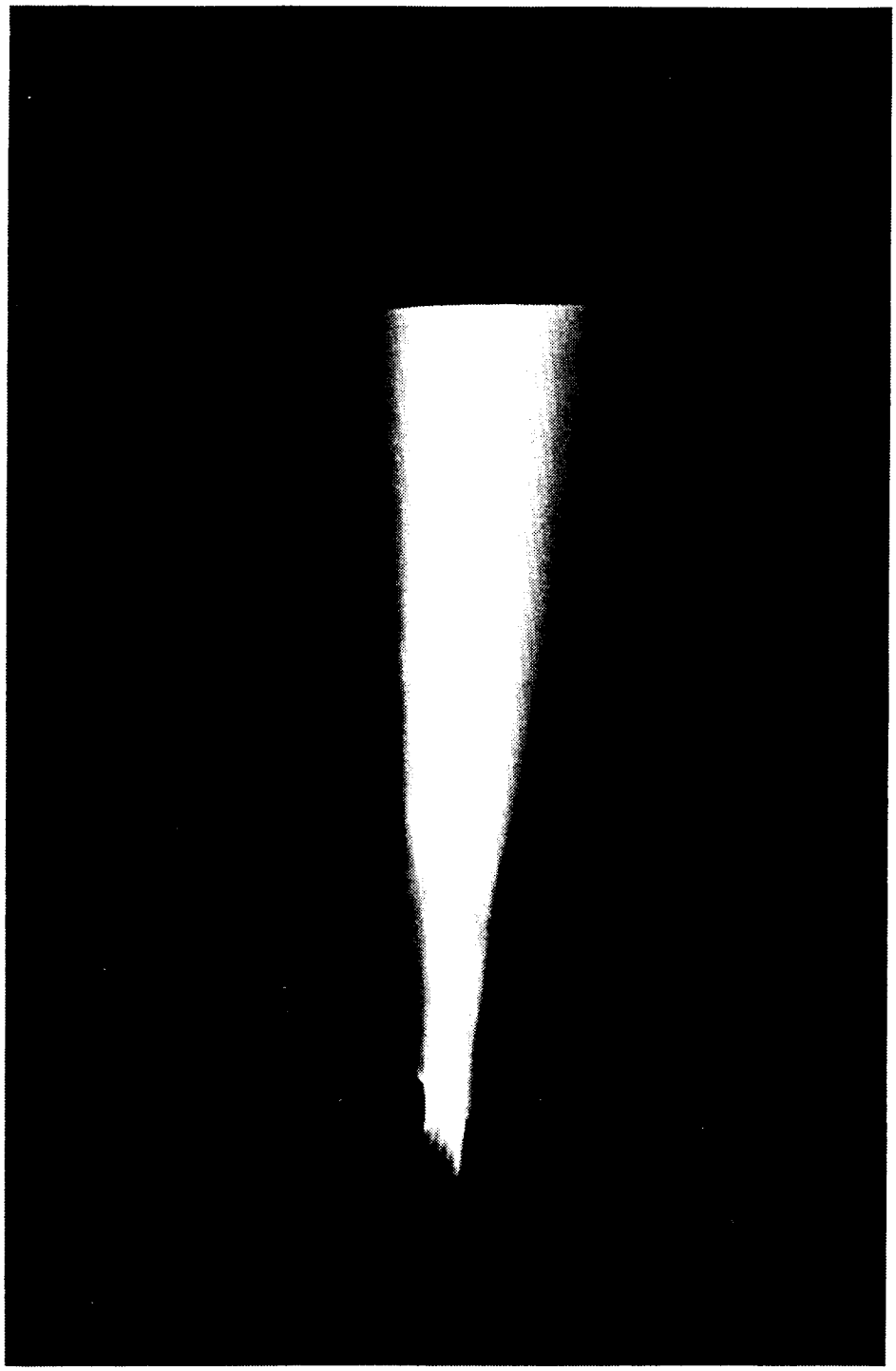

Fig. 49. Photograph of autoignition, pilot fuel and primary fuel injection. (T_t = 2850 R, ϕ_1 = 0.052, ϕ_2 = 0.39)

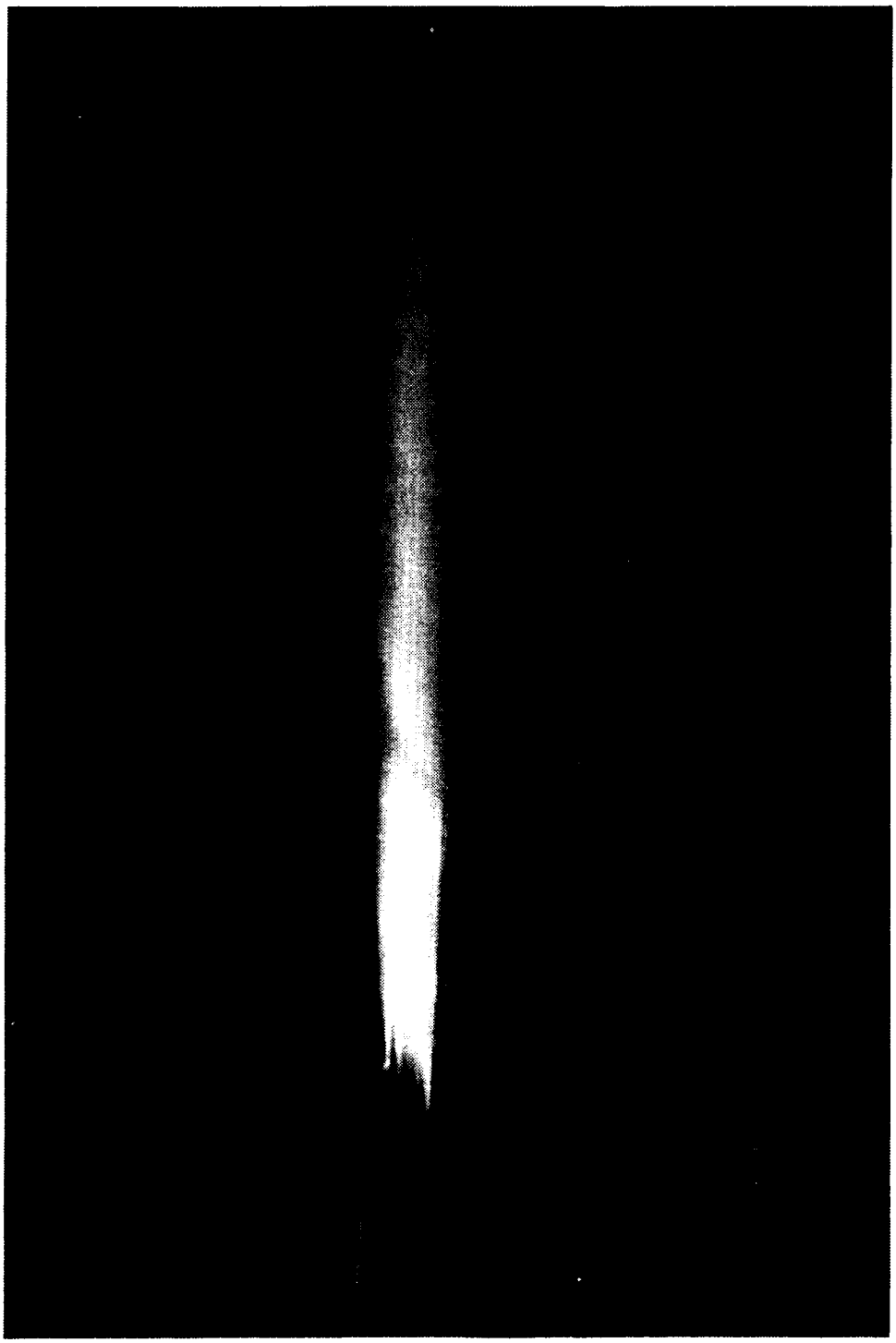

Fig. 50. Photograph of autoignition, pilot fuel injection. (T_t = 3200 R, ϕ_1 = 0.053)

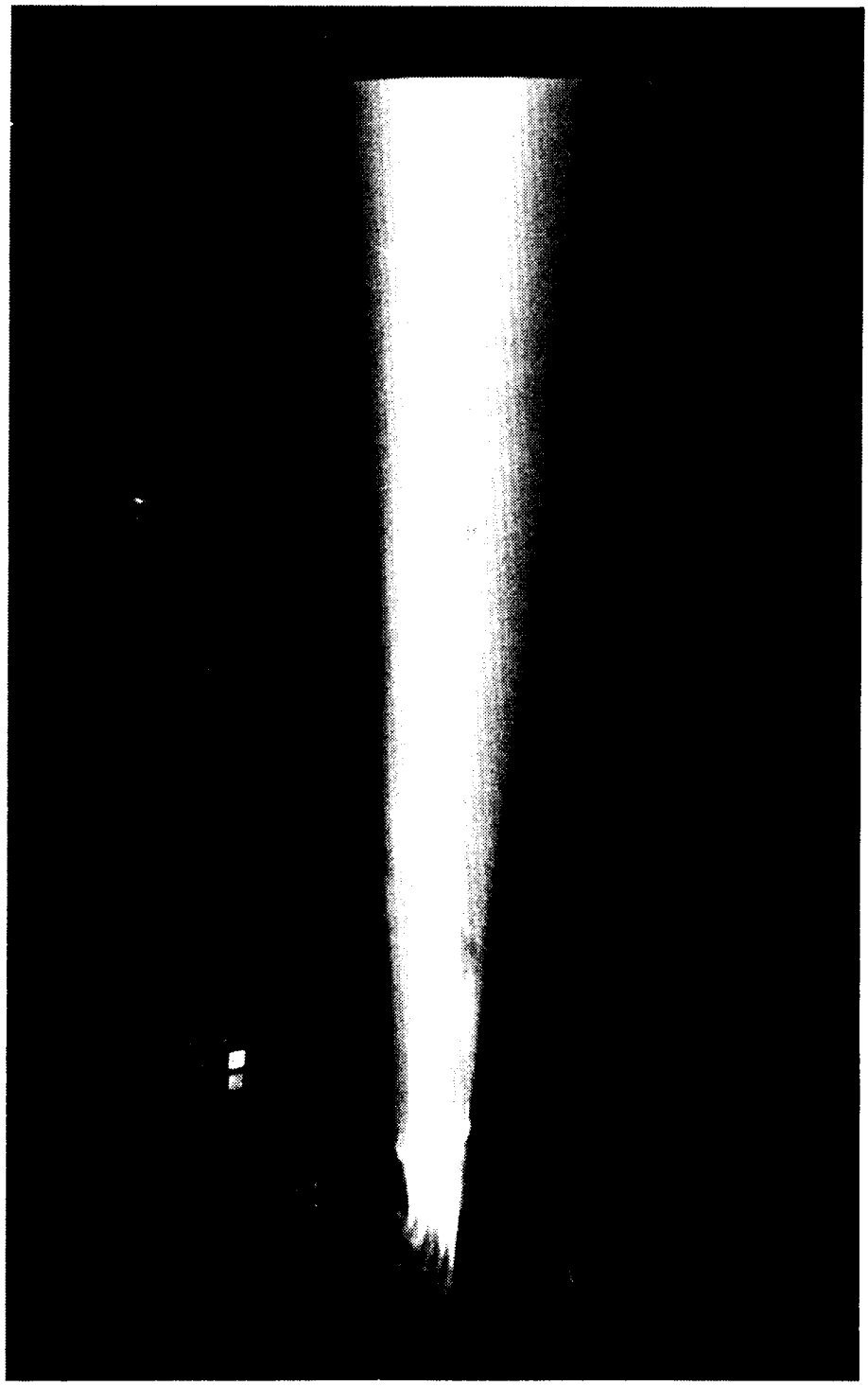

Fig. 51. Photograph of autoignition, pilot fuel and primary fuel injection. (T_t = 3200 R, ϕ_1 = 0.053, ϕ_2 = 0.24)

combustion was observed immediately upstream of the step (see Fig. 52). However, very little combustion was observed at the upstream fuel injectors for the conditions tested. Vigorous combustion was observed downstream of the reattachment shock during both the pilot fuel combustion and combined fuel combustion for tests with total temperatures above 3500 R. The above observations, which were verified by the UV-TV, indicate that the blockage created by the downstream fuel injection is necessary for flame stabilization for some flow conditions with the unconfined hardware. However, the fuel from the downstream injectors does not appear to be drawn into the recirculation region (see Fig. 51). Furthermore, the blockage created by the upstream fuel injectors does not appear to be sufficient to stabilize the flame at the upstream injector location, even at the highest temperatures tested (see Fig. 52).

Shadowgraph pictures were also taken of the flowfield. A shadowgraph picture of the flowfield with no fuel injection and no plasma injection is shown in Fig. 53. The view of the test section is similar to that of the UV-TV (see Fig. 42(a)). Once again the igniter and primary fuel injectors are hidden in the recessed portion of the injector block. Unlike the UV-TV picture, the upstream fuel injectors are visible in the shadowgraphs. The shock wave originating near the top left corner of the picture was the result of a discontinuity between a flange and the nozzle exit. Although this shock wave was located in the test section, it was not thought to have any significant effect on the results. A shadowgraph picture of the flow with the plasma torch operating is shown in Fig. 54. Note that

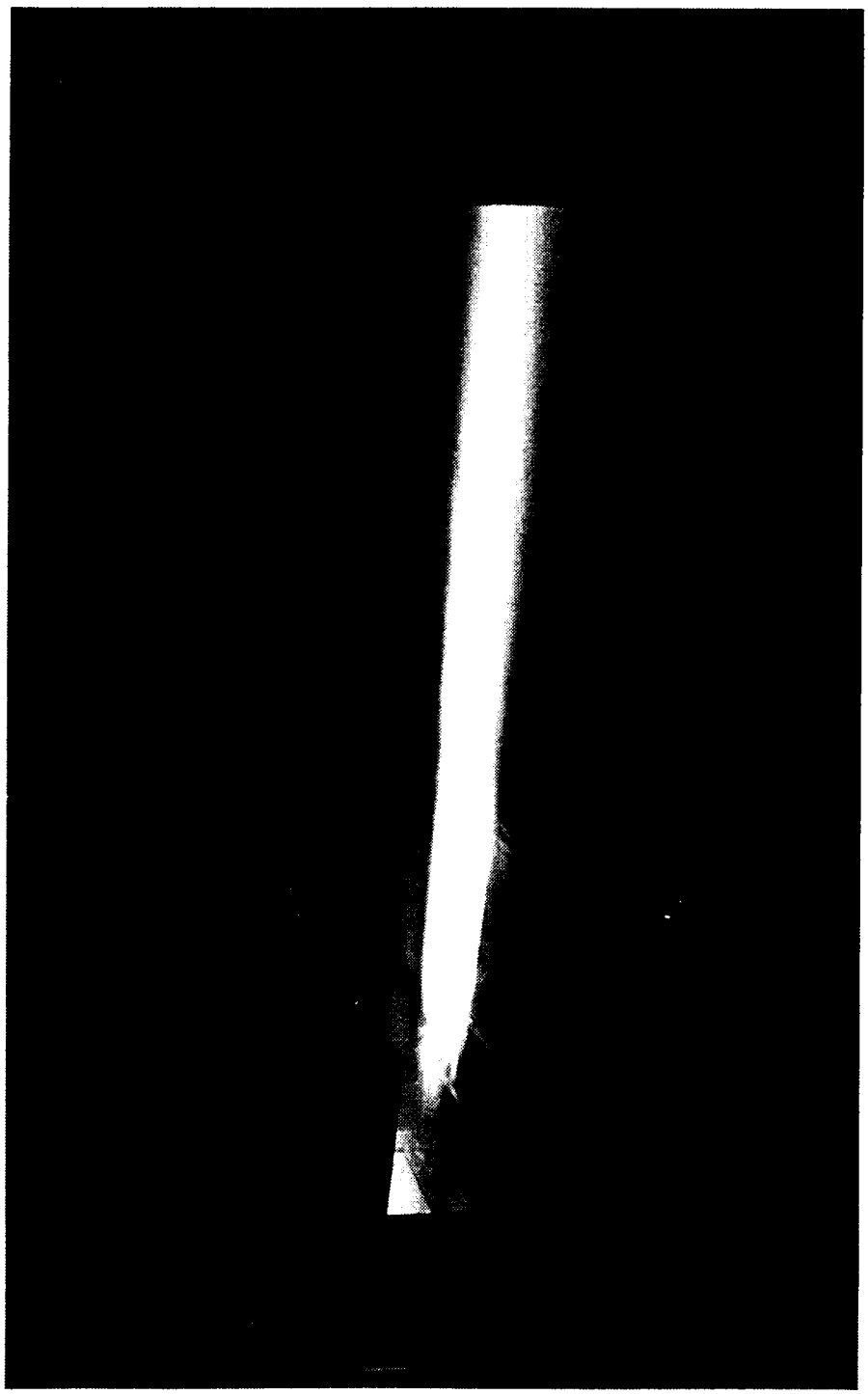

Fig. 52. Photograph of autoignition, pilot fuel injection. (T_t = 3500 R, ϕ_1 = 0.058)

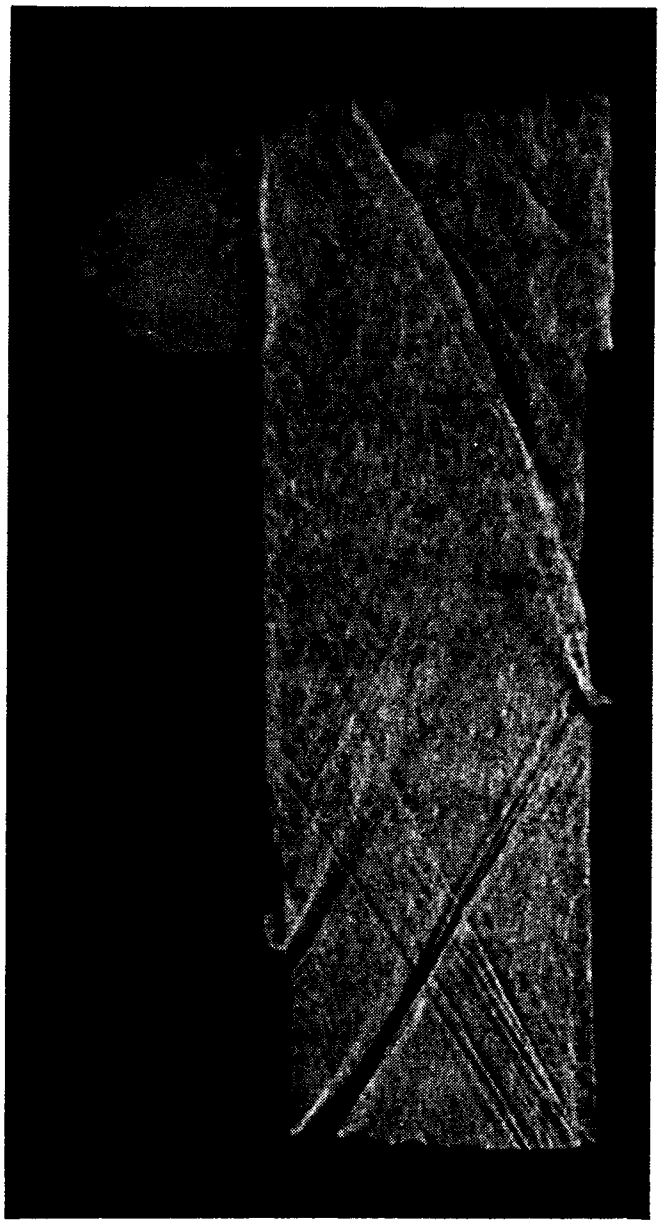

Fig. 53. Shadowgraph of flowfield, no injection.
(T_t = 1550 R)

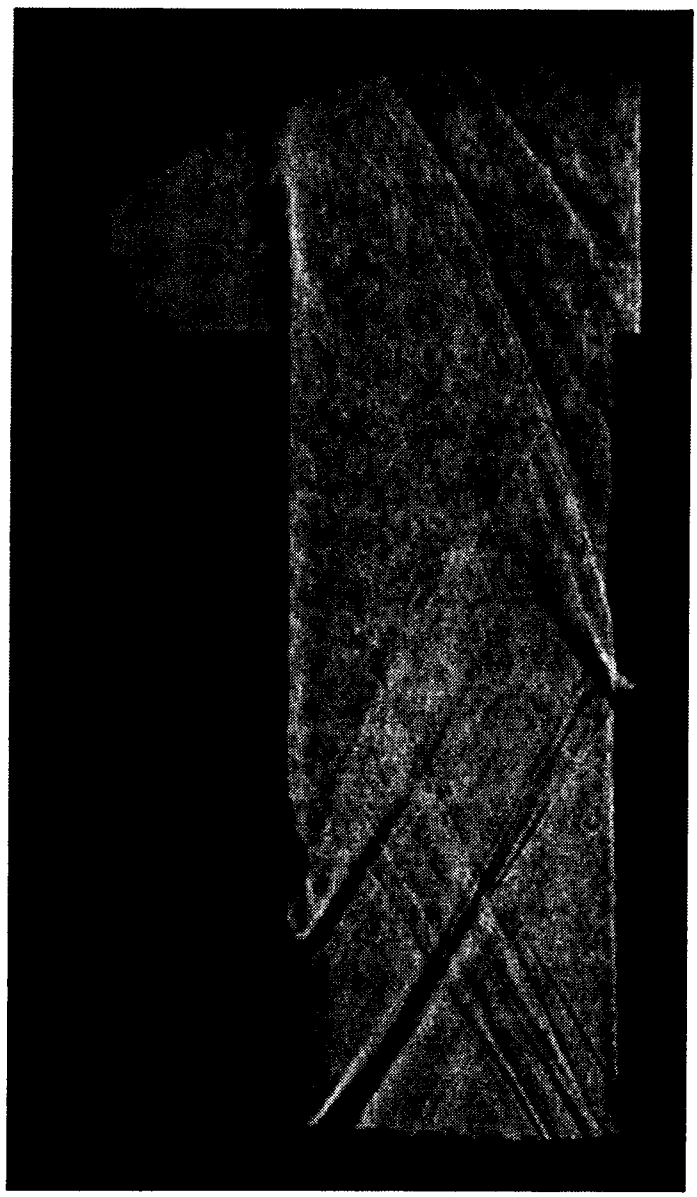

Fig. 54. Shadowgraph of flowfield, plasma injection.
(T_t = 1540 R, P = 1410 W, Q = 40.0 scfh, α = 1.0)

the plasma torch did not create a disturbance in the freestream. A shadowgraph picture of the flow with both pilot and primary fuel injection is shown in Fig. 55. The significant observation from this photograph is that the shock wave originating at the reattachment point coalesces with the bow shock waves from the primary fuel injectors, providing the potential for increased flame stability.

The characteristics of the injector design were studied during the unducted tests by varying the amount of fuel injected through the pilot injectors. This investigation was conducted at a total temperature of approximately 1750 R with the plasma torch as an igniter. Both the power and the feedstock flow to the plasma torch were turned off once combustion was established. These tests were monitored both visually and with the UV-TV. Visual observation indicated that ignition was not obtained when no pilot fuel was injected. For the lowest non-zero value of upstream fuel flow tested ($\phi_1 = 0.009$), ignition did occur and flameholding was demonstrated. However, when the equivalence ratio of the fuel injected upstream was 0.066 or greater, the flame blew off when the torch was extinguished. These visual observations were substantiated by the relative intensities measured by the UV-TV. In fact, the relative intensity of the UV radiation from the flame, measured before the plasma torch was extinguished, was indicative of whether a flame would blow off without the plasma torch. The relative intensity was measured behind the bow shock wave of the primary fuel injectors and at the end of the injector block. Both measurements revealed similar trends. Typically, combustion which persisted without the plasma torch was 40 percent more intense behind

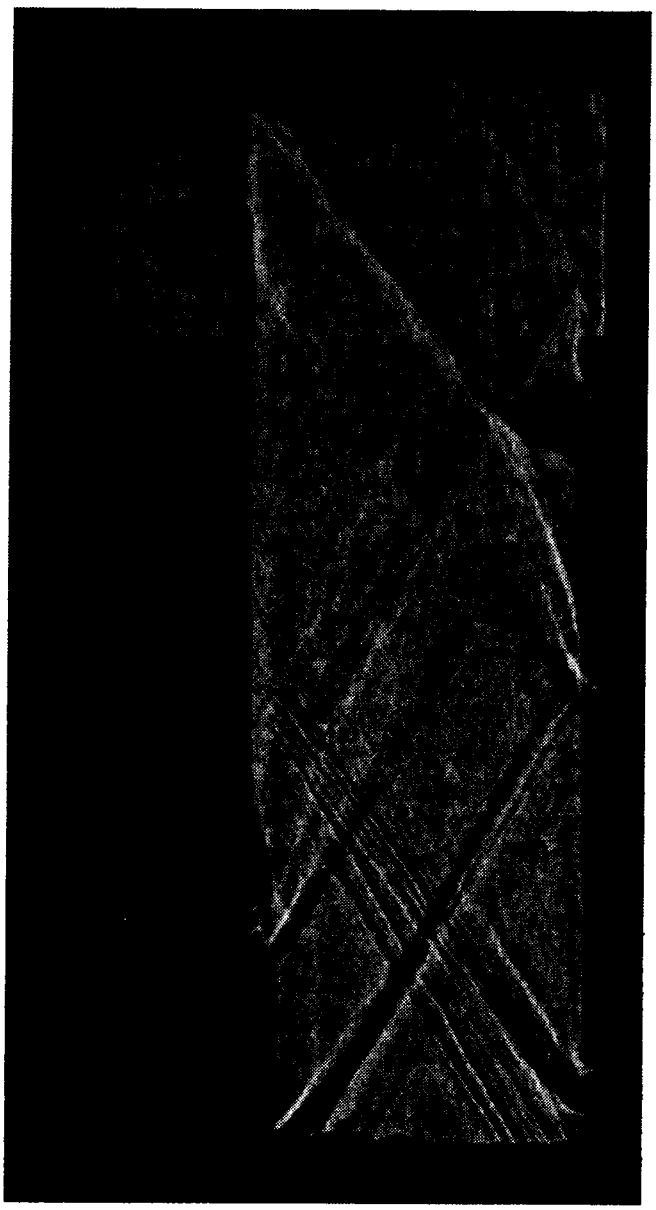

Fig. 55. Shadowgraph of flowfield, pilot and primary fuel injection with torch feedstock flow. (T_t = 1530 R, ϕ_1 = 0.042, ϕ_2 = 0.25, P = 0 W, Q = 40.0 scfh, α = 1.0)

the bow shock wave than that which would blow off without the plasma torch.

The performance of the injector configuration was characterized during the ducted tests using the measured pressure distributions and calculated combustion efficiencies. The effect of various amounts of fuel injected upstream was studied first. These tests were conducted at temperatures below the autoignition temperature. The argon-hydrogen plasma torch was used as the igniter. As in the unducted tests, no combustion was detected when there was no upstream fuel injection. It was also demonstrated that if the pilot fuel injection was turned off after ignition of the primary fuel flow was established, the flame blew off. However, the results of tests with various non-zero values of upstream equivalence ratio were different from the unducted test results. Flameholding was demonstrated for all non-zero values of upstream equivalence ratio tested, the lowest value being 0.02. The pressure effects resulting from the confined combustion appear to be sufficient to stabilize the flame.

With the upstream bulk equivalence ratio held constant at approximately 0.04, the effect of the amount of fuel injected through the primary fuel injectors was investigated. For a downstream equivalence ratio of 0.09 and a total temperature of approximately 1800 R, the flame blew off when the torch was extinguished. The flame persisted after the plasma torch was extinguished for values of the downstream equivalence ratio of 0.22 and 0.29 under similar test conditions. This result differs from the unducted tests, where the

upstream pilot fuel would flamehold without injection downstream. The reason for this difference is not understood.

The igniter/flameholder configuration was also tested with igniters other than a plasma torch. Two igniters were tested, a pyrophoric mixture of 20 percent by volume silane in hydrogen and a surface discharge plug. Both injectors were situated at the same location as the plasma torch. The silane-hydrogen mixture was injected through a small orifice about the size used for the plasma torch. The data from these test are summarized in Table VI. The silane hydrogen mixture did not produce ignition for total temperatures less than 1780 R for any flow rates tested (3.33×10^{-4} to 4.65×10^{-3} lb/s). For total temperatures above 1780 R the silane-hydrogen mixture produced ignition even for the lowest flow rate tested, 3.33×10^{-4} lb/s. The observation that the silane-hydrogen flowrate had no effect on the minimum ignition temperature was a surprising result. Figure 56 presents a comparison of the pressure distributions from two tests with different silane-hydrogen mass flows and a test with the argon-hydrogen plasma. The estimated combustion efficiencies were 47 +/- 1 percent. Note that the increased mass flow of the silane-hydrogen mixture did not affect the pressure distribution. This result is in agreement with the results from the argon-hydrogen plasma tests in which the torch operating conditions had no effect on the combustion efficiency.

The surface discharge plug was a Champion Model FHE 283-1. This device and its associated power supply create a spark approximately once a second. The energy and duration of the spark are 159 Btu

Table VI. Summary of data from tests with 20/80 SiH_4-H_2.

RUN	BATCH	$\dot{m}$ x10^3 (lb_m/s)	ϕ_1	ϕ_2	T_t (R)	η_c
23	5	0.33	0.043	0.24	1580	*
	6	0.37	0.046	0.26	1600	*
	7	1.39	0.046	0.26	1620	*
	8	3.25	0.047	0.26	1620	*
	9	4.65	0.041	0.26	1620	*
24	2	2.32	0.000	0.26	1600	*
	3	2.10	0.009	0.26	1600	*
	4	2.27	0.086	0.26	1620	*
	5	2.33	0.130	0.26	1620	*
	6	4.67	0.130	0.26	1620	*
	7	4.56	0.000	0.26	1640	*
	8	0.31	0.048	0.32	2460	0.52
	9	2.32	0.048	0.32	2480	0.53
	10	2.32	0.16	0.30	2480	0.53
	11	2.31	0.043	0.27	1780	0.47
	12	0.33	0.043	0.27	1780	0.46
	13	0.35	0.041	0.26	1610	*

* No ignition

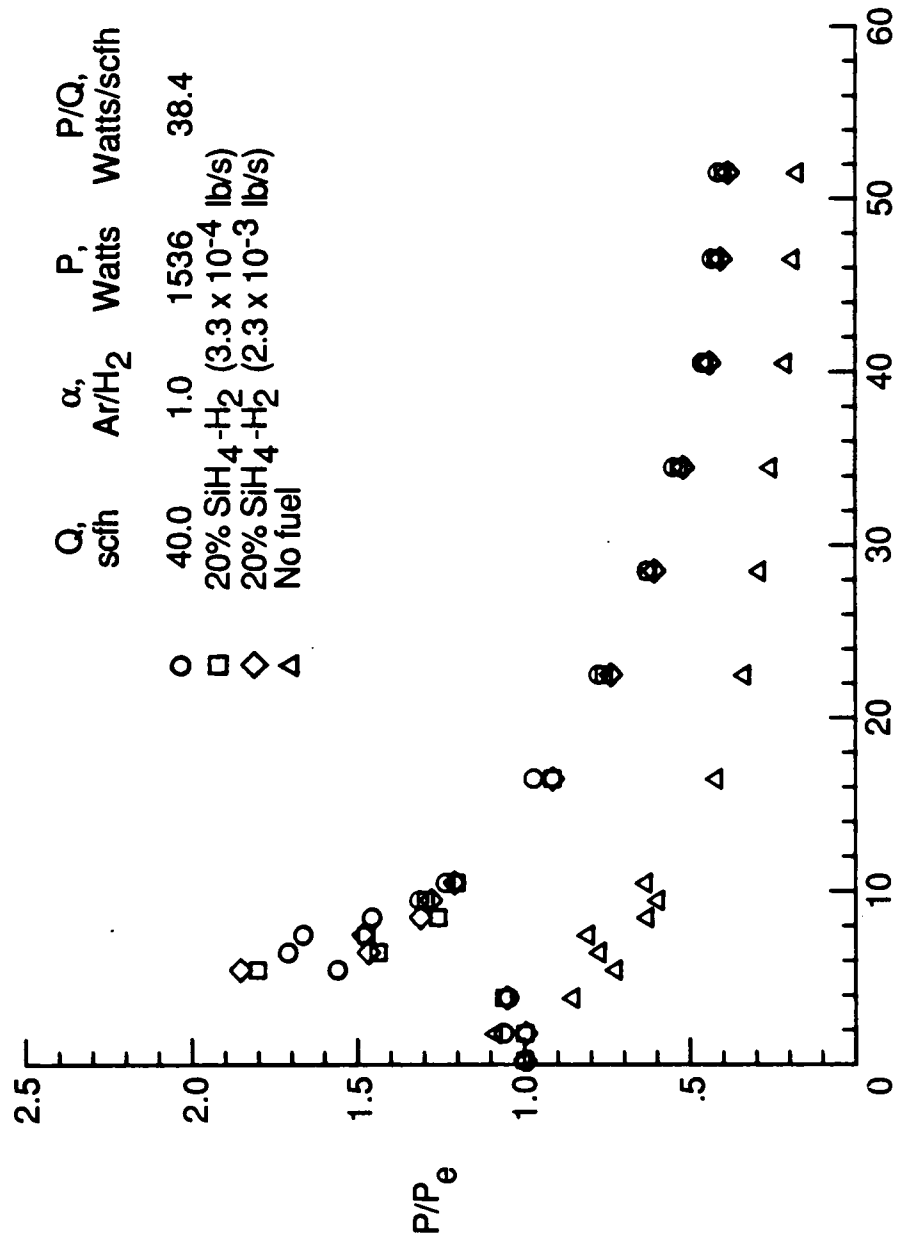

Fig. 56. Pressure distributions: Ar/H_2 plasma and 20 percent SiH_4-H_2. (T_t = 1780 R, ϕ = 0.31)

and 7 microseconds, respectively. The surface discharge plug ignited the flow during a test with a total temperature of 1610 R. However, this result could not be repeated in five attempts. Tests with total temperatures of 1800 R and 2450 R were also conducted without successful ignition. Therefore, the spark igniter was considered a poor igniter under these conditions, and was not equivalent to the plasma torch or the silane-hydrogen mixture as an ignition source.

9.4 Additional Torch Tests

A very limited test program was conducted with the VPI plasma torch installed in a flat plate configuration similar to that used in some of the Plasmadyne torch tests. The purpose of these tests was to demonstrate that the low-power plasma torch alone is an igniter and a flameholder for total temperatures of 1600 R. Fuel injectors were located both upstream and downstream of the plasma torch. Ignition occurred during all tests involving downstream injection or the combination of upstream and downstream injection. For tests with only upstream injection, ignition occurred only for the case of maximum fuel injection. Apparently, only for the case of maximum injection pressure was the lateral spread of hydrogen sufficient to fuel the region near the torch. It was also demonstrated that the flame would blow off when the torch was extinguished. Therefore, the VPI plasma torch was an effective igniter and flameholder at power levels of less than 1 kW without the aid of a geometric flameholder.

10. SUMMARY

An experimental and analytical investigation of the use of radicals for ignition and flameholding in supersonic flow was conducted. The analytical investigation was conducted using a finite-rate chemical kinetics code to calculate the effects on ignition delay time of additions of small quantities of radicals to hydrogen-air mixtures. The results of these calculations indicated that additions of H, O, N, and OH were all effective in reducing the calculated ignition delay time. A review of the literature indicated that H, O, N, and OH had all been used successfully for combustion enhancement.

An experimental investigation was conducted to explore the use of radicals as an ignition and flameholding source in supersonic flows. Since the results of the analytical investigation did not indicate a preferred radical, hydrogen atoms were selected after a search of the literature. Atomic hydrogen was selected because hydrogen atoms participate in a chain branching reaction. Furthermore, experiments have shown that the hydrogen atom concentration is decreased when a flame inhibitor is present, while the concentrations of oxygen atoms and hydroxyl radicals are unaffected by inhibitors.

A plasma torch was chosen as the hydrogen atom generator for this investigation because it provides continuous operation at the pressure level required for scramjet operation over the entire flight envelope (0.2-2 atmospheres). Two plasma torches were used in this investigation. A commercially-available plasma torch was used during the

initial tests, while a low-power plasma torch was developed for later tests.

Diagnostic experiments were conducted with both torches to verify the presence of hydrogen atoms in the torch exhaust. The first and simplest diagnostic technique was visual observation, which indicated the exhaust was pink. This pink radiation signified the presence of the first transition in the Balmer series of the hydrogen atom, thereby indicating the presence of atomic hydrogen. A second verification was obtained using the Stark broadening technique. Finally, a large portion of the visible spectrum of the exhaust from the low-power plasma torch was analyzed spectroscopically. The results of this investigation also verified the presence of hydrogen atoms and indicated an increase in hydrogen atom density with increasing power level.

The theory that hydrogen atoms should be effective for ignition and flameholding in supersonic flows was first experimentally tested using a commercially-available plasma torch. Unconfined flow tests were conducted to allow optical access to the fuel injection and pilot region of the Mach 2 flow. The heater total temperature and the torch power levels were varied, and an OH visualization system (UV-TV) was used to sense ignition/no-ignition. Ignition and flameholding limits, in terms of minimum total temperature, were determined for hydrogen, ethylene, ethane and methane. Confined flow tests were also conducted using an expanding duct to simulate a scramjet combustor. During the ducted tests the combustion efficiency was inferred from measured wall static pressures using a one-dimensional analysis.

For the fuels tested the minimum ignition total temperatures with the plasma torch pilot were: hydrogen - 1065 R (lowest temperature tested), ethylene - 2000 R, ethane - 2200 R, methane - 2700 R. These temperatures were obtained while operating the torch at a nominal net power of 2 kW. The torch was shown to be a good igniter and flameholder in that flames of both hydrogen and hydrocarbon fuels could be stabilized by the torch and would blow off when the torch was extinguished. The effectiveness of the torch was very sensitive to relative fuel injection location. The best combustion resulted when fuel was injected both upstream and downstream of the torch.

During confined flow tests with supersonic hydrogen combustion, the estimated efficiency of the torch-ignited combustion was 60 percent, which was essentially identical to that obtained in a similar configuration ignited with a pyrophoric silane-hydrogen mixture. However, when the fuel flow was increased a sufficient amount to choke the constant area section, the plasma torch acted as a flameholder and prevented upstream propagation. Changing from hydrogen to hydrocarbon fuels with the same injector configuration resulted in poor combustor performance with the ducted model. The results of these initial tests indicated that hydrogen atoms from a plasma torch operating at about 2 kW could be an effective igniter and flameholder for high-speed combustion.

Once the concept of using hydrogen atoms for ignition and flameholding in supersonic flow had been demonstrated, a low-power plasma torch (VPI torch) and a pilot injector configuration were designed to extend these early results to lower power levels. The low-

power torch was uncooled and operated on argon-hydrogen mixtures at power levels of 630 to 2590 W. The injector design incorporated small upstream pilot fuel injectors, a step for recirculation and primary fuel injectors downstream of the step. The upstream injectors fueled the recirculation zone. The downstream injectors were located far enough downstream of the step to prevent the primary fuel from affecting the concentration of fuel in the recirculation region. The torch was located in the recirculation region. Both unconfined and ducted tests were conducted in a Mach 2 flow with hydrogen fuel. During the unconfined flow tests the UV-TV was again used to document ignition and the flameholding location. Wall static pressures were again used to estimate the combustion efficiency during the ducted tests.

The argon-hydrogen plasma produced ignition for all temperatures tested with the unducted hardware, including a total temperature of 530 R. For total temperatures simulating a flight Mach number of approximately 4, the argon-hydrogen plasma produced ignition for a power input of 630 W, the lowest torch power possible for the 1:1 argon-hydrogen mixture. Once ignition was established, the plasma torch had no measurable effect on performance, even for power levels of 1860 W. For the lowest burner temperature tested (T_t = 1400 R), the flame persisted when the torch was extinguished. Stabilization was provided by the recirculation zone between the rearward facing step and the disturbance created by the downstream injection.

For the ducted tests the argon-hydrogen plasma again produced ignition for all temperatures tested. The pressure distributions and

the corresponding estimated efficiencies were not affected by changes in the torch parameters. For the lowest burner temperature tested (T_t = 1400 R), the flame persisted even when the torch was extinguished. During tests at 530 R, flow separation occurred, so it is unclear to what extent combustion would have occurred if Mach 2 flow had been maintained.

The observation that torch power had no effect on performance once ignition was established should not be surprising. The flow of hydrogen through the torch was less than one percent of the flow through the pilot fuel injectors. Therefore, once hydrogen atoms were being formed in the recirculation zone by reaction, the hydrogen atom addition through the torch was insignificant.

An argon plasma, a pyrophoric mixture of silane and hydrogen, and a spark igniter were tested in the new injector configuration as a comparison to the argon-hydrogen plasma. These tests were also used to characterize the injector configuration for ignition sources other than the argon-hydrogen plasma. The argon plasma produced ignition for total temperatures greater than 1600 R. The silane-hydrogen mixture produced ignition for total temperatures in excess of 1780 R. The spark igniter was ineffective. Once combustion was established, the efficiency was independent of the choice of igniter/pilot.

11. CONCLUSIONS

The following conclusions were drawn from the results of this investigation:

1. With transverse injection, an argon-hydrogen plasma generated by a plasma torch operating at a power level of 780 W is an effective ignition and flameholding source for hydrogen-fueled Mach 2 flows at total temperatures as low as 1400 R and possibly as low as 520 R.
2. Hydrogen atoms are believed to be responsible for the observed results for three reasons.
   (a) The analytical investigation demonstrated that replacing 0.5 percent of the fuel with hydrogen atoms reduces the calculated ignition delay time of the hydrogen-air reaction by a factor of two at 1750 R.
   (b) The diagnostic tests demonstrated the presence of hydrogen atoms in the argon-hydrogen plasma.
   (c) An argon plasma with an energy input approximately equal to that of the argon-hydrogen plasma (800 W) was only effective at total temperatures above 1600 R. (A thermal or radiative effect of the argon plasma was assumed responsible for the ignition.)
3. Hydrogen atoms are effective in reducing the minimum total temperature required for ignition of ethylene, ethane, and methane in a Mach 2 flow by more than 33 percent.

4. The two-stage injector design flameholds with hydrogen fuel at a total temperature of 1400 R.
5. The two-stage injector configuration used in conjunction with an argon-hydrogen plasma igniter is a very effective igniter and flameholder combination for scramjet combustors even at igniter power levels of 780 W. (The combination may also be effective for lower igniter power levels; 780 W was the lowest power level tested.) This conclusion is based on tests simulating scramjet operation in the range of Mach 3 to Mach 6 at low to moderate altitudes. It is expected that this igniter and flameholder combination will be effective over a broader operating range.

LITERATURE CITED

1. Andrews, E. H.; Northam, G. B.; Torrence, M. G.; Trexler, C. A.; and Pinckney, S. Z.: Mach 4 Wind Tunnel Tests of a Hydrogen-Burning Airframe-Integrated Scramjet Engine. NASA TM-85688, 1984. (Conf.)

2. Sanlorenzo, E. A.; Venkataramani, S. K.,; and Deere, M. M.: Design, Fabrication, and Tests of a Scramjet Model at Mach 4. General Applied Science Laboratories, NASA CR-165,787, 1981.

3. Anderson, G. Y. and Mackley, E. A.: Mach 7 Performance of the Langley Airframe-Integrated Modular Scramjet. Presented at the 1983 JANNAF Propulsion Meeting, February 1983. CPIA Publication 370, Vol. 5, pp. 493-508 February 1983. (Conf.)

4. Schmotolocha, S. N.; Economos, C.; and Tamagno, J.: Supersonic Combustion of Hydrocarbon Fuels with Air Pilots. Technical Report AFAPL-TR-69-71, September 1969.

5. Weinberg, F. J.: Plasma Jets in Combustion. C 45/83 IMechE, 1983.

6. Clements, R. M.: Review of Plasma Jet Ignition. The Chemistry of Combustion Processes, ACS Symposium Series 249, American Chemical Society, pp. 193-204, 1984.

7. Tozzi, L. and Dabora, E. K.: Plasma Jet Ignition in a Lean-burn CFR Engine. Nineteenth Symposium (International) on Combustion, The Combustion Insititute, Pittsburgh, pp. 1467-1474, 1982.

8. Mittinti, D. N. and Dabora, E. K.: Plasma Jet Ignition Studies. Presented at Twentieth Symposium (International) on Combustion, The Combustion Institute, Pittsburgh, 1984.

9. Mittinti, D. N. and Dabora, E. K.: Flame Jet Ignition of Lean Fuel-Air Mixtures. Progress in Astronautics and Aeronautics, American Institute of Astronautics and Aeronautics, Inc., New York, Vol. 105, pp. 38-68, 1985.

10. Kimura, I.; Aoki, H.; and Karo, M.: The Use of a Plasma Jet for Flame Stabilization and Promotion of Combustion in Supersonic Air Flows. Combustion and Flame, Vol. 42, pp. 297-305, 1981.

11. Kimura, I. and Imajo, M.: An Experimental Investigation of an Arc-Heated Stirred Reactor. Sixteenth Symposium (International) on Combustion, The Combustion Institute, Pittsburgh, pp. 809-815, 1977.

12. Tachibana, T.; Kobayashi, T.; Matsuda, T.; and Kimura, I.: The Use of Electrical Discharges for Ignition and Control of Combustion of Solid Propellants. Japan Society for Aeronautical and Space Sciences, Journal. Vol. 33, No. 378, pp. 433-437, 1985.

13. Weber, R. J. and MacKay, J. S.: An Analysis of Ramjet Engines Using Supersonic Combustion. NACA Technical Note 4386, September 1958.

14. Ferri, A: Review of Problems in Application of Supersonic Combustion. Journal of The Royal Aeronautical Society, Vol. 68, No. 645, pp. 575-595, September 1964.

15. Stull, F. D.: Scramjet Combustion Prospects. Astronautics and Aeronautics, Vol. 3, No. 12, pp. 48-52, December 1965.

16. Ferri, A. and Fox, H.: Analysis of Fluid Dynamics of Supersonic Combustion Process Controlled by Mixing. Twelfth Symposium (International) on Combustion, The Combustion Institute, Pittsburgh, pp. 1105-1112, 1969.

17. Ferri, A.: Review of Scramjet Propulsion Technology. Journal of Aircraft, Vol. 5, No. 1, pp. 3-10, January-February 1968.

18. Waltrup, P. J.; Anderson, G. A.; Stull, F. D.: Supersonic Combustion Ramjet (Scramjet) Engine Development in the United States. Presented at the Third International Symposium on Air Breathing Engines, Munich, Germany, March 7-12, 1976.

19. Jones, R. A. and Huber, P. W.: Toward Scramjet Aircraft. Astronautics and Aeronautics, Vol. 16, No. 2, pp. 38-48, February 1978.

20. Beach, H. L., Jr.: Hypersonic Propulsion Paper No. XII, CP-2092, NASA Lewis Research Center, 1979.

21. Billig, F. S.: Ramjets with Supersonic Combustion. AGARD-NATO PEP Lecture Series No. 136, Ramjet and Ramrocket Propulsion Sytems for Missiles.

22. Northam, G. B.: Combustion in Supersonic Flow. Workshop Report, Twenty-first JANNAF Combustion Meeting, October 1984.

23. Billig, F. S.: Combustion Processes in Supersonic Flow. Presented at the Seventh International Symposium on Air Breathing Engines, Beijing, China, September 2-6, 1985.

24. Northam, G. B. and Anderson, G. Y.: Supersonic Combustion Ramjet Research at Langley, AIAA-86-0159, January 1986.

25. Waltrup, P. J.: Liquid Fueled Supersonic Combustion Ramjets: A Research Perspective of the Past, Present, and Future. AIAA-86-0158, January 1986.

26. Kaufman, L. G., II: Hypersonic Flows Past Transverse Jets. Final Report, Grumman Research Department, Report RE-263, August 1966.

27. Schetz, J. A. and Billig, F. S.: Penetration of Gaseous Jets Injected into a Supersonic Stream. Journal of Spacecraft and Rockets, Vol. 3, No. 11, pp. 1658-1665, November 1966.

28. Henry, J. R.: Fuel Injection and Mixing in Scramjet Combustor. NASA TM X-1437, October 1967.

29. Torrence, M. G.: Concentration Measurements of an Injected Gas in a Supersonic Stream. NASA TN D-3860, April 1967.

30. Orth, R. C. and Funk, J. A.: An Experimental and Comparative Study of Jet Penetration in Supersonic Flow. Journal of Spacecraft and Rockets, Vol. 4, No. 9, pp. 1236-1242, September 1967.

31. Henry, J. R.: Recent Research on Fuel Injection and Mixing and Piloted-Ignition for Scramjet Combustors. Twelfth Symposium (International) on Combustion, The Combustion Institute, Pittsburgh, pp. 1175-1182, 1969.

32. Orth, R. C.; Schetz, J. A.; and Billig, F. S.: The Interaction and Penetration of Gaseous Jets in Supersonic Flow. NASA CR 1386, 1969.

33. Torrence, Marvin G.: Effect of Injectant Molecular Weight on Mixing of a Normal Jet in a Mach 4 Airstream. NASA TN D-6061, January 1971.

34. McClinton, C. R.: The Effect of Injection Angle on the Interaction Between Sonic Secondary Jets and a Supersonic Freestream. M.S. Thesis, George Washington University, February 1967.

35. Thayer, W. J., III and Corlett, R. C.: Dynamic and Transport Phenomena in the Two-Dimensional Jet Interaction Flowfield. AIAA-71-561, June 1971.

36. Thayer, W. J., III: The Two-Dimensional Separated Flow Region Upstream of Inert and Chemically Reactive Transverse Jets. Boeing Scientific Research Laboratories Document D1-82-1C, March 1971.

37. Rogers, R. C.: A Study of the Mixing of Hydrogen Injected Normal to a Supersonic Airstream. NASA TN D-6114, March 1971.

38. Rogers, R. C.: Mixing of Hydrogen Injected From Multiple Injectors Normal to a Supersonic Airstream. NASA TN D-6476, September 1971.

39. Anderson, G. Y.: An Examination of Injector/Combustor Design Effects on Scramjet Performance. Presented at the Second International Symposium on Air Breathing Engines, Sheffield, England, March 24-29, 1974.

40. McClinton, C. R.: Effect of Ratio of Wall Boundary-Layer Thickness to Jet Diameter in Mixing of a Normal Hydrogen Jet in a Supersonic Stream. NASA TM X-3030, June 1974.

41. McClinton, C. R.; Torrence, M. G.; Gooderum, P. B.; and Young, I. G.: Nonreactive Mixing Study of a Scramjet Swept-Strut Fuel Injector. NASA TN D-8069, December 1975.

42. Rogers, R. C.: A Model of Transverse Fuel Injection Applied to the Computation of Supersonic Combustor Flow. AIAA-79-0359, January 1979.

43. Schetz, J. A.: Injection and Mixing in Turbulent Flow. Progress in Astronautics and Aeronautics, American Institute of Astronautics and Aeronautics, Inc., New York, Vol. 68, pp. 154-162, 1980.

44. McDaniel, J. C. and Graves, J., Jr.: A Laser-Induced-Fluorescence Visualization Study of Transverse, Sonic Fuel Injection in a Nonreacting Supersonic Combustor. AIAA-86-0507, January 1986.

45. Allen, H., Jr. and Fletcher, E. A.: Combustion of Various Highly Reactive Fuels in a 3.84- by 10-Inch Mach 2 Wind Tunnel. NASA Memo 1-15-59E, April 1959.

46. Allen, H., Jr. and Fletcher, E. A.: A Study of the Combustion of Aluminum Borohydride in a Small Supersonic Wind Tunnel. NASA TN D-296, July 1960.

47. Stevenson, C. W. and Hartsfield, B. W.: Demonstration of Supersonic Combustion of Hydrazine in a Short Length Combustor. Technical Report AEDC-TR-69-262, December 1969.

48. Billig, F. S.: Hydrocarbon, High Energy and Reactive Fuels for Supersonic Combustion Engines. Notes for lecture presented at the "Scramjet Engine Technology and Applications" course, July 1965.

49. Huber, P. W. and Schexnayder, C. J., Jr.: Criteria for Self-Ignition of Supersonic Hydrogen-Air Mixtures. NASA Technical Paper 1457, August 1979.

50. McClinton, C. R.: Autoignition of Hydrogen Injected Transverse to Supersonic Airstream. AIAA-79-1239, June 1979.

51. Slutsky, S.; Tamagno, J.; and Trentacoste, N.: Supersonic Combustion in Premixed Hydrogen-Air Flows. AIAA Journal, Vol. 3, No. 9, pp. 1599-1605, September 1965.

52. Anderson, G. Y. and Gooderum, A. R.: An Experimental Study of Flame Propagation in Supersonic Premixed Flows of Hydrogen and Air. NASA TN D-4631, June 1968.

53. Schetz, J. A. and Jannone, J.: The Ignition of Flowing Hydrocarbon/Air Mixtures by a Hydrogen Pilot Flame. Pyrodynamics, Vol. 2, pp. 1-14, 1965.

53. Bray, K. N. C. and Fletcher, R. S.: Ignition of a High Speed, Cold, Combustible Flow by Means of a Hot, Turbulent Jet. AIAA-70-148, January 1970.

54. Bray, K. N. C.; Fletcher, R. S.; and Spalding, D. B.: Ignition and Combustion in Ducted Turbulent Supersonic Flow. AIAA-70-720, June 1970.

55. Kay, I. W.; McVey, J. B.; Kepler, C. E.; and Chiappetta, L.: Hydrocarbon-Fueled Scramjet. Technical Report AFAPL-TR-68-146, Vol. VIII, May 1971.

56. Edelman, R. B.; Schmotolocha, S.; and Slustsky, S.: Combustion of Liquid Hydrocarbons in a High Speed Air Stream. AIAA-70-88, January 1970.

57. Schmotolocha, S. N. and Edelman, R. B.: High Speed Ignition and Combustion Characteristics of Storable Fuels Using a Hot Gas Pilot Igniter. Technical Report AFOSR-TR-72-1304, April 1972.

58. McFarlin, D. J. and Kepler, C. E.: Mach 5 Test Results of Hydrogen-Fueled Variable-Geometry Scramjet. Technical Report AFAPL-TR-68-116, October 1968.

59. Burnette, T. D.: Dual Mode Scramjet. Technical Report AFAPL-TR-67-132, Part III, June 1968.

60. Kay, I. W.; Chiappetta, L.; and McVey, J. B.: Hydrocarbon-Fueled Scramjet. Technical Report AFAPL-TR-68-146, Vol. IV, 1969.

61. Diskin, Glenn S.: Evaluation of a Storable Fluorine Based Ignitor/Pilot for Scramjets. M.S. Thesis, George Washington University, February 1986.

62. Diskin, G. S. and Northam, G. B.: Evaluation of a Storable Fluorine Based Pilot for Scramjets. AIAA-86-0372, January 1986.

63. Carlson, C. H.: Scramjet Performance Parametrics for Hypersonic Airbreathing Missile Application. NASA CR 3575, 1981. (Conf.)

64. Quarterly Report: Fuels Research for Supersonic Combustion. Supported by Air Force Aero Propulsion Laboratory Ramjet Technology Branch (APRT), July-September 1969.

65. Siminski, V. J.; Wright, F. J.; Edelmann, R.; Economos, C.; and Fortune, O.: Research on Methods of Improving the Combustion Characteristics of Liquid Hydrocarbon Fuels. Technical Report AFAPL-72-74, Vol. I and II, 1972.

66. Siminski, V. J. and Wright, F. J.: The Effect of Homogeneous Additives on the Autoignition of Hydrocarbon Fuels. AIAA-72-71, January 1972.

67. Beach, H. L., Jr.; Mackley, E. A.; and Guy, R. W.: Mach 7 Tests of the Langley Airframe-Integrated Scramjet. NASA TM-84595, June 1983. (Conf.)

68. Northam, G. B. and McLain, A. G.: Supersonic Combustion of a Silane/Methane Mixture. Presented at the 22nd JANNAF Combustion Meeting, Pasadena, California, October 7-11, 1985.

69. Gerstein, M. and Choudhury, P. R.: Use of Silane/Methane Mixtures for Scramjet Ignition. AIAA-84-1407, June 1984.

70. Isaac, J. J.: A Study of Ignition and Combustion in Ducted Supersonic Flow. Ph.D. Thesis, Cranfield Institute of Technology, 1974.

71. Cookson, R. A. and Isaac, J. J.: Aided Supersonic Combustion of Transversely Injected Fuels. AIAA Journal, Vol. 14, No. 1, January 1976.

72. Isaac, J. J. and Cookson, R. A.: Jet Flame Stabilization in Subsonic and Supersonic Flows. Combustion and Flame, Vol. 30, pp. 187-192, 1977.

73. Cookson, R. A.: Aided Combustion of Liquid and Gaseous Fuels Injected Transversely into a Supersonic Air-Stream. Technical Report AD-780-615, March 1974.

74. Investigation of Low Speed Fixed Geometry Scramjet. Technical Report AFAPL-TR-6-105, October 1968.

75. Faucher, J. E., Jr.; Goldstein, S.; Taback, E.: Supersonic Combustion of Fuels Other Than Hydrogen for Scramjet Applications. Technial Report AFAPL-TR-67-12, February 1967.

76. Billig, F. S.; Waltrup, P. J.; and Stockbridge, R. D.: Integral-Rocket Dual-Combustion Ramjets: A New Propulsion Concept. Journal of Spacecraft and Rockets, Vol. 17, No. 5, p. 416, September-October 1980.

77. Brabbs, T. A. and Olson, S. L.: Fuel-Rich Catalytic Combustion. NASA Technical Paper 2468, 1985.

78. Brabbs, T. A.: Fuel-Rich Catalytic Preburner for Volume-Limited Hydrocarbon Scramjet. NASA Technical Memorandum 87111, October 1985.

79. Guy, R. W. and Mackley, E. A.: Initial Wind Tunnel Tests at Mach 4 and 7 of a Hydrogen-Burning, Airframe-Integrated Scramjet. Presented at the Fourth International Symposium on Air Breathing Engines, Lake Buena Vista, Florida, April 1-6, 1979.

80. Billig, F. S.: Design of Supersonic Combustors Based on Pressure-Area Fields. Eleventh Symposium (International) on Combustion, The Combustion Institute, Pittsburgh, pp. 755-769, 1967.

81. Longwell, J. P.; Frost, E. E.; and Weiss, M. A.: Flame Stability in Bluff Body Recirculation Zones. Industrial and Engineering Chemistry, Vol. 45, No. 8, pp. 1629-1633, August 1953.

82. Longwell, J. P.: Flame Stabilization by Bluff Bodies and Turbulent Flames in Ducts. Fourth Symposium (International) on Combustion, The Combustion Institute, Pittsburgh, pp. 90-97, 1954.

83. Longwell, J. P.: Combustion Problems in Ramjets. Fifth Symposium (International) on Combustion, The Combustion Institute, Pittsburgh, pp. 48-56, 1955.

84. Kundu, K. M.; Banerjee, D.; Bhaduri, D.: Theoretical Analysis on Flame Stabilization by a Bluff-Body. Combustion Science and Technology, Vol. 17, pp. 153-162, 1977.

85. Kundu, K. M.; Banerjee, D.; and Bhaduri, D.: On Flame Stabilization by Bluff Bodies. Journal of Engineering for Power, Vol. 102, pp. 209-214, Janury 1980.

86. Ballal, D. R. and Lefebvre, A. H.: Weak Extinction Limits of Turbulent Flowing Mixtures -- Flame Stabilization. ASME Paper 78-GT-144, 1978.

87. Lees, L.: Fluid-Mechanical Aspects of Flame Stabilization. Jet Propulsion, Vol. 24, pp. 234-236, 1954.

88. Zukoski, E. E. and Marble, F. E.: Experiments Concerning the Mechanism of Flame Blowoff from Bluff Bodies. From proceedings of the Gas Dynamics Symposium on Aerothermochemistry, August 22, 23, 24, 1955.

89. Plee, S. L. and Mellor, A. M.: Characteristic Time Correlation for Lean Blowoff of Bluff-Body-Stabilized Flames. Combustion and Flame, Vol. 35, pp. 61-80, 1979.

90. Ballal, D. R. and Lefebvre, A. H.: Some Fundamental Aspects of Flame Stabilization. Presented at the Fifth International Symposium on Air Breathing Engines, Bangolore, India, 1981.

91. Rizk, N. K. and Lefebvre, A. H.: On the Relationship Between Flame Stability and Drag of Bluff-Body Flameholders. Presented at the Seventh International Symposium on Air Breathing Engines, Beijing, China, September 2-6, 1985.

92. Rogers, R. C. and Schexnayder, C. J., Jr.: Chemical Kinetic Analysis of Hydrogen-Air Ignition and Reaction Times. NASA Technical Paper 1856, 1981.

93. Winterfeld, G.: On Process of Turbulent Exchange Behind Flameholders. Tenth Symposium (International) on Combustion, The Combustion Institute, Pittsburgh, pp. 1265-75, 1965.

94. McClinton, C. R. and Jakubowski, A. K.: Parametric Investigation of Hydrogen Fuel Scramjet Flameholding. Twentieth JANNAF Combustion Meeting, Naval Postgraduate School, Monterey, 1983. (Conf.)

95. Jakubowski, A.: Hydrogen Fuel Scramjet Flameholding. Unpublished.

96. Huber, P. W.: Conceptual Model for Turbulent Flameholding for Scramjet Combustors. NASA Technical Paper 1543, 1980.

97. Winterfeld, G.: On the Burning Limits of Flame-Holder-Stabilized Flames in Supersonic Flow. Deutsche Versuchsanstalt Fuer Luft- Und Raumfahrt E.V., Institut Fuer Luftstahlantriebe, Porz-Wahn/Germany, August 1968.

98. Waltrup, P. J.; Dugger, G. L.; Billig, F. S.; and Orth, R. C.: Direct-Connect Tests of Hydrogen-Fueled Supersonic Combustors. Sixteenth Symposium (International) on Combustion, The Combustion Institute, Pittsburgh, pp. 1619-1629, 1977.

99. Anderson, G. Y. and Gooderum, P .B.: Exploratory Tests of Two-Strut Fuel Injectors for Supersonic Combustion. NASA TN D-7581, February 1974.

100. Harsha, P. T.; Colley, W. C.; and Kenworthy, M. J.: Hypersonic Ramjet Research Engine - Combustor Design. General Electric, Cincinnati, Ohio, Report Number R66FPD56.

101. Anderson, G. Y.; Eggers, J. M.; Waltrup, P. J.; and Orth, R. C.: Investigation of Step Fuel Injectors for an Integrated Modular Scramjet Engine. Presented at the Thirteenth JANNAF Combustion Meeting, Montery, California, September 13-17, 1976.

102. McClinton, C. R. and Gooderum, P. B.: Direct-Connect Test of a Hydrogen-Fueled Three-Strut Injector for an Integrated Modular Scramjet Engine. Presented at the Fourteenth JANNAF Combustion Meeting, Colorado Springs, Colorado, August 15-17, 1977.

103. Eggers, J. M.; Reagon, P. G.; and Gooderum, P. B.: Combustion of Hydrogen in a Two-Dimensional Duct with Step Fuel Injectors. NASA Technical Paper 1159, May 1978.

104. McClinton, C. R.: Interaction Between Step Fuel Injectors on Opposite Walls in a Supersonic Combustor Model. NASA Technical Paper 1174, May 1978.

105. Northam, G. B.; Trexler, C. A.; and McClinton, C. R.: Flameholding Characteristics of a Swept-Strut H_2 Fuel-Injector for Scramjet Applications. Presented at the Seventeenth JANNAF Combustion Meeting, Hampton, Virginia, September 22-26, 1980.

106. Levy, M. E.; Cerkanawicz, A. E.; and McAlevy, R. F., III: Ignition of Subatmospheric Gaseous Fuel-Oxidant Mixtures by Ultraviolet Irradiation. AIAA-69-88, 1968.

107. Cerkanowicz, A. E.; and McAlevy, R. F., III: Photochemical Ignition and Combustion Enhancement in High Speed Flows of Fuel-Air Mixtures. AIAA-73-216, 1973.

108. McAlevy, R. F., III: Photochemical Combustion of Hydrogen. Unpublished.

109. Lavid, M.; Stevens, J. G.; and Westbrook, C. K.: Enhancement of Premixed H_2/Air Flames with Photochemically Produced Radicals: Analytical Modeling. Presented at the Fall Technical Meeting of the Eastern Section of the Combustion Institute, Philadelphia, Pennsylvania, November 4, 1985.

110. Tanford, C. and Pease, R. N.: Equilibrium Atom and Free Radical Concentrations in Carbon Monoxide Flames and Correlations with Burning Velocities. The Journal of Chemical Physics, Vol. 15, No. 7, pp. 431-433, July 1947.

111. Tanford, C.: Theory of Burning Velocity. I. Temperature and Free Radical Concentrations Near the Flame Front, Relative Importance of Heat Conduction and Diffusion. The Journal of Chemical Physics, Vol. 15, No. 7, pp. 433-439, July 1947.

112. Tanford, C. and Pease, R. N.: Theory of Burning Velocity. II. The Square Root Law for Burning Velocity. The Journal of Chemical Physics, Vol. 15, No. 12, pp. 861-865, December 1947.

113. Gaydon, A. G. and Wolfhard, H. G.: Flames - Their Structure, Radiation and Temperature. John Wiley & Sons, Inc., New York, Fourth Edition, 1979.

114. Jachimowski, C. J. and McLain, A. G.: A Chemical Kinetic Mechanism for the Ignition of Silane/Hydrogen Mixtures. NASA Technical Paper 2129, 1983.

115. Chinitz, W.: Theoretical Studies of the Ignition and Combustion of Silane-Hydrogen-Air Mixtures. NASA CR 3876, 1985.

116. Biordi, J. C.; Lazzara, C. P.; and Papp, J. F.: Chemical Flame Inhibition Using Molecular Beam Mass Spectrometry. Reaction Rates and Mechanisms in a 0.3 Percent CF_3Br Inhibited Methane Flame. Bureau of Mines RI 8029, May 1975.

117. Dabora, E. K.: Effect of NO_2 on the Ignition Delay of CH_4-Air Mixtures. Combustion and Flame, Vol. 24, No. 2, pp. 181- 184, April 1975.

118. Slack, M. W. and Grillo, A. R.: Shock Tube Investigation of Methane-Oxygen Ignition Sensitized by NO_2. Combustion and Flame, Vol. 28, No. 2, pp. 155-177, February 1977.

119. Harrison, A. J. and Weinberg, F. J.: Flame Stabilization by Plasma Jets. Proceedings of the Royal Society of London A, Vol. 321, pp. 95-103, 1971.

120. Hilliard, J. C.: Methods of Improving Combustion by Electrical Means. Ph.D. Thesis, Imperial College of Science and Technology, London, November 1979.

121. Ziegler, G. R. W.; Wagner, E. P.; and Maly, R. R.: Ignition of Lean Methane Air Mixtures by High Pressure Glow and Arc Discharges. Twentieth Symposium (International) on Combustion, The Combustion Institute, Pittsburgh, pp. 1817-1824, 1984.

122. Cobine, J. D.: Gaseous Conductors. Dover Publications, Inc., New York, 1958.

123. Finkelnburg, W. and Maecker, H.: Electric Arcs and Thermal Plasma. Translation of "Elektrische Bogen und thermisches Plasma," Handbook of Physics, Vol. XXII, Gas Discharges II, Springer-Verlag, Berlin, 1956.

124. Pfender, E.: Electric Arcs and Arc Gas Heaters. Chapter 5, Gaseous Electronics, Vol. 1, Electrical Discharges, Edited by M. N. Hirsch, pp. 291-351, 1978.

125. Hoyaux, M. F.: Arc Physics. Springer-Verlag, Berlin, 1968.

126. Gordon, S. and McBride, B. J.: Computer Program for Calculation of Complex Chemical Equilibrium Compositions, Rocket Performance, Incident and Reflected Shocks, and Chapman-Jouguet Detonations. NASA SP-273, 1971.

127. Patch, R. W.: Components of a Hydrogen Plasma Including Minor Species. NASA TN D-4993, January 1969.

128. Capitelli, M.; Ficocelli, E.; and Molinari, E.: Equilibrium Compositions and Thermodynamic Properties of Mixed Plasmas - III. Argon-hydrogen plasmas at 10^{-2} - 10^{3} atmospheres between 2,000 K and 35,000 K, Centro di Studio per la Chimica dei Plasmi del C.N.R., Bari, 1971.

129. Lawton, J. and Weinberg, F. J.: Electrical Aspects of Combustion. Clarendon Press, Oxford, 1969.

130. Lawton, J.; Payne, K. G.; and Weinberg, F. J.: Flame-Arc Combination. Nature, Vol. 193, pp. 736-738, 1962.

131. Chen, D. C. C.; Lawton, J.; and Weinberg, F. J.: Augmenting Flames with Electric Discharges. Tenth Symposium (International) on Combustion, The Combustion Institute, Pittsburgh, pp. 743-754, 1965.

132. Waterson, K.: Some Operating Characteristics of Novel Ignition Devices for Hydrocarbon/Air Mixtures. Ph.D. thesis, University of Oxford, September 1973.

133. Hilliard, J. C. and Weinberg, F. J.: Effect of Nitrogen-containing Plasmas on Stability, NO formation and Sooting of Flames. Nature, Vol. 259, pp. 556-557, 1976.

134. Weinberg, F. J.: Hom, K; Oppenheim, A. K.; and Teicham, K.: Ignition by Plasma Jet. Nature, Vol. 272, pp. 341-343, 1978.

135. Orrin, J. E.; Vince, I. M.; and Weinberg, F. J.: Ignition by Radiation from Plasmas. Combustion and Flame, Vol. 37, pp. 91-93, 1980.

136. Orrin, J. E.; Vince, I. M.: and Weinberg, F. J.: A Study of Plasma Jet Ignition Mechanisms. Eighteenth Symposium (International) on Combustion, The Combustion Institute, Pittsburgh, pp. 1755-1765, 1981.

137. Carleton, F. B.; Vince, I. M., and Weinberg, F. J.: Energy and Radical Losses from Plasma Jet Igniters to Solid Surfaces. Nineteenth Symposium (International) on Combustion, The Combustion Institute, Pittsburgh, pp. 1523-1531, 1982.

138. Klein, N.; Carleton, F. B.; and Weinberg, F. J.: Methods for Evaluation of Ignition Stimuli for Liquid Propellants.

139. Clements, R. M.; Smy, P. R.; Topham, D.; Vince, I. M.; Vovelle, C.; and Weinberg, F. J. Chemical Activity and Transport Processes in the Vicinity of a Plasma Jet Igniter. Combustion and Flame, Vol. 57, pp. 265-274, 1984.

140. Vince, I. M.; Vovelle, C.; and Weinberg, F. J.: The Effect of Plasma Jet Ignition on Flame Propagation and Sooting at the Rich Limit of Flammability. Combustion and Flame, Vol. 56, pp. 105-112, 1984.

141. Warris, A. M.: Electric Plasmas for Flame Stabilization and Ignition in Fast Gas Streams. Ph.D. Thesis, March 1983.

142. Warris, A. M.; and Weinberg, F. J.: Ignition and Flame Stabilization by Plasma Jets in Fast Gas Streams. Presented at Twentieth Symposium (International) on Combustion, The Combustion Institute, Pittsburgh, pp. 1825-1831, 1984.

143. Boston, P. M.; Bradley, D.; Lung, F. K-K.; Vince, I. M.; and Weinberg, F. J.: Flame Initiation in Lean, Quiescent and Turbulent Mixtures with Various Igniters. Twentieth Symposium (International) on Combustion, The Combustion Institute, Pittsburgh, pp. 141-149, 1984.

144. Colver, G. M.; and Weinberg, F. J.: Quenching Magnetically Rotated Augmented Flames and Plasma Jets in Mixtures Containing Methane, Oxygen and Nitrogen. Proceedings of the Royal Society of London A, Vol. 326, pp. 375-391, 1972.

145. Jagoda, I. J. and Weinberg, F. J.: Optical Studies of Plasma Jets. Journal of Physics D: Applied Physics, Vol. 13, pp. 551-561, 1980.

146. Chan, A. K. F.; Hilliard, J. C.; Jones, A. R.; and Weinberg, F. J.: An Electrically Efficient, Finely Tunable, Low-Power Plasma Generator. Journal of Physics D: Applied Physics, Vol. 13, pp. 2309-2320, 1980.

147. Behbahani, H. F.; Fontijn, A.; Muller-Dethlefs, K.; and Weinberg, F. J.: The Destruction of Nitric Oxide by Nitrogen Atoms from Plasma Jets. Combustion Science and Technology, Vol. 27, pp. 123-132, 1982.

148. Behbahani, H. F.; Warris, A. M.; and Weinberg, F. J.: The Destruction of Nitric Oxide by Nitrogen Atoms from Plasma Jets: Designing for Thermal Stratification. Combustion Science and Technology, Vol. 30, pp. 289-302, 1983.

149. Barbi, E.: Uncooled Choked Plasma Torch for Ignition and Flameholding in Supersonic Combustion. M.S. Thesis, Virginia Polytechnic Institute and State University, August 1986.

150. McKelliget, J; Szekely, J.; Vardelle, M.; and Fauchais, P.: Temperature and Velocity Fields in a Gas Stream Exiting a Plasma Torch. A Mathematical Model and Its Experimental Verification. Flame Chemistry and Plasma Processing, Vol. 2, No. 3, pp. 317-332, 1982.

151. Vaessen, P. H. M.: Heat and Momentum Transfer From an Atmospheric Argon Hydrogen Plasma Jet to Spherical Particles. M.S. Thesis, Eindhoven, Technische Hogeschool, Netherlands, 1984.

152. Boffa, C.; and Pfender, E.: Enthalpy Probe and Spectrometric Studies in an Argon Plasma Jet. Heat Transfer Laboratory, University of Minnesota, 1967.

153. Weise, W. L.; Paquette, D. R.; and Solarski, J. E.: Profiles of Stark-Broadened Balmer Lines in a Hydrogen Plasma. Physical Review, Vol. 129, No. 3, pp. 1225-1232, February 1, 1963.

154. Huddlestone, R. H. and Leonard, S. L. (editors): Plasma Diagnostic Techniques. Academic Press, New York, 1965.

155. Brundin, C. L.; and Talbot, L.: The Application of Langmuir Probe Techniques to Flowing Ionized Gases. North Atlantic Treaty Organization Report 478, September 1964.

156. Clements, R. M.; and Smy, P. R.: Langmuir-probe Measurement of Electron Temperature in a Flowing High-density Plasma. Electronics Letters, Vol. 6, No. 17, pp. 538-539, August 20, 1970.

157. Swift, J. D. and Schwar, M. J. R.: Electrical Probes for Plasma Diagnostics. London Iliffe Books, LTD., 1970.

158. Chung, P. M.; Talbot, L.; and Touryan, K. J.: Electric Probes in Stationary and Flowing Plasmas: Theory and Application. Springer-Verlag, Berlin, 1975.

159. Cherrington, B. E.: The Use of Electrostatic Probes for Plasma Diagnostics - A Review. Plasma Chemistry and Plasma Processing, Vol. 2, No. 2, pp. 113-140, 1982.

160. Grey, J. and Jacobs, P. F.: Cooled Electrostatic Probe. AIAA Journal, Vol. 5, No. 1, pp. 84-90, 1967.

161. Weise, W. L.: Line Broadening. Plasma Diagnostic Techniques, ed. R. H. Huddlestone and S. L. Leonard, Academic Press, New York, pp. 265-317, 1965.

162. Goode, S. R. and Deavor, J. P.: Determination of Electron Density in an Atomic Plasma by Least-squares Fit to the Stark Profile. Spectrochimica Acta, Vol. 39B, No. 6, pp. 813-818, 1984.

163. Vidal, C. R.; Cooper, J.; and Smith, E. W.: Hydrogen Stark-Broadening Tables. The Astrophysical Journal Supplement Series, No. 214, Vol. 25, pp. 27-136, 1973.

164. Clyne, M. A. A. and Thrush, B. A.: Reaction of Hydrogen Atoms with Nitric Oxide. Transactions of the Faraday Society, Vol. 57, pp. 1305-1314, 1961.

165. Phillips, L. F. and Schiff, H. I.: Mass Spectrometric Studies of Atomic Reactions. III. Reactions of Hydrogen Atoms with Nitrogen Dioxide and with Ozone. The Journal of Chemical Physics, Vol. 37, No. 6, pp. 1233-1238, September 15,1962.

166. Clyne, M. A. A. and Stedman, S. H.: Reactions of Atomic Hydrogen with Hydrogen Chloride and Nitrosyl Chloride. Transactions of the Faraday Society, Vol. 62, pp. 2164-2174, 1966.

167. Suttrup, F.: Ignition of Gaseous Hydrocarbon Fuels in Hypersonic Ramjets. Presented at the First International Symposium on Air Breathing Engines, Marseille, France, June 1972.

168. McClinton, C. R.: Personal communication.

APPENDIX

DISCUSSION OF EXPECTED ERROR

A discussion of the expected error for the various experimental measurements involved in this research is presented.

TORCH GAS FLOW MEASUREMENT

The flows of argon and hydrogen to the torch were calculated from pressures measured upstream of choked orifices according to the relation

$$\dot{m} = C\, p_t / T_t$$

where C is a constant which incorporates the area, discharge coefficient, specific heat ratio and molecular weight. The pressures were measured with transducers which had been calibrated using a dead weight tester traceable to the National Bureau of Standards (NBS). A value for the constant was determined from a calibration using a Hastings mass flow meter which was also traceable to NBS. The calibration procedure was to measure the flowrate and pressure at several points in the operating range and to use a least squares method to determine the constant. The error was estimated by repeating the calibration procedure and comparing the Hastings output to the calculated value. The error was never greater than 3 percent.

ELECTRICAL MEASUREMENTS

The voltage and current to the torch were measured by analog meters with an expected accuracy of +/- 2.5 volts and +/- 0.5 amps, respectively. Although these were never thoroughly calibrated, they were checked against a calibrated digital voltmeter and found to be in good agreement. The power was calculated as the product of the voltage and the current.

$$P = VI$$

The Kline and McClintock method may be used to determine the uncertainty. The uncertainty in the power measurement is:

$$W_P = \left[\left(\frac{\partial P}{V}\right) W_V^{\ 2} + \left(\frac{\partial P}{I}\right) W_I^{\ 2} \right]^{\frac{1}{2}}$$

which reduces to

$$W_P = \left[\left(IW_V\right)^2 + \left(VW_I\right)^2 \right]^{\frac{1}{2}}$$

For typical torch conditions of 80 volts and 15 amps (P = 1200 W), the uncertainty is

$$W_P = \left[\left[(15)(2.5)\right]^2 + \left[(80)(0.5)\right]^2 \right]^{\frac{1}{2}}$$

or

$$W_P = 55 \text{ W} \sim 5 \text{ percent}$$

WIND TUNNEL CONDITIONS

The conditions of the air leaving the vitiated heater (m, T_t, P_t, and γ) are estimated or calculated from facility instrumentation. These instruments are regularly calibrated and maintained. The accepted accuracy of the total temperature is +/- 50 R. The total pressure is measured with a transducer and is therefore known to be accurate to within +/- 5 psi.

The two page vita has been removed from the scanned document. Page 1 of 2

The two page vita has been removed from the scanned document. Page 2 of 2